



---

## **Voltage Control of Hybrid Photovoltaic/ Battery Power System for Low Voltage DC Micro grid**

---

**Aalborg University**  
**Institute of Energy Technology**

**DRAGOS OVIDIU OLTEANU**

## **Master Thesis**

---

# **Voltage Control of Hybrid Photovoltaic/ Battery Power System for Low Voltage DC Micro grid**

---

**Aalborg University**  
Institute of Energy Technology  
Denmark, June 2016

**Supervisor:**

**Amin Hajizadeh**

**Student:**

**Dragos Olteanu**  
**Project group –OES9-3**

## **Acknowledgement**

First of all I would like to express my gratitude to my supervisor Amin Hajizadeh for his important contribution to this project and for his motivation during the semester.

I would like also to express my appreciation to Henry Enevoldsen Assistant Engineer from the Department of Energy Technology for his cooperation and professional support.

Many thanks to my colleagues at AAU, for friendly companion and constructive discussions at any time, no matter the place or the hour.

Finally, I would like to thank my family for their continuous moral support in the past 2 years.

## Abstract

Data in this report includes the work on the design of a stand-alone low voltage DC micro grid system to power a fully DC single house in remote areas. The main objective of this report was to investigate a maximum power point tracking (MPPT) algorithm. By simulation, the behavior and efficiency of the system, together with the implemented algorithm were analyzed.

First the Photovoltaic module was build using MATLAB's SimPowerSystems block, delivering power to a boost converter, controlled by the MPPT algorithms feeding a DC load and a battery.

MPPT is a technique which is responsible for extracting the maximum power from the Photovoltaic (PV) System. The algorithm used for tracking the maximum power point of the Photovoltaic module is the Perturb and Observer (P&O) method which is written in an m. files in MATLAB and used to calculate the maximum power point for different weather conditions. Different data such as input voltage, current and output voltage, power for each simulation have been recorded.

## Table of Contents

1. Introduction.....	1
1.1 The current state of integration of photovoltaic sources in electricity networks .....	3
1.1.1The evolution of the photovoltaic sources worldwide .....	3
1.1.2 The evolution of the photovoltaic sources in Europe.....	4
2. Problem formulation .....	5
2.1 The problem.....	5
2.2 Task at hand.....	5
2.3 Project Delimitations .....	6
3. Modelling of PV Panel.....	7
3.1 Photovoltaic cell.....	7
3.2 Mathematical model of PV Module.....	9
3.3 PV Array .....	13
3.5 Matlab- Simulink Model of Photovoltaic module .....	16
3.6 Electrical characteristics PV module Simulink .....	19
4. The Boost Converter .....	21
4.1 Closed switch operation of the Boost converter .....	24
4.2 Open switch operation of the Boost converter .....	26
5. Maximum Power Point Tracking Algorithm .....	33
5.1 MPPT main characteristics.....	33
5.2 Perturb and Observe MPPT algorithm.....	34
6. Simulations and results .....	37
6.1 Constant Irradiance and constant Temperature without battery .....	37
6.2 Constant Irradiance and constant Temperature with battery connected.....	43
6.3 Fluctuating Irradiance and fluctuating Temperature.....	50
7. Experiments Chapter .....	56
7.1Test Experiment.....	56
7.2 First Boost converter experiment .....	58
7.2.1 Experiment results .....	60
7.3 Second boost converter experiment .....	62

8. Conclusion.....	65
8.1 Future research and improvements .....	66
9. Nomenclature .....	67
9.1 Abbreviations .....	69
10. References .....	71
Appendices:.....	73
A. Boost Converter .....	73
a. Subsystem of the Converter .....	73
b. Matlab .m file for calculating inductor and capacitance value .....	74
c. Perturb and Observe .m file.....	74
B. Battery graphs Chapter 6.3 .....	77
C. Photovoltaic Panel Array.....	79
a. Block Parameters defined by the user in Simulink .....	79
b. Diode current equation in detail.....	79
D. Datasheets for Inductor, Diode, Capacitor, MOSFET Transistor.....	80
a. Fast recovery rectifier diode datasheet .....	80
b. Aluminum Capacitor Axial Standard datasheet .....	81
c. MOSFET transistor .....	85
d. Inductor.....	88

## 1. Introduction

Fossil fuels such as coal, oil, and gas have been for many centuries the primary source of the energy generation around the globe. Burning of the fossil fuels is leading to a considerable amount of CO<sub>2</sub> emission in the atmosphere that will enhance the greenhouse effect to increase, causing higher temperature. When the temperature is increasing, that triggers the release of more CO<sub>2</sub> from the oceans and from the permafrost areas. All the factors mentioned above are causing the global warming which have a direct implication on the sea level rises, extreme weather conditions, and other serious natural and social impacts. [1-renewable course]

The growing energy demand due to the economically aspects and population growth are shifting the world energy production from the conventional to sustainable energy sources in order to produce enough power. At the UN Climate Change Conference held in Paris at the end of 2015, 186 countries had announced their action plan towards the decreasing of their greenhouse gas emissions. The target plan for the next 5 years is to keep the rise temperature below 2 °C. The main aim of the conference was to make all the countries aware of the global warming impact and to outline that the transition towards renewable energy is needed now. Solar energy will play an important role in this transition. [3]

In some countries, the price that people are paying for 1KWh of solar energy is almost the same with the price that people are paying for 1KWh coal energy. In the last 10 years the price of Photovoltaic Systems has drop dramatically of around 75%. [2]

The low solar price is not the only advantage of the solar power implementation. The Photovoltaic systems that are produced around the globe can be installed as grid connection modules or can be operated as standalone mode for the remote areas where the grid connection is not feasible. Some of the standalone or off grid systems are used also in some applications such as outside playgrounds for children's, street lighting. In some cases the off grid systems are installed together with a battery backup which is needed during the evening hours when the irradiance level is very low. [4]

Photovoltaic systems are harvesting the solar energy and are converting it into electricity and in this process two main advantages can be mentioned: firstly is an environmental friendly

process and secondly the maintenance cost of such a system is low in comparison with the maintenance cost of other renewable energy technologies.

After highlighting the main advantages of the photovoltaic technology, some of the disadvantages of PV should be mentioned. There are two main disadvantages of PV technology, the first one is the high initial installation cost and in the second place the low efficiency achieved for the commercial crystalline silicon solar panels around 22%. [6]

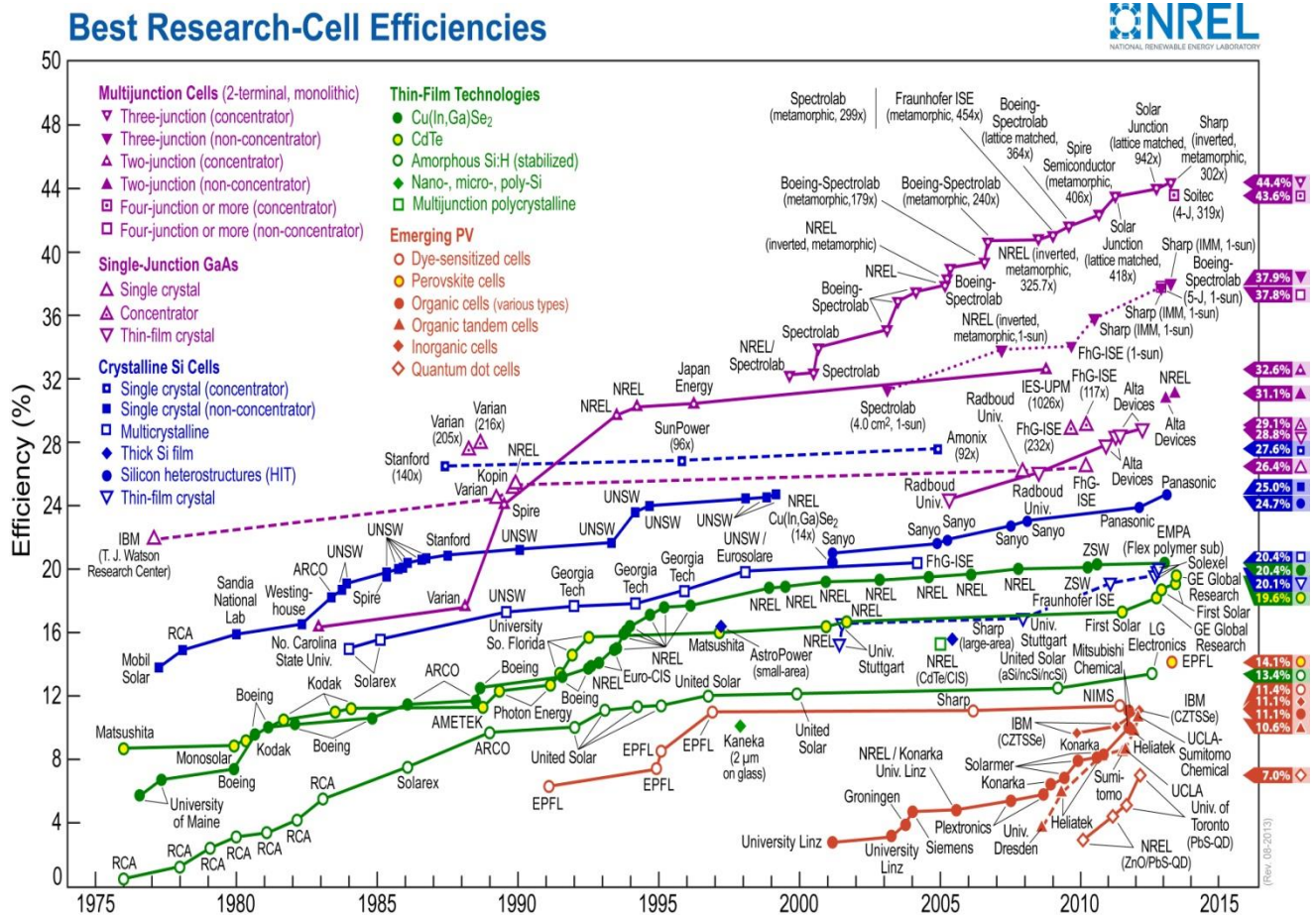


Figure 1-1 Best research solar cells in production by year [7]

The technology development in the PV industry has shown in the last 50 years an increasing in the efficiencies from around 10% in the 1975 to 40%-44% in 2015 for the different Multi-junction solar cell (two-junction or three junction solar cells).

Usually the time interval between the development of a new materials and better technology for developing higher efficiencies solar cells is around 10 years. In this time period a lot of



researches are going on and the main goal is to reduce the manufacturing costs and to optimize the manufacturing process.

## 1.1 The current state of integration of photovoltaic sources in electricity networks

### 1.1.1 The evolution of the photovoltaic sources worldwide

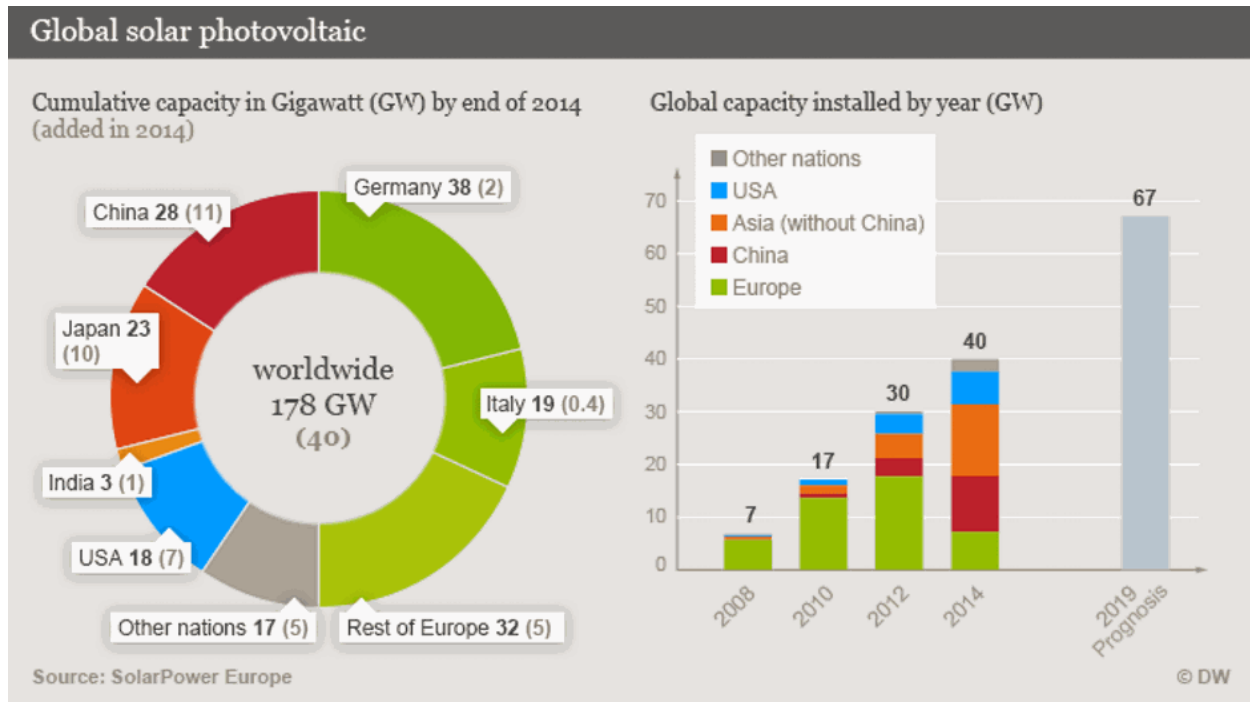


Figure 1-2: Global solar photovoltaic cumulative capacity [8]

According to the report of Solar Power Europe (SPE) in its Global Market Outlook 2015-2019 in 2014 around 40 GW of new solar capacity was installed worldwide, compared to 38.4 GW in 2013. This 40 GW was setting a new record in the solar PV market, which globally has a 178 GW installed capacity. As we can observe from the graph, Germany has the highest rate of installed PV in the world, with a cumulative capacity of 38 GW. Italy has the second biggest installed capacity in Europe with 19GW of photovoltaic technology. [2]

### 1.1.2 The evolution of the photovoltaic sources in Europe

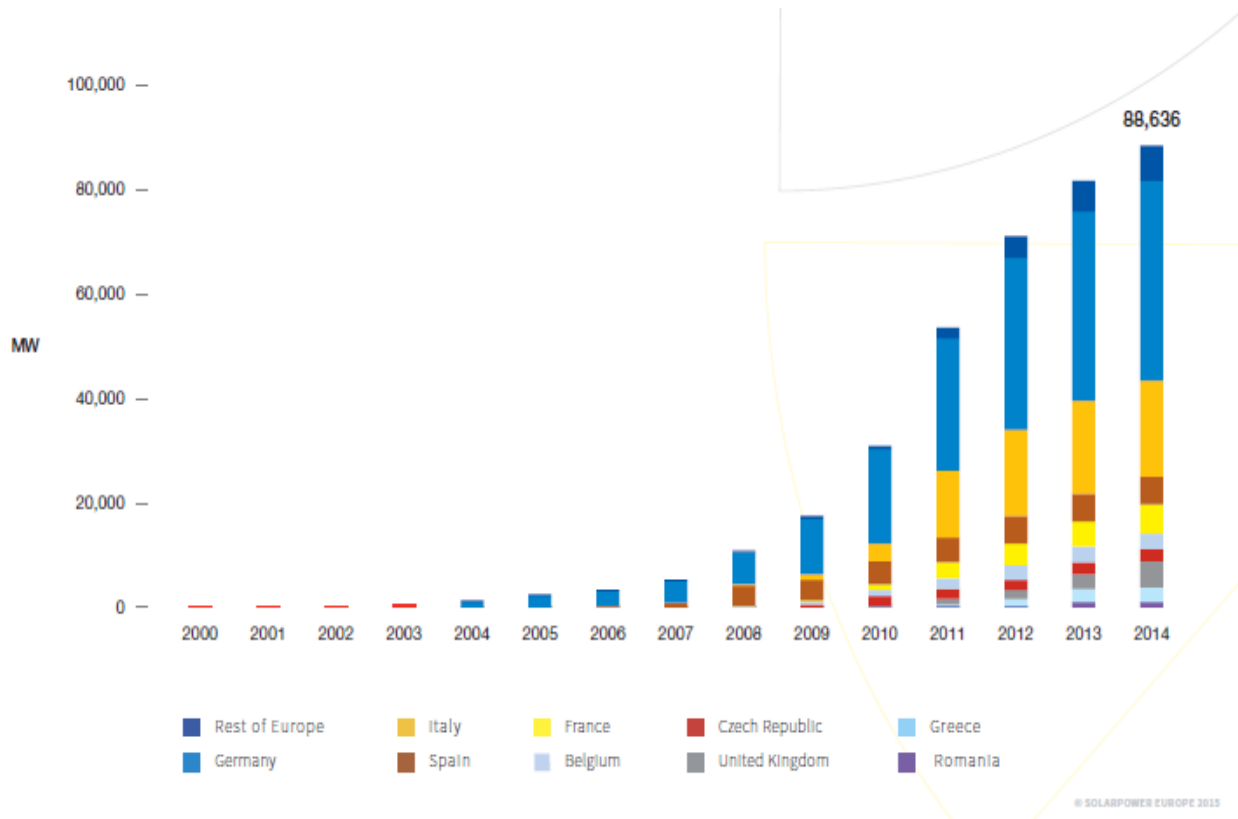


Figure 1-3: The evolution of cumulative PV installed capacity in Europe in the period 2000-2014. [2]

In 2009 the European Union defined the targets for the 2020 total PV installed capacity in Europe and their targets were much rapidly reached than they expected. Already in 2014 these targets were reached and in the same year the total installed capacity in Europe was around 90GW of PV which is consolidating Europe as a global leader for the cumulative installed capacity. Germany is the European and global leader of these industry, with a lot of research project carrying out in different field areas such as improving the maximum power point tracking methods or developing new materials in order to reduce the production costs. [2]

Denmark cumulative PV installed capacity is not shown in the graph, because the percentage of this renewable energy source is very low. Denmark has decided to invest more in the wind industry and today is the world leader when we are referring to the wind power installed capacity. The percentage of energy supply coming from the wind power technology is more than 40% and the targets for 2020 are optimistic nearly 50% of the energy should come from the wind power plants. [9]

## 2. Problem formulation

### 2.1 The problem

Commonly, when a PV module is directly coupled to a load, the operating point is rarely at the maximum power point or MPP. Having a satisfactory Maximum Power Point Tracking algorithm working together with a high efficiency converter is a must if you are investing in the photovoltaic industry. Whether you are using, P&O algorithm connected to a boost converter, buck converter or a boost-buck converter any external factors such as temperature, irradiance and shadings can lead to overpowering consequences, such as shifting of the I-V curve and implicit shifting of the maximum power point.

In order to overcome these problems and to maintain the MPP different control strategies have to be analyzed and optimized according to the selected algorithm.

In this case the Perturb and Observe strategy has to be analyzed together with the advantages and disadvantages of this method. The main problem is making the simulation work, since we already know the PV array is producing a non-linear output power which has to be properly controlled in order to interface it to the DC loads and the battery.

### 2.2 Task at hand

This project will analyze a DC micro grid system. The first step was the research part, the understanding of the PV array model and the working principle of the DC/DC converters. Later a PV array model was built together with a DC/DC converter model in Simulink. A control strategy was implemented which will be directly connected to the DC/DC boost converter. This converters are connected to the PV array output for MPPT objective, such as extracting the maximum available power for a given irradiance level.

Specifically the DC system that combines all the components that makes the PV array to respond to the different external factors has to be modeled.

## 2.3 Project Delimitations

- The PV array block used in the Simulation part has not the identically same parameters as the one used for the Experimental part
- The PV block is a prebuilt block that is available in the Simulink library
- Two different solar module were used in this project
  - For the Chapter 3.5 the solar module : **Soltech 1STH-215-P** with a Maximum Power  $P_{max} = 213.15 \text{ W}$
  - For the Chapter ..... **and for the experimental part the solar moduel: Solar Panel Model: JTM90-36M** with a Maximum Power  $P_{max} = 90 \text{ W}$
- A fixed step change (Increment value used to increase/decrease the duty cycle D) was used for each perturbation
- The practical implementation of the whole system wasn't possible and just the boost converter prototype was built.

## 3. Modelling of PV Panel

### 3.1 Photovoltaic cell

Photovoltaic (PV) module consists of a number of PV cells connected in series or in parallel depending on the desired specification of voltage and current. The arrangement of the cells in a series connection is needed due to the fact that their operating voltage is in the range of hundreds of millivolts and the current produced when the solar cell is absorbing the incident light is in the range of some amperes. For this series connection the voltage is added and the PV module is now operating at a voltage range of tens of volts and the current range is remaining in the same range of some amperes. In order to increase the current level of a PV module a number of strings are connected in parallel and in this manner the preferred power level of the PV module is achieved. In order to calculate and represent the (I-V) characteristic of a PV module, the voltage value has to be multiplied with the number of cells in series and the value of the cell current has to be multiplied with the number of strings of module connected in parallel.

In practice when the PV panel is mounted on the roof of the house the nominal current and voltage values can differ from manufactures datasheet (STC 25 C) characteristics because of shadowing effect or due to different orientation of the module in respect to the sun position. The fluctuating operating conditions are known as mismatching and can conduct to a serious decrease in the overall output power of the PV module.

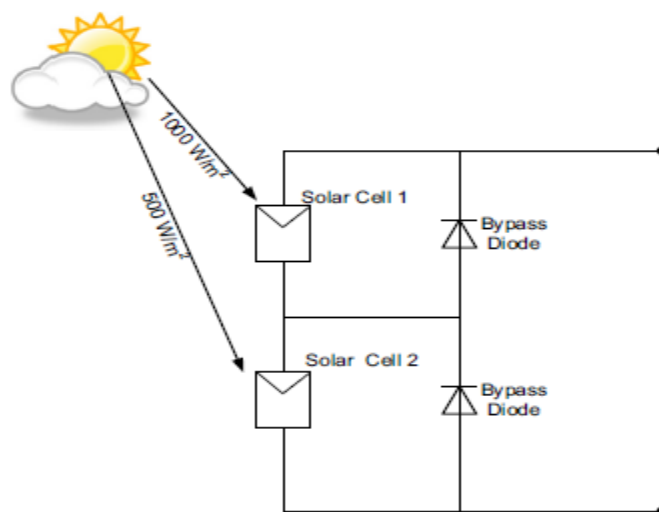


Figure 3-1: Operation of solar PV under partial shading condition [21]

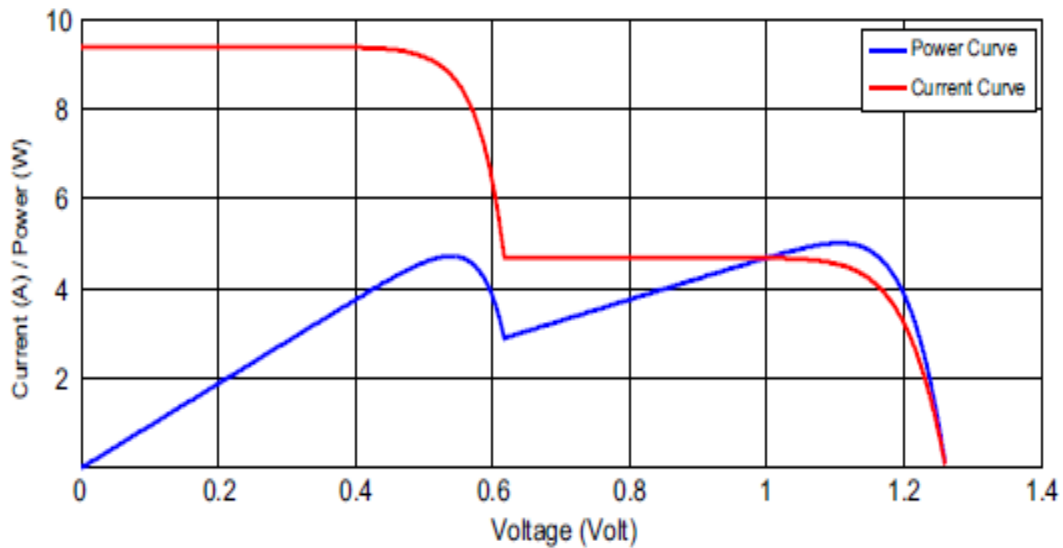


Figure 3-2: I–V and P–V Curve under partial shading condition [21]

In order to reduce the effect of mismatching or the effect caused by broken cells the PV manufactures are connecting two or three bypass diodes in parallel to a string of series connected cells, depending on each manufactures.

The bypass diodes are installed on the rear side of the panel and normally in a passive mode. They will be active and ready to bypass the exceeding current when a group of cells are not working or are producing a current lower than the one of the other subpanels in the string.

By adding a second diode in parallel with the first diode the model can enhance and a better performance can be achieved. [10]

### 3.2 Mathematical model of PV Module

Photovoltaic modules are modeled using an equivalent circuit type, based on the behavior of the diode with a characteristic exponential, which differ in the procedure of calculation, accuracy and number of parameters involved in the calculation of the characteristic I-V. The model shown in the Fig 1.4 is a single diode model, but also other models with two or three diodes can be implemented.

When the PV cell is absorbing the incident light coming from the sun, electron-holes pairs are generated creating an internal electric field which result in a photo-induced current generation. The generated photo-current flows in the opposite direction to the forward diode dark current. [1]

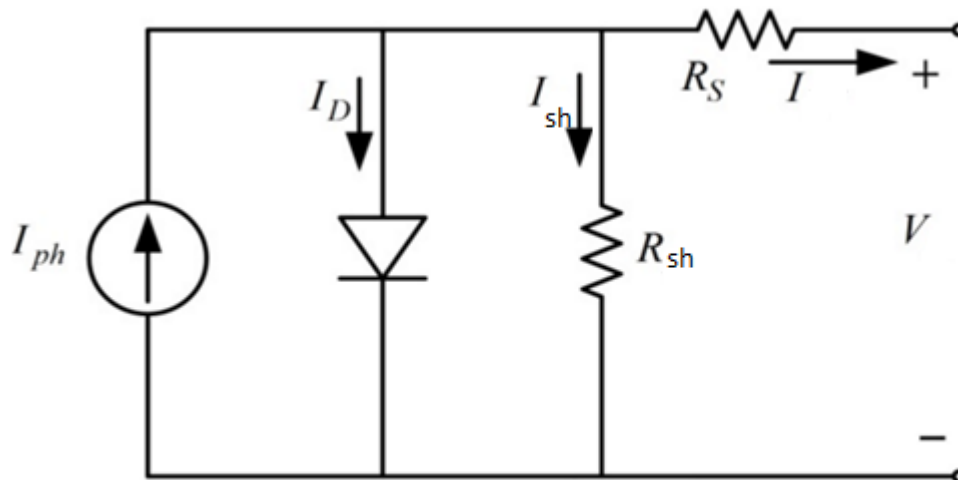


Figure 3-3: Single diode model accounting for Ohmic losses [10]

The equation Eq. 3.1 represents the photo-induced current which is clearly dependent on the different features of the semiconductor material used in the manufacturing process of the solar cell. The photo current varies linearly in respect with the irradiation level and temperature.

$$I_{ph} = I_{ph,STC} * \frac{G}{G_{STC}} [1 + \alpha_1 * (T - T_{STC})]$$

Eq. 3-1

Where:

$G$  - Solar irradiation

$G_{STC}$  - Reference solar irradiation

$T_{STC}$  - Reference cell temperature

$I_{ph,STC}$  - Photo-current at  $G_{STC}$  and  $T_{STC}$

$\alpha_1$  - The temperature coefficient of the current, defined in STC as:

$$\alpha_1 = \frac{dI}{dT}$$

Eq. 3-2

When no external voltage is applied, the photo-current continues to flow and it can be measured as the short circuit current ( $I_{sc}$ ).

The current through the diode  $I_d$  is representing the non-linearity of the I-V curve. By applying the Kirchhoff's current law, based on the equivalent circuit presented in the Fig 1.4 the following equation is found:

$$I = I_{ph} - I_d - I_{sh}$$

Eq.3-3

Where:

$I$  - Output current of the Photovoltaic module

$I_d$  - Current flowing through the diode

$I_{sh}$  - Shunt current

$I_{ph}$  - Light generated current

$$I = I_{ph} - I_0 \left[ e^{\frac{e(V - I R_s)}{A k T}} - 1 \right] - \left( \frac{V - I R_s}{R_{sh}} \right)$$

Eq.3-4



Where:

$R_{sh}$  - Shunt resistance

$R_s$  - Series resistance

A - Dimensionless factor

k - Boltzmann constant

e - Electron charge

T - Temperature

$I_0$  - Reverse saturation current of the diode

The series resistance  $R_s$  represented in the single diode model is essentially influencing the slope of the I-V curves at high voltage levels. If we are referring at the open-circuit voltage, it can be stated that any decreasing in the cell quality is resulting in a decreasing in the curve slope because of the high voltage drop that over the series resistance.

An approximated equation can be written:

$$R_s \approx \left. \frac{dV}{dI} \right|_{V=V_{oc}}$$

Eq.3-5

In the case of the shunt resistance  $R_{sh}$ , the lower the value of the chosen resistance, the higher the amount of current that is drawn by the resistance is. That will result in a decrease of the output current, and in the same time in a decline of the slope of the curve at low voltage level.

The approximated definition can be written as following:

$$R_{sh} \approx \left. \frac{dV}{dI} \right|_{I=I_{sc}}$$

Eq.3-6

The cell efficiency is directly influenced by the values of the two resistances which is expressed through the curve factor or through so called fill factor. The expression for the fill factor is defined as ration between the multiplication of the voltage and current values of maximum power point and the multiplication of the open-circuit voltage and short-circuit current.[10]

The fill factor is defined as: [11]

$$FF = \frac{V_{MPP} * I_{MPP}}{V_{OC} * I_{SC}}$$

Eq.3-7

Where:

FF - Fill factor

$V_{MPP}$  - Voltage value at maximum power point

$I_{MPP}$  - Current value at maximum power point

$V_{OC}$  - Open-circuit voltage

$I_{SC}$  - Short-circuit current

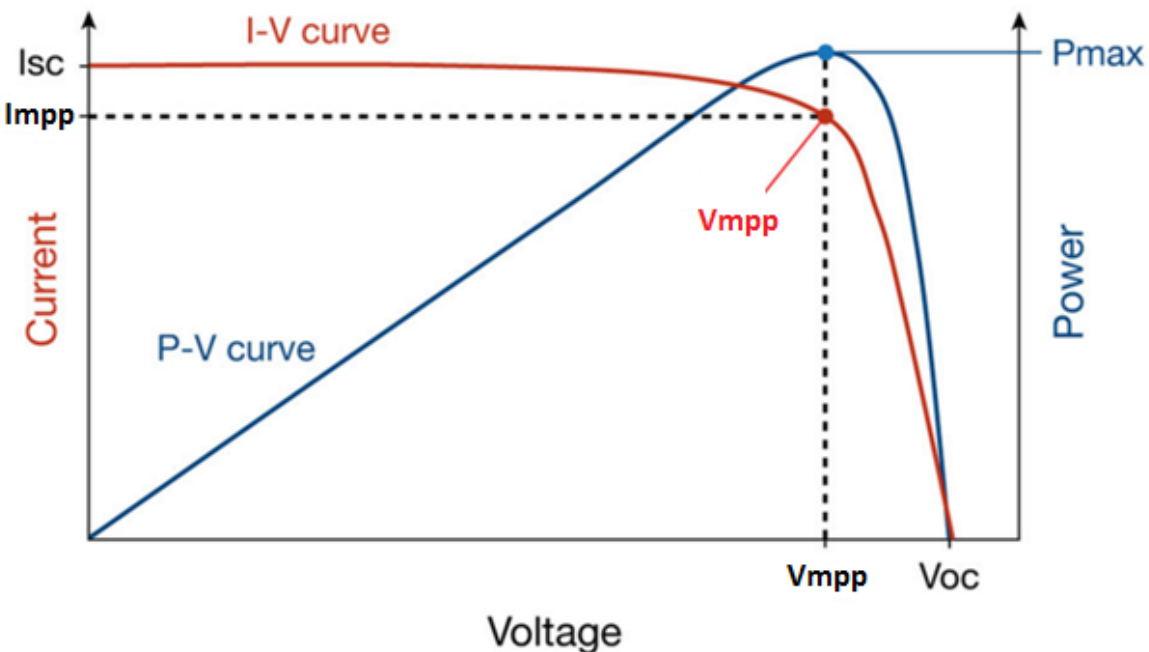


Figure 3-4: Characteristic I-V and P-V curves of a photovoltaic module [13]

The solar cell efficiency  $\eta$  can be expressed as following: [11]

$$\eta = \frac{P_{mpp}}{P_{in}} = \frac{I_{mpp} * V_{mpp}}{\text{Incident solar irradiance} * \text{Area of the solar cell}}$$

Eq.3-8

$$\eta = \frac{V_{oc} * I_{SC} * FF}{G(t) * A_{C1}}$$

Eq.3-9

Where:

$G(t)$  - Incident solar irradiance

$A_{C1}$  - Area of solar cell

$P_{mpp}$  –maximum power point

### 3.3 PV Array

A Photovoltaic array is build-up of multiple solar PV module which are wired together in order to produce the necessary amount of power that is needed for fulfilling the requirements of a house or office building. The PV modules that are constructing the PV array are producing direct current (DC) and can be firstly connected in series to achieve the desired voltage and in order to produce more current the individual strings are coupled in parallel.

There are four main factors which are playing an important role in the calculation of any photovoltaic module output. Firstly the efficiency of converting the solar energy into electricity has to be taken into account, which for the today's commercial use the efficiency is between 15%-24%. Secondly the load resistance decides where the module will operate on the curve of current and voltage (I-V). The most efficient operating point is where the maximum power can be extracted, the function of maximum power point tracking method is to move this changing operating point to the point (Pmax) where the panel produces the maximum power. [11]

In Figure 3-5 the I-V curve is represented under different temperature conditions but constant irradiance.

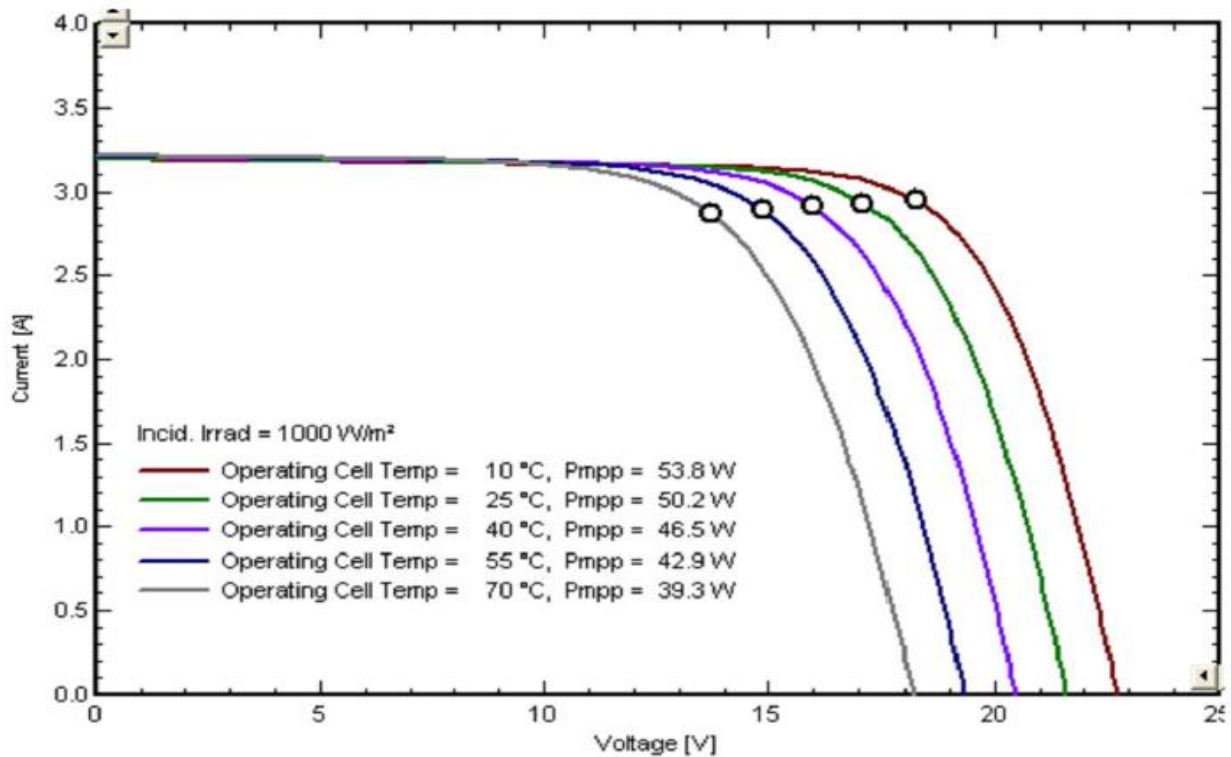


Figure 3-5: Output I-V characteristics of the PV module with different temperatures under constant irradiance [12]

The current that is generated by the solar cell is directly proportional to the solar irradiance and is not highly influenced by the temperature. One of the most affected parameters by the increase in the temperature is the open circuit voltage. While temperature is increasing the voltage is decreasing.

The voltage output of crystalline-silicon cells falls about 0.5% per degree centigrade temperature grows. For that reason the module are more efficient in areas where the outside temperatures are moderate and the person who is mounting the PV module will leave enough space behind the module in order to allow the air to circulate for cooling the panel.

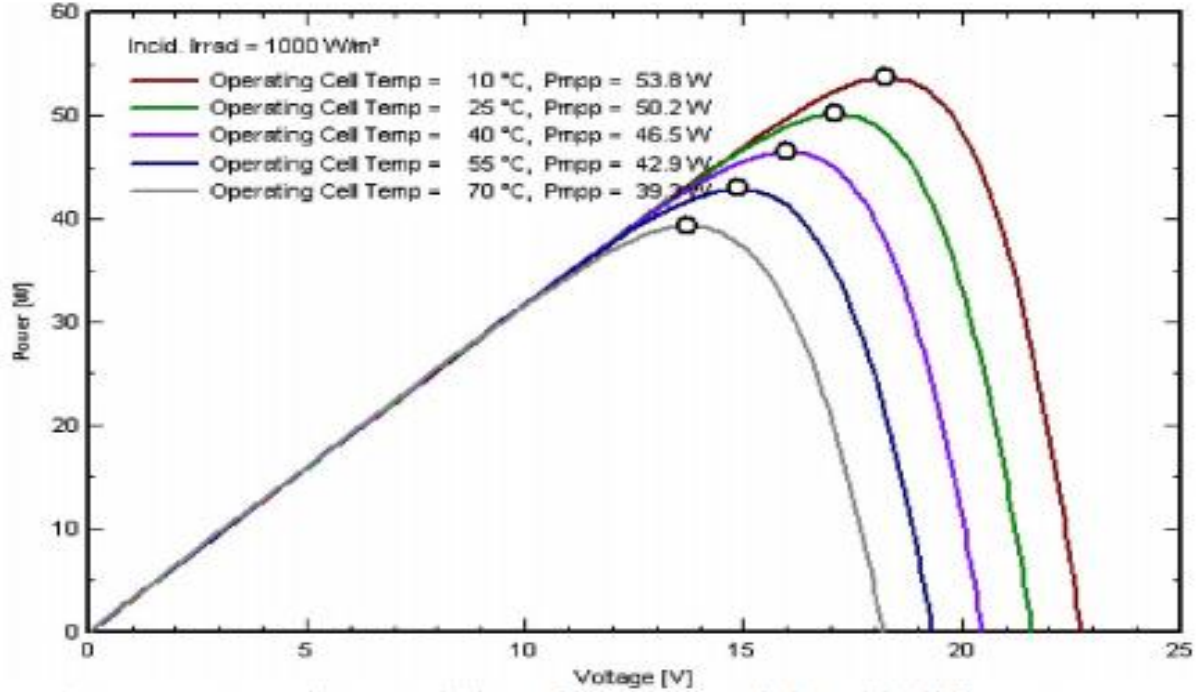


Figure 3-6: The effect of temperature on the P-V characteristic of PV module under constant irradiance [12]

In figure 3-6 it is shown the effect of temperature on the P-V characteristic of the PV module under constant irradiance (STC irradiance  $1000\text{W}/\text{m}^2$ ). As the cell temperature is increasing from  $10\text{ }^\circ\text{C}$  up to  $70\text{ }^\circ\text{C}$  the power is decreasing from  $53.8\text{W}$  to  $39.3\text{W}$ . As already mentioned the current is not highly influenced by the temperature but on the other hand, the voltage is directly influenced by the temperature.

The common configuration for the solar PV panels is a series connection with 30 to 36 cells. Each cell is transforming into electricity around  $0.5\text{ V}$  so in total the panel can deliver  $15\text{V}$  to  $18\text{V}$  depending on the configuration. The modules are design to charge  $12\text{V}$  batteries, but without a control method they will not charge the battery completely. The produced current of a PV cell is around  $2\text{A}$  to  $3\text{A}$  depending on the manufacture and because of the series configuration the same amount of current is flowing through all the cells.

### 3.5 Matlab- Simulink Model of Photovoltaic module

For the Simulation part of the Photovoltaic module the PV block from the Simscape library was used and the configuration of the Panel was modified in respect with the desired output power.

**Table 1. Solar Module Datasheet [Solar Panel Model: Soltech 1STH-215-P]**

Specifications Details	Values
Maximum Power ( $P_{max}$ )	213.15 W
Open Circuit Voltage ( $V_{oc}$ )	36.3 V
Short Circuit Current ( $I_{sc}$ )	7.84 A
Maximum Power Voltage ( $V_{mpp}$ )	29 V
Maximum Power Current ( $I_{mpp}$ )	7.35 A
Temperature coefficient of $V_{oc}$ (%/deg. C)	-0.38
Temperature coefficient of $I_{sc}$ (%/deg. C)	0.065

After understanding the behavior of a Photovoltaic panel under different irradiance and temperatures a small simulation experiment was conducted for a better understanding of the system behavior under different changes in irradiance. The first part of this simulation was to perform a manual MPP tracking under different level of irradiance and constant temperature.

The module was connected to a resistive load and by varying the load resistance from 0.5 ohms to 13 ohms the maximum power point of the module was found. A current measurement block was connected in series in order to measure the current produced by the panel and for the voltage measurement a voltage measurement block was connected in parallel to the PV output. Four different irradiance level where tested and the measurements values where wrote down in an Excel file and then I-V curves and P-V curves for all four irradiance levels where plotted on the same graph.

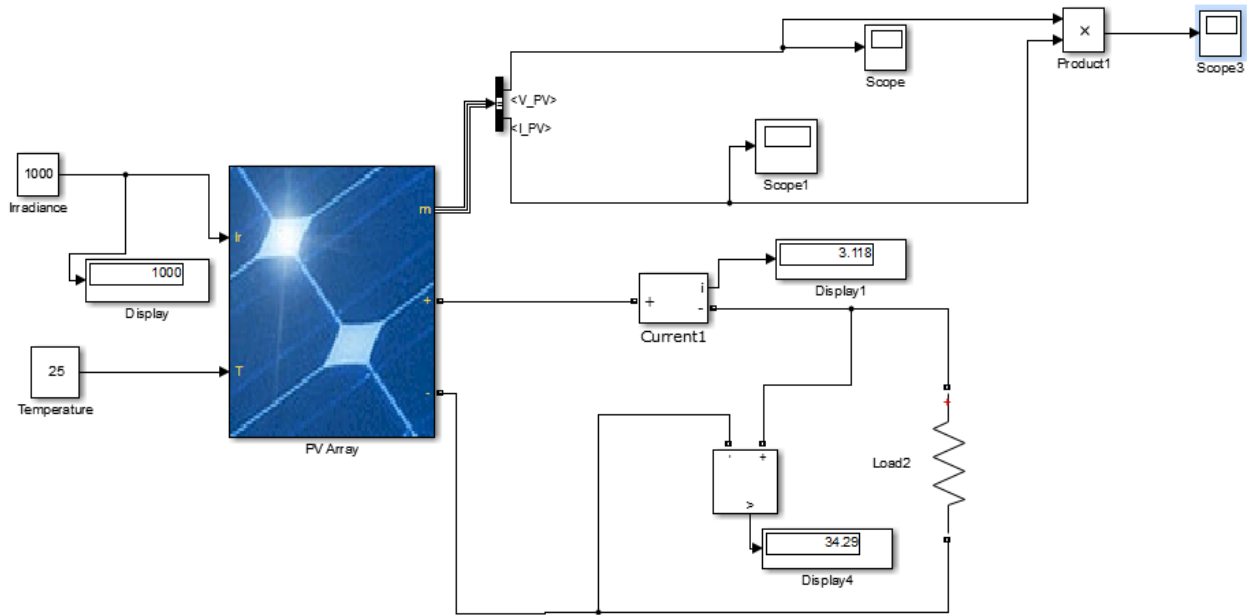


Figure 3-7: PV module and the load simulation for manual MPP

After changing the resistance load values for each irradiance case, the following I-V curves were plotted.

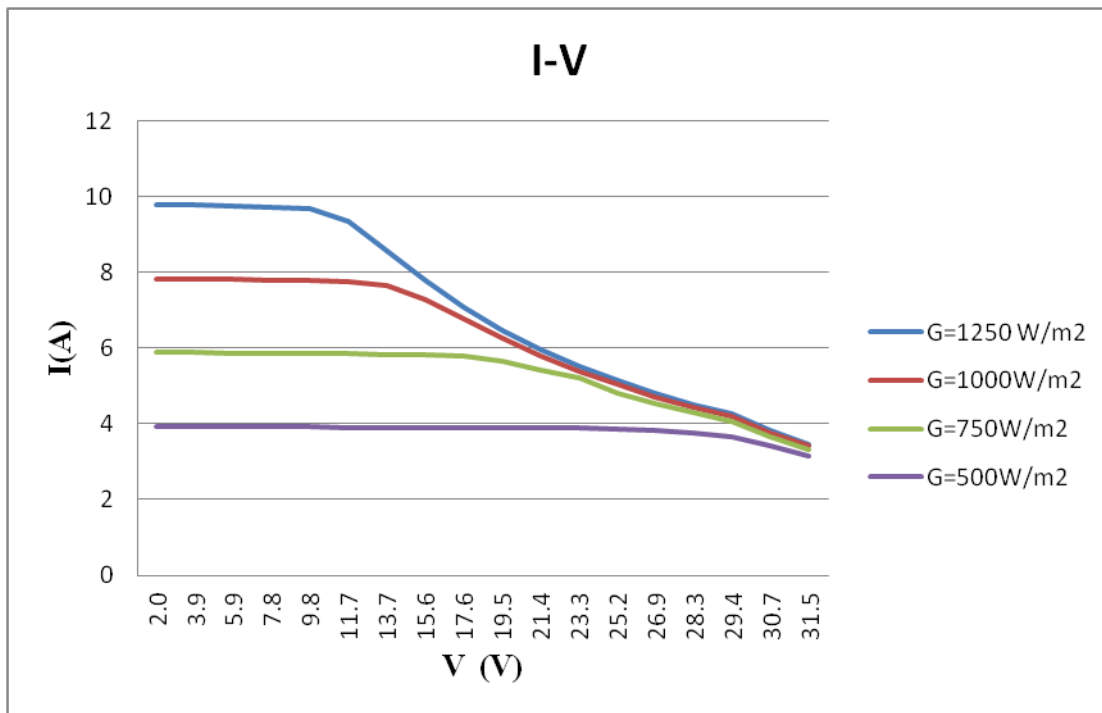


Figure 3-8: I-V curve for different irradiance levels

Different illuminations are changing the values of the short circuit current of the PV module. With a low irradiance value we expect a decreasing in the short circuit current, which will shift the curve further down to the X-axis. The magnitude of the current output from a PV module depends directly on the solar irradiance and can be increasing by connecting solar cells in parallel or by increasing the irradiance level.

In the case when the irradiance level is bigger than the standard test condition one, therefore we will observe an increasing in the short circuit current value and the curve it will shifted up.

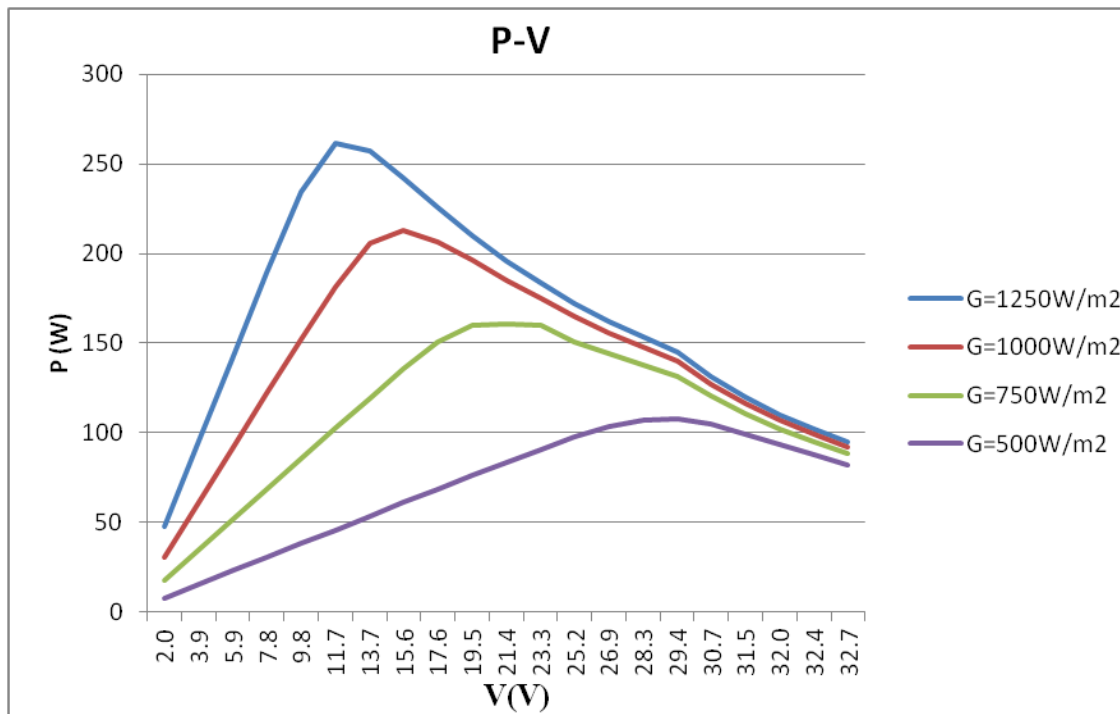


Figure 3-9: P-V curve for different irradiance levels.

Because the power is a function of the current and voltage, we are expecting that the maximum power point it will also shifted to a lower value. For the irradiance values lower than the standard test condition value 1000W/m<sup>2</sup> the P-V curves are shifted down, and different operating points were manual founded. The operating point for each irradiance level was found with the same procedure, namely by varying the load resistance from 0.5 ohms to 13 ohms. Because the current is influenced directly by the incident light, the P-V curve it will be also shifted up, above the reference value of the P-V curve.



### 3.6 Electrical characteristics PV module Simulink

In the table below the electrical characteristics of the PV module used for the simulation part are shown. The solar panel type is a 90 W mono crystalline module.

**Table 2. Electrical characteristics of PV Module [Solar Panel Model: JTM90-36M ]**

Specifications Details	Values
Maximum Power ( $P_{max}$ )	90 W
Open Circuit Voltage ( $V_{oc}$ )	22.5 V
Short Circuit Current ( $I_{sc}$ )	5.3 A
Maximum Power Voltage ( $V_{mpp}$ )	18 V
Maximum Power Current ( $I_{mpp}$ )	4.99A
Temperature coefficient of $V_{oc}$ (%/deg. C)	-0.38
Temperature coefficient of $I_{sc}$ (%/deg. C)	0.065
Cells	36

The I-V and P-V curves for the module are shown in the following graphs. Also the maximum power point can be seen on the graphs.

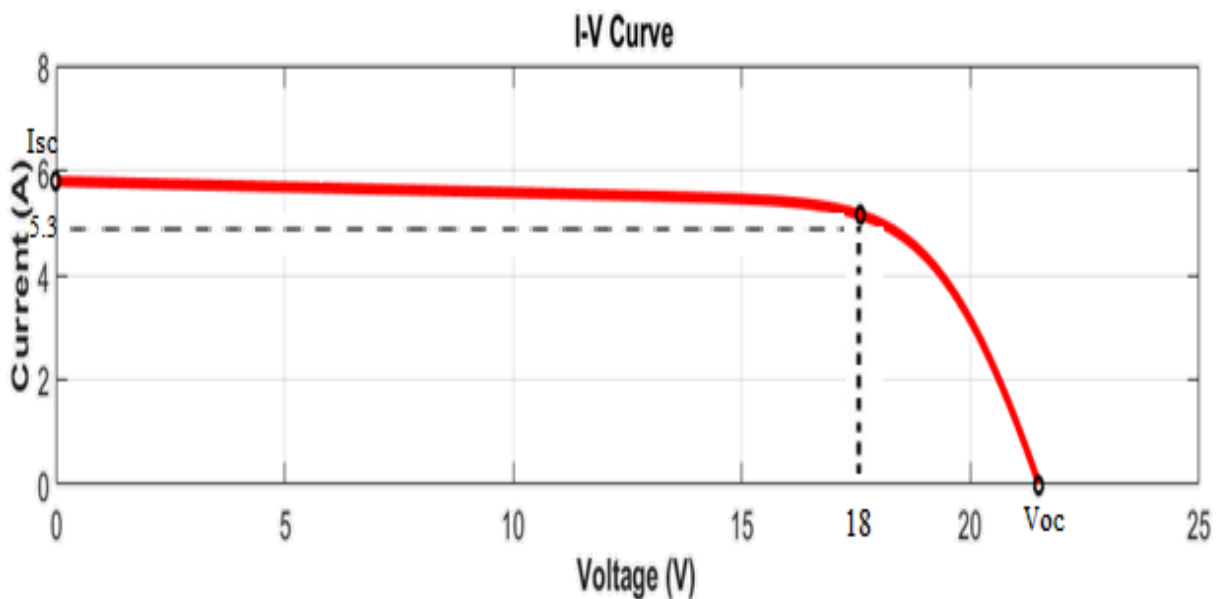


Figure 3-10: I-V curve characteristic

Some of the important parameters of the PV panel are define below:

- Short-Circuit Current,  $I_{sc}$

When the voltage over the terminals is equal with zero, a short-circuit current can be measured. The short-circuit current can be define as the maximum value of the photo generated current in the PV module. It is pictured in the upper left corner in the Fig.15.

- Open-Circuit Voltage,  $V_{oc}$

If no current flows through the external circuit, the open-circuit voltage can be measured and is representing the maximum voltage of the PV module. The open-circuit voltage is illustrated in the bottom right corner in the Fig 15.

- Maximum Power Point,  $M_{pp}$

A PV module can have a single maximum power point under fixed irradiance and temperature, which is representing the maximum possible output power that can be extracted. Some of the literature are defining the maximum power point as the operating point of the PV module. The  $M_{pp}$  is illustrated below in the Figure 15. [16]

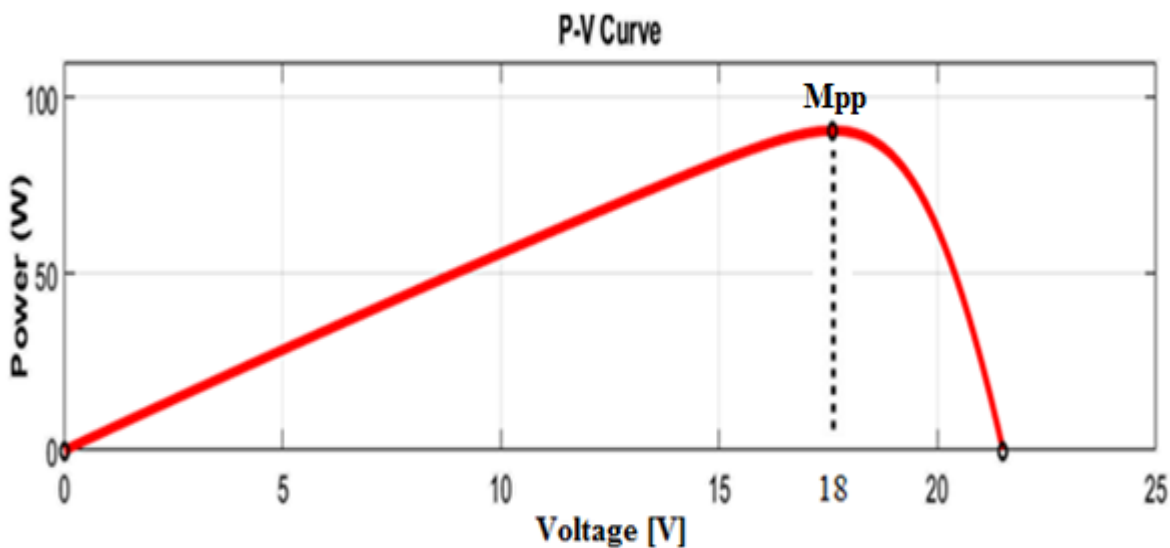


Figure 3-11: P-V curve characteristic

## 4. The Boost Converter

The boost converter is used to step-up the voltage from a low voltage level to a high voltage level. From the equation of power, we know that  $P = \text{voltage (V)} \times \text{current (I)}$ , in case that the output voltage will raise, the output current is necessary to decrease.

A DC boost converter can be supplied from many sources such as DC voltage sources, batteries, fuel cells. The working principle of the converter is to frequently opening and closing an electronic switch. Two operation modes of the converter will be presented in the following chapter.

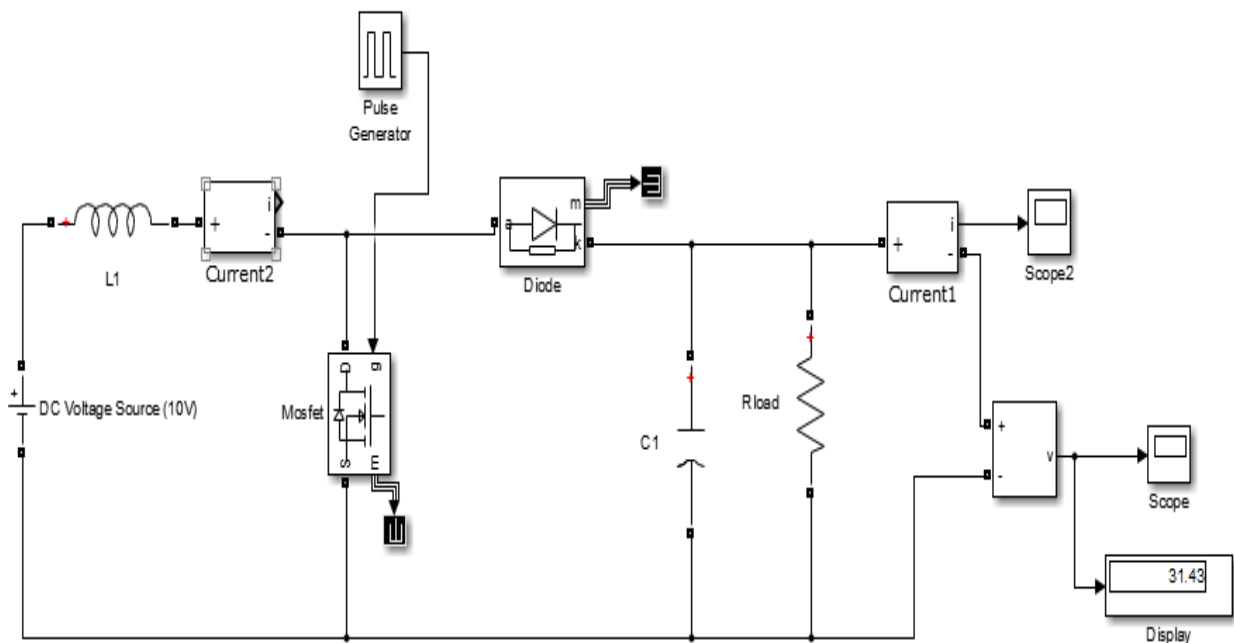


Figure 4-1: The boost converter Simulink circuit with a DC voltage source

In the Figure 4-1 an equivalent circuit of a DC-DC boost converter is shown. The circuit was built in Simulink, and the input source is a constant 10V DC voltage source. Other components such as an inductor, capacitor, diode and a MOSFET transistor are used in order to build the convert. The input for the transistor is a pulse generator signal with a frequency of 10 kHz and a pulse width of 70%. A 50 ohms resistance is considered the load of the system.

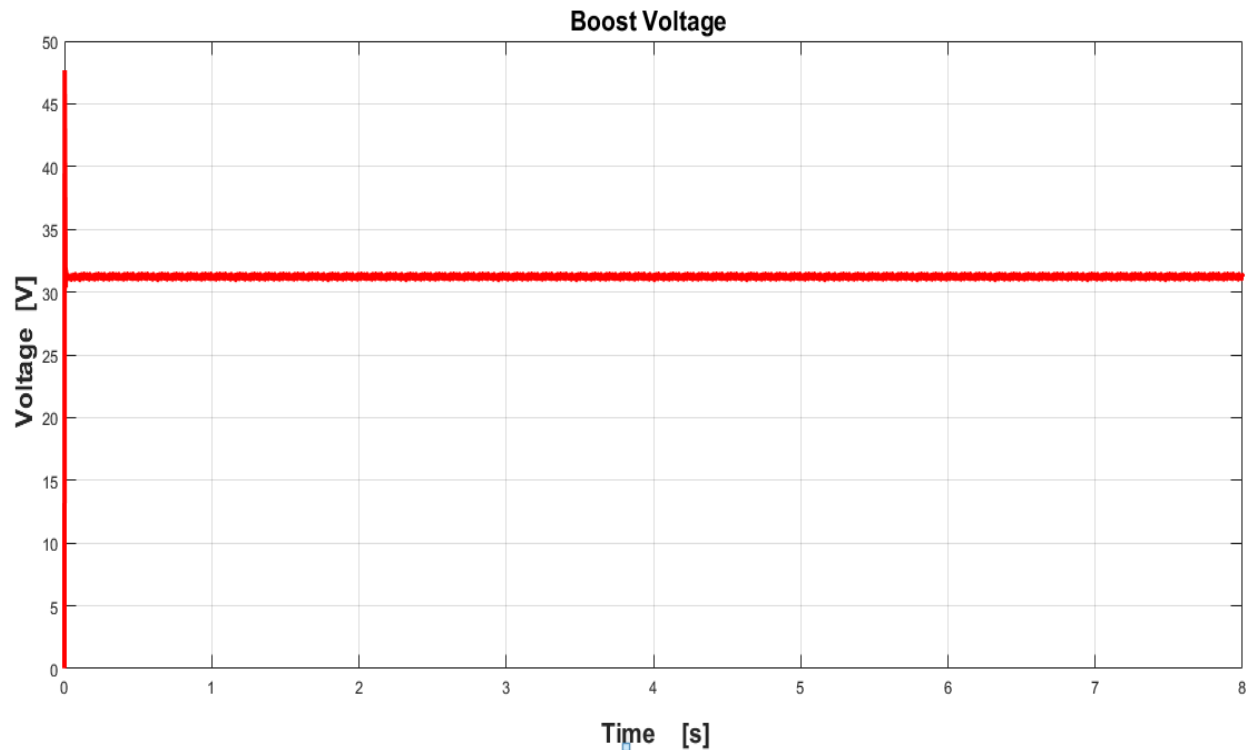


Figure 4- 2: The output voltage is boosted and the converter is working as expected.

The converter is boosting the voltage from 5V to 23.8V and in the case of the current, the input current will be higher than the output current. The input current can be calculated from the Eq.4 assumed that we know the desired output boosted voltage, the load current, the efficiency and the peak to peak ripple current values.

$$I_{in} = I_{out} * \left( \frac{V_{out}}{V_{in}} \right) * \frac{1}{\eta} + \frac{\Delta I_L}{2}$$

Eq.4-1

The power out of the boost converter is equal with the input power multiplying with losses, and the losses are expressed by the efficiency factor  $\eta$ .

$$P_{in} = \frac{P_{out}}{\eta}$$

Eq.4-2

In the design process of the boost converter, each component of the converter has to be chosen carefully in order to satisfy the system requirements. The MOSFET transistor has to be able to operate with currents bigger than the input current from the Eq.4-1.

When you are searching for the transistor, the maximum rated voltage at which the transistor is working is a very important limitation. The value of the maximum rated voltage can be found in the datasheet and paying attention to this limitation can prevent a possible damage of the MOSFET.

The maximum duty ratio at which the converter can operate is another important practical limitation, which has to be taken into account.

The duty ratio can be defined as following:

$$D = 1 - \frac{V_{in}}{V_{out}}$$

Eq.4-3

The value for the maximum duty cycle can be determined from the below equation Eq.4-02. Each boost converter has a maximum duty cycle, above which the regulator will not be able to work as a boost. [15]

$$D = \frac{V_{in} - I_{out} * [R_1 + R_2 + 2 * R_L]}{V_{in} + I_{out} * [R_1 - R_2]}$$

Eq.4-4

Where:

$R_1$  - Parasitic resistance of inductor

$R_2$  - Parasitic resistance of transistor

$R_L$  - Load resistance

## 4.1 Closed switch operation of the Boost converter

In this chapter the closed switch operation of the Boost converter will be discussed in detail. When the gate of the MOSFET transistor used in the Simulation is closed, the diode is reversed (like an open circuit). Applying Kirchoff's voltage law in the loop including the source, the inductor and the MOSFET transistor. The voltage across the inductor is equal in this case to the voltage source. [14]

$$v_L = V_s = L * \frac{di_L}{dt} \quad \text{Or} \quad \frac{di_L}{dt} = \frac{V_s}{L}$$

Eq. 4-5

Where:

$v_L$  - Voltage across the inductor

$V_s$  - Source voltage

$L$  - Inductor

$i_L$  - Inductor current

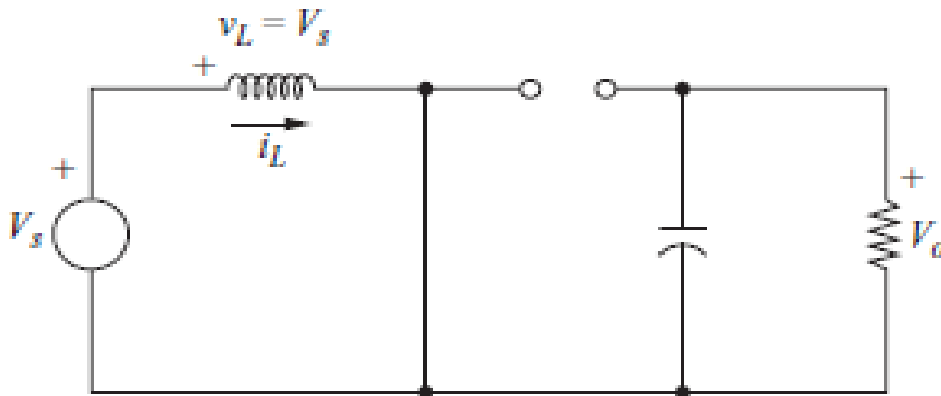


Figure 4- 3: Equivalent circuit for the switch is closed [14]

From the above figure of the equivalent circuit for the closed switch can be stated that the rate of change in current is constant and as a consequence the current raises linearly during the time that the switch is closed. The change in inductor current can be calculated as following:

$$\frac{\Delta i_L}{\Delta t} = \frac{\Delta i_L}{D \cdot T} = \frac{V_s}{L}$$

Eq. 4-6

Where:

D - Duty cycle

T - Switching period

From the Eq. 4-6 the  $\Delta i_L$  can be computed as following:

$$(\Delta i_L)_{closed} = \frac{V_s \cdot D \cdot T}{L}$$

Eq.4-7

Where:

$\Delta i_L$  - Inductor current ripple

When the switch is in closed operation mode, the inductor will store energy in the inductor in the form of a magnetic field. We have some amount of current flowing through the inductor and some amount of energy stored in the inductor.

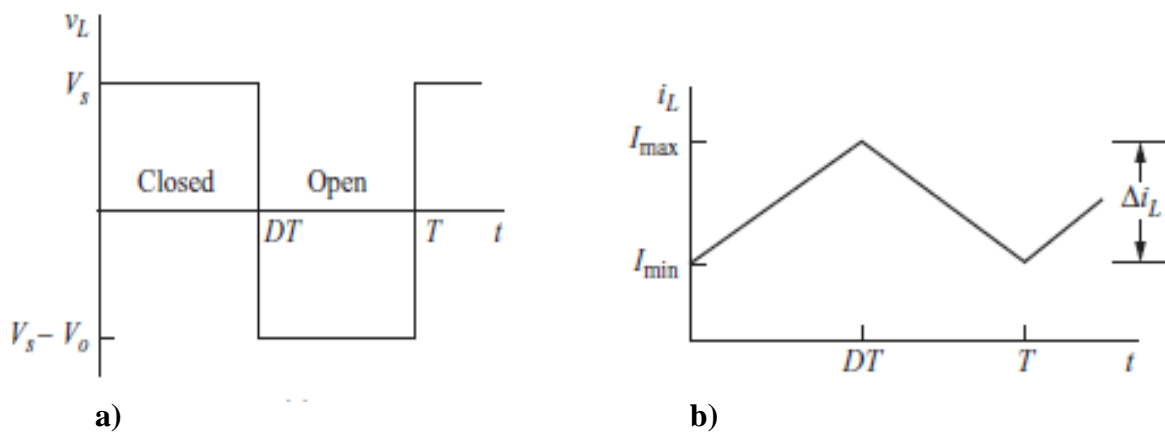


Figure 4- 4: Boost converter waveform a) Inductor voltage b) Inductor current [14]

## 4.2 Open switch operation of the Boost converter

At the time when the switch is opened, since the inductor current cannot change immediately, the diode turns into a short circuit or so called forward-biased in order to allow the inductor current to flow through. Energy gets transferred from the inductor to the output capacitor. [14]

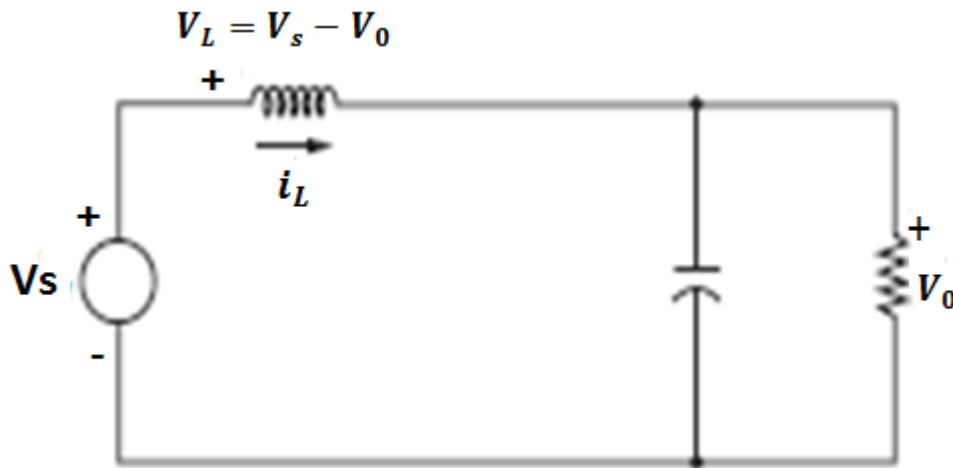


Figure 4- 5: Equivalent circuit for the switch is open [14]

Making the assumption that the output voltage  $V_0$  is constant, applying Kirchhoff's voltage law, the voltage across the inductor can be founded:

$$V_L = V_s - V_0 = L * \frac{di_L}{dt}$$

Eq.4-8

The above equation can be rearranged and written as:

$$\frac{di_L}{dt} = \frac{V_s - V_0}{L}$$

Eq.4-9

Where:

$V_s$  - Source voltage

$V_0$  - Output voltage



As in the previews mode operation, the rate of change of inductor current is a constant, but in this case the sloop is negative and the current is changing linearly. The equation for the change in inductor current of the open switch mode is expressed below:

$$\frac{\Delta i_L}{\Delta t} = \frac{\Delta i_L}{(1-D)T} = \frac{V_s - V_0}{L}$$

Eq.4-10

Solving the Equation 4-10 for  $\Delta i_L$  -inductor current ripple the following equation can be solved:

$$(\Delta i_L)_{open} = \frac{(V_s - V_0)(1-D)T}{L}$$

Eq.4-11

Using the Equations. 4-7 and Eq. 4-11 for the condition of steady-state operation, the net change in inductor current must be equal to zero:

$$(\Delta i_L)_{closed} + (\Delta i_L)_{open} = 0$$

Eq.4-12

$$\frac{V_s * D * T}{L} + \frac{(V_s - V_0)(1-D)T}{L} = 0$$

Eq.4-13

Solving the Equation 4-13 for  $V_0$

$$V_s(D + 1 - D) - V_0(1 - D) = 0$$

Eq.4-14

$$V_0 = \frac{V_s}{1-D}$$

Eq.4-15

From the Equation. 4-15 we can state that the output voltage is the ratio between input voltage and (1- duty cycle).

The duty cycle can takes values between zero and one, and in the case that the switch is kept always open, the value of the duty cycle is equal to zero and solving Eq.4-15 it is found that the output voltage in this case is the same with the input voltage.

By increasing the duty cycle, the denominator of the Eq.4-15 is becoming smaller, and that is conducting to the rise of the output voltage.

For the computation of the average current passing the inductor, will start with the supposition that the average power provided by the source will be equal with the average power absorbed by the load resistor. The output power can be calculated as: [14]

$$P_0 = \frac{V_0^2}{R} = V_0 * I_0$$

Eq.4-16

Where:

$P_0$ - Output power of the boost converter

$R$  - Load resistance

$V_0$  - Output voltage

$I_0$  - Output current

The input power can be defined as:

$$V_S * I_S = V_S * I_L$$

Eq.4-17

By equating the Eq.4-16 and Eq.4-17 and by applying the formula for the output voltage from Eq.4-15 the following equation resulting: [14]

$$V_s * I_L = \frac{V_0^2}{R} = \frac{[V_s/(1-D)]^2}{R} = \frac{V_s^2}{(1-D)^2} * R$$

Eq.4-18

The next step is to solve the above equation for the average inductor current and after making different replacements, the expression for  $I_L$  can be written in the following form:

$$I_L = \frac{V_s}{(1-D)^2 * R} = \frac{V_0^2}{V_s * R} = \frac{V_0 * I_0}{V_s}$$

Eq.4-18

In order to calculate the maximum and minimum inductor currents, firstly the values for the average inductor current has to be calculated. Second step will be the use of Eq.4-7, where the values for  $I_{L,max}$  and  $I_{L,min}$  can be found as following:

$$I_{L,max} = I_L + \frac{\Delta i_L}{2} = \frac{V_s}{(1-D)^2 * R} + \frac{V_s * D * T}{2L}$$

Eq.4-19

$$I_{L,min} = I_L + \frac{\Delta i_L}{2} = \frac{V_s}{(1-D)^2 * R} - \frac{V_s * D * T}{2L}$$

Eq.4-20

Where:

$I_{L,max}$ - Maximum inductor current

$I_{L,min}$  - Minimum inductor current

The output voltage Eq.4-15 was founded starting from the assumption that the inductor current is continuous, and that is implying that the current is always positive. Under the condition of continuous inductor current, the minimum value of the inductor can be found from the Eq. 4-20. [14]

In the next equation the boundary between continuous and discontinuous inductor current can be expressed as following:

$$I_{L,min} = 0 = \frac{V_s}{(1-D)^2 * R} - \frac{V_s * D * T}{2 * L} \quad \text{Eq.4-21}$$

$$\frac{V_s}{(1-D)^2 * R} = \frac{V_s * D * T}{2 * L} = \frac{V_s * D}{2 * L} \quad \text{Eq.4-22}$$

From Eq.4-22 the minimum value of the inductor current can be found solving the equation in respect with the variable L:

$$L_{min} = \frac{D * (1-D)^2 * R}{2 * f} \quad \text{Eq.4-23}$$

In order to provide a margin to ensure continuous-current operation the actual value of the inductor will be higher than the  $L_{min}$  value.

In the design process of a boost converter is often favorable to define L in terms of a desired  $\Delta i_L$  as following: [14]

$$L = \frac{V_s * D * T}{\Delta i_L} = \frac{V_s * D}{\Delta i_L * f} \quad \text{Eq.4-24}$$

Where:

$L_{min}$  - Minimum inductor current

$L$  - Inductor current

$f$  - Switching frequency

$\Delta i_L$  - Inductor current ripple

## Output Voltage Ripple

The previous equations were defined under the hypothesis of constant output voltage, meaning an infinite capacitance. The effect of such a capacitance can be seen in the output voltage fluctuation or ripple.

The change in capacitor charge can be found from the following expression:

$$|\Delta Q| = \left(\frac{V_0}{R}\right) * D * T = C * \Delta V_0$$

Eq.4-25

If we solve the equation 4-25 in respect to the voltage ripple the next equation can be found:[14]

$$\Delta V_0 = \frac{V_0 * D * T}{R * C} = \frac{V_0 * D}{R * C * f}$$

Eq.4-26

$$\frac{\Delta V_0}{V_0} = \frac{D}{R * C * f}$$

Eq.4-27

Where:

$\frac{\Delta V_0}{V_0}$  - Output voltage ripple

$R$  -resistance

The capacitance can be calculated from the Eq.4-26 and the expression is given as following:

$$C = \frac{D}{R * \left(\frac{\Delta V_0}{V_0}\right) * f}$$

Eq.4-28

The equivalent series resistance of the capacitor has an important influence on the output voltage ripple. The voltage ripple of the equivalent series resistance can be found with the help of the next expression: [14]

$$\Delta V_{0,ESR} = \Delta i_c * r_c = I_{L,max} * r_c$$

Eq.4-29

Where:

$\Delta V_{0,ESR}$  - Output voltage ripple due to capacitor equivalent series resistance

$I_{L,max}$  - Maximum inductor current

$r_c$  - Equivalent series resistance

## 5. Maximum Power Point Tracking Algorithm

### 5.1 MPPT main characteristics

The maximum power point tracking algorithm has the purpose of extracting the maximum power from the photovoltaic module and transmit the maximum power to the load.

During a day under different irradiance conditions, different maximum power points can be observed. If the Photovoltaic module is connected straight to a load, the operating point is seldom the maximum power point. Even in the case when a battery is connected directly to solar module, the panel is not working at his maximum power point and the battery can be damaged.

The connection of the panel directly to the battery without of a MPPT means that the module is forced to operate at battery voltage, which is in most of the cases lower than the maximum operating voltage. In order to overcome this power losses, a maximum power point tracking have to be implemented together with a power converter.

A power converter is necessary for the sake of adjusting the energy flow from the PV array to the load. For this project a boost converter was used to track the maximum power point of the array.

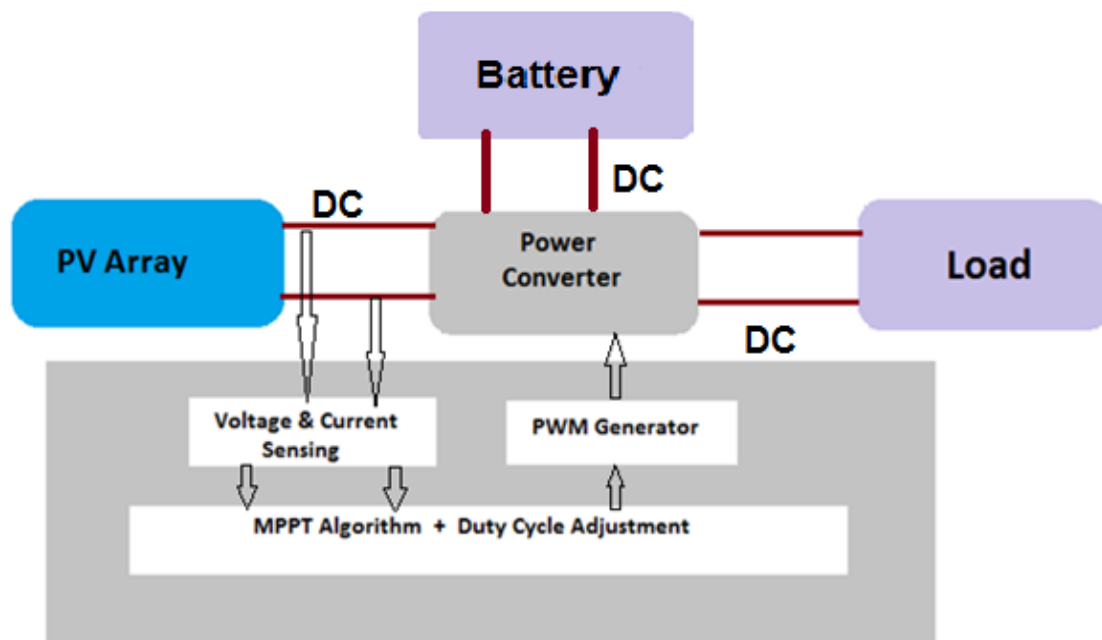


Figure 5- 1: System schematic PV array-MPPT-Load [17]

In the figure 5-1 it is shown the system schematic of the simulated model. As the panel is operating, the voltage and current of the photovoltaic module will be sensed and the corresponding power will be calculated. The second step is to determine if you want to move up or down on the duty cycle of the converter in order to adjust the maximum power. Different maximum power point algorithms are used in the literature for the duty cycle calculations.

For this project the Perturb and Observe algorithm was used, and the main idea of the algorithm consists in the increase or decrease of the duty cycle based on the comparison of the powers.

## 5.2 Perturb and Observe MPPT algorithm

The perturb and observe (P&O) algorithm is the most well-known maximum power point tracking algorithm which is suitable for any photovoltaic system. As described above the algorithm is used for finding the maximum power point. A PV module has a single maximum power point under constant irradiance and temperature and the P-V curve is described by a parabolic function.

Supposing that the operating voltage of the photovoltaic module is perturbed and whether the power produced by the PV array is increasing, the operating point has been driven toward the MPP. In this particular case the operating voltage has to be perturbed in the same direction.

If the power produced by the PV module is decreasing, as a consequence the operating point has been driven away from the MPP. In this case, the direction of the perturbed operating voltage has to be reversed. In this manner, the operating point of the PV module will progressively reach the maximum power point and will fluctuate around it. A detailed visualization of the P-V curve can be seen in the figure 5-2

In the simulation part of the algorithm, a fixed step change (Increment value used to increase/decrease the duty cycle  $D$ ) was used for each perturbation.

For a better efficiency a dynamic step value can be used, but that requires more knowledge in the specific MPPT algorithms for PV and is beyond the scope of this thesis. [18]



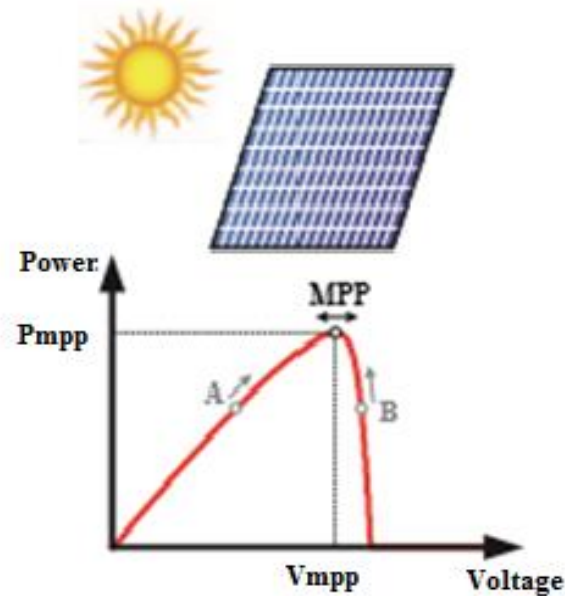


Figure 5-2: P-V characteristic with MPP [19]

One of the main reasons for choosing the Perturb and Observe (P&O) algorithm instead of other well-known was that this method is suitable for any PV module, doesn't need any knowledge about the PV array and works fairly well under different environmental conditions. Another advantage of this algorithm is the quickly implementation on digital controllers.

There are also some disadvantages of P&O algorithm which will be highlighted below. In the first instance after finding the operating point its keeps fluctuating around the MPP and a small amount of energy is wasted. Another drawback is that this algorithm has a poor performance in case of the rapidly changing of irradiance level and the probability to track the MPP in the wrong way. [16]

For a better understanding of the algorithm, one can take a look at the flow chart of the Perturb and Observe algorithm which can be seen below in the figure 5-3.

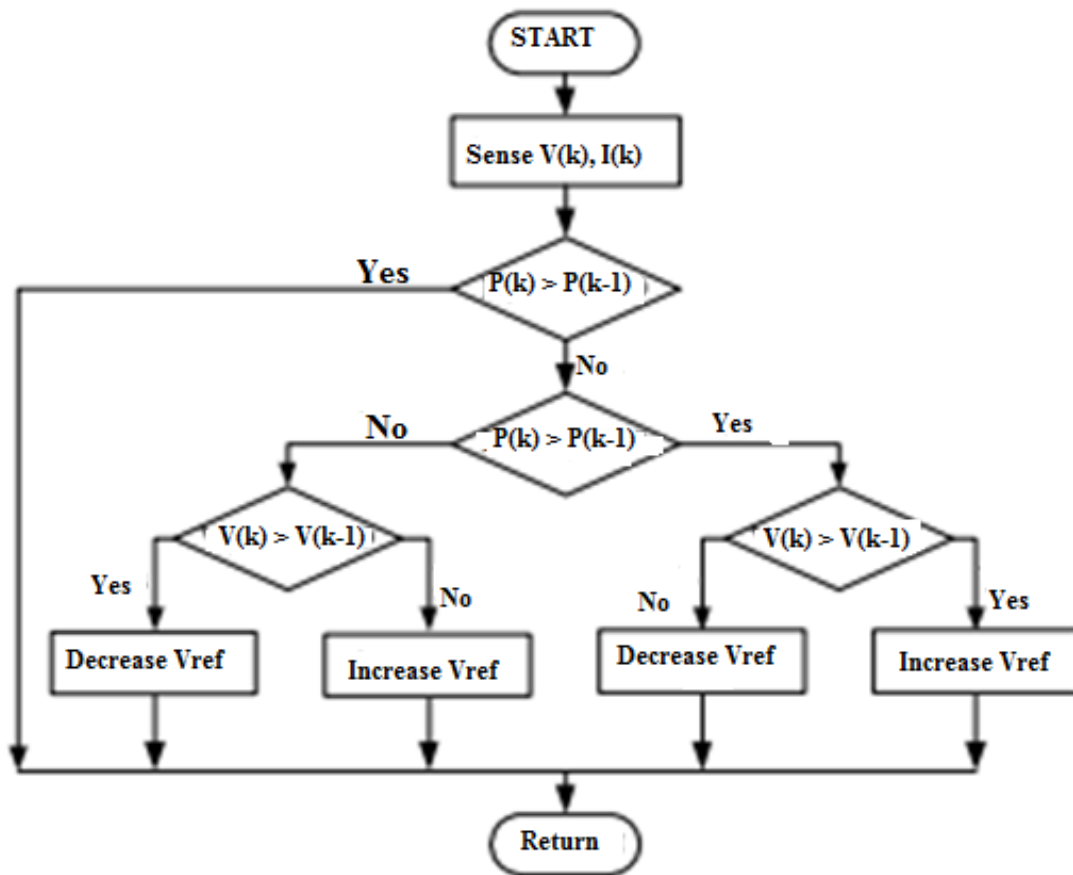


Figure 5- 3: Flow chart Perturb and Observe method [17]

As can be seen from the above flowchart the P&O algorithm is fairly easy to follow, transforming this into Matlab /C code inside a Simulink function. The final C code of P&O algorithm can be found in the Appendix [A. c]

## 6. Simulations and results

### 6.1 Constant Irradiance and constant Temperature without battery

After understanding the working principle of the boost converter chosen for this project, and after deciding which maximum power point tracking method is more suitable, a Simulink model was built in order to simulate different environmental conditions, like changing irradiance, changing temperatures.

The first model was simulated with constant irradiance and constant temperature as can be seen in the next picture. The simulation was conducted without a battery connected to the output of the system.

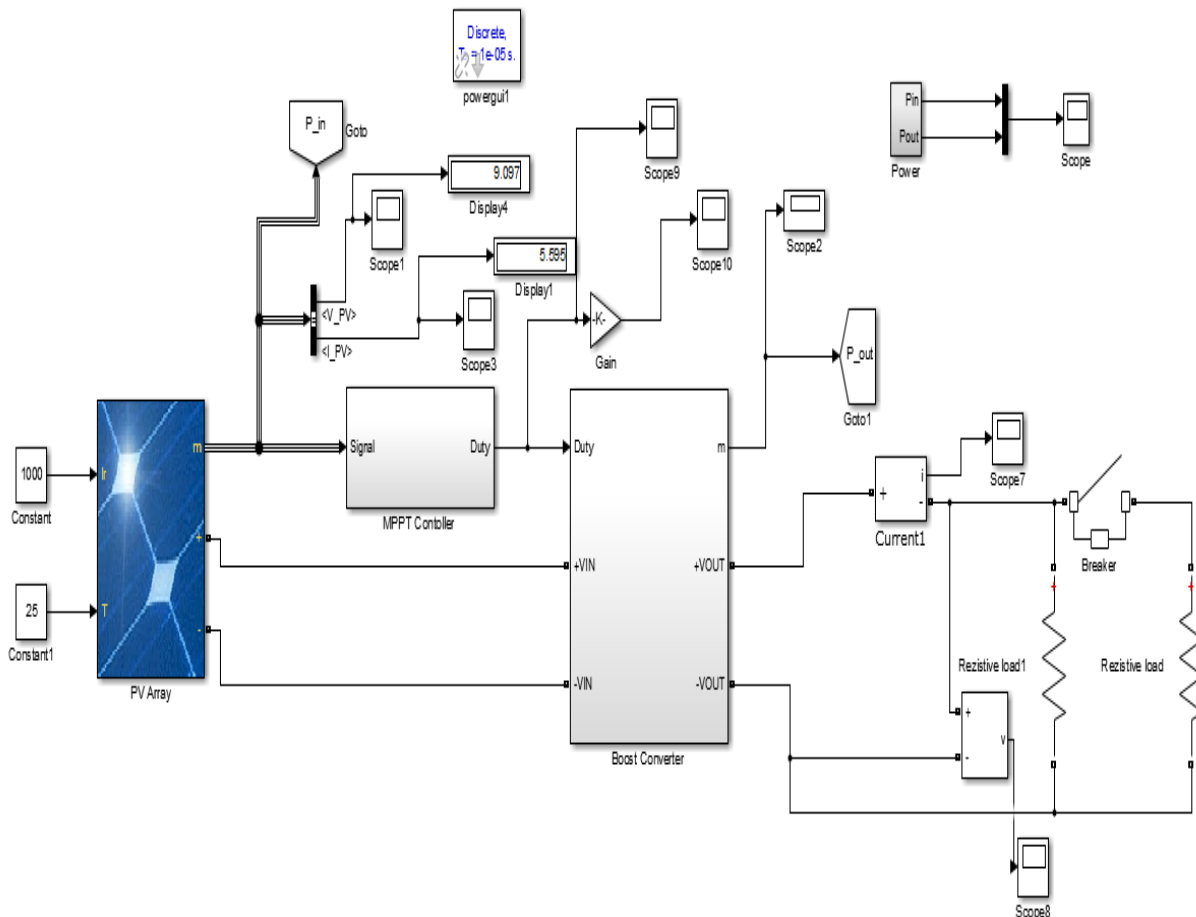


Figure 6-1: System schematic PV-MPPT-Boost converter-Load with constant irradiance and constant temperature

In the above simulation, it have been used the 90 W mono crystalline module described in figure 6-1 which is connected to a MPPT controller. The boost converter is needed to adjust the energy flow from the PV module to the load. The converter is designed to boost the voltage from the 18V the  $V_{mpp}$  value of the PV to a constant 44V the desired output voltage value. The photovoltaic electrical characteristics can be found in Chapter 3-6. The photovoltaic panel is connected to DC resistive loads but in this scenario the battery was not connected at the output of the system. The frequency chosen for the simulation was 20 KHz and the values for the inductor and capacitor of the boost converter were calculated in order to meet the design considerations. In the above simulation the module is connected to a resistive load of 25ohms. A breaker is added in the Simulink model which after 10s will added to the system another resistance which is connected in parallel with the first resistance.

In table 3 can be found the boost converter components together with their characteristics. The derived formulas and calculations can be found in Appendix [A. b]

**Table 3. Boost converter components**

Components	Characteristics
Inductor	44 $\mu$ H-11A
Capacitor	160 $\mu$ F -63V
Diode	Fast recovery rectifier diode 1N400
MOSFET	60V - 0.07 $\Omega$ - 16A
Resistive load	25 ohms –after 10s (breaker) 15ohms

Below the graphs for voltage, current, input-output power of photovoltaic panel can be found.

The 90W mono crystalline panel used for the simulations has a:

$$V_{mpp} = 18 V$$

$$I_{mpp} = 4.9A \text{ (voltage and current close to maximum power point of the PV)}$$

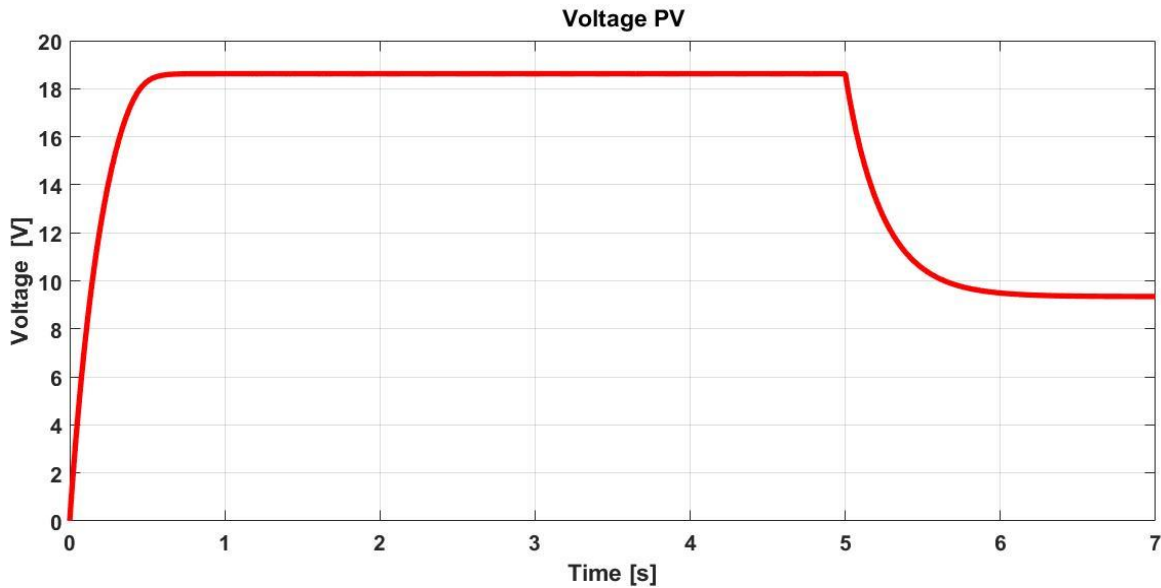


Figure 6-2: Photovoltaic voltage with breaker

As can be seen in figure 6-2 after connecting the second resistive load, the voltage is dropping from the  $V_{mpp}$  value to a smaller value of around 10V. By adding a new resistance load to the system, the value of the equivalent parallel resistance will be always smaller than any other resistance existing in the circuit. Without a battery connected to the output of the system the voltage will decrease depending on the value of the second resistance. The decrease in the voltage level will affect also the input and output power of the module. Both powers will decrease and the PV module will not operate anymore at maximum power point.

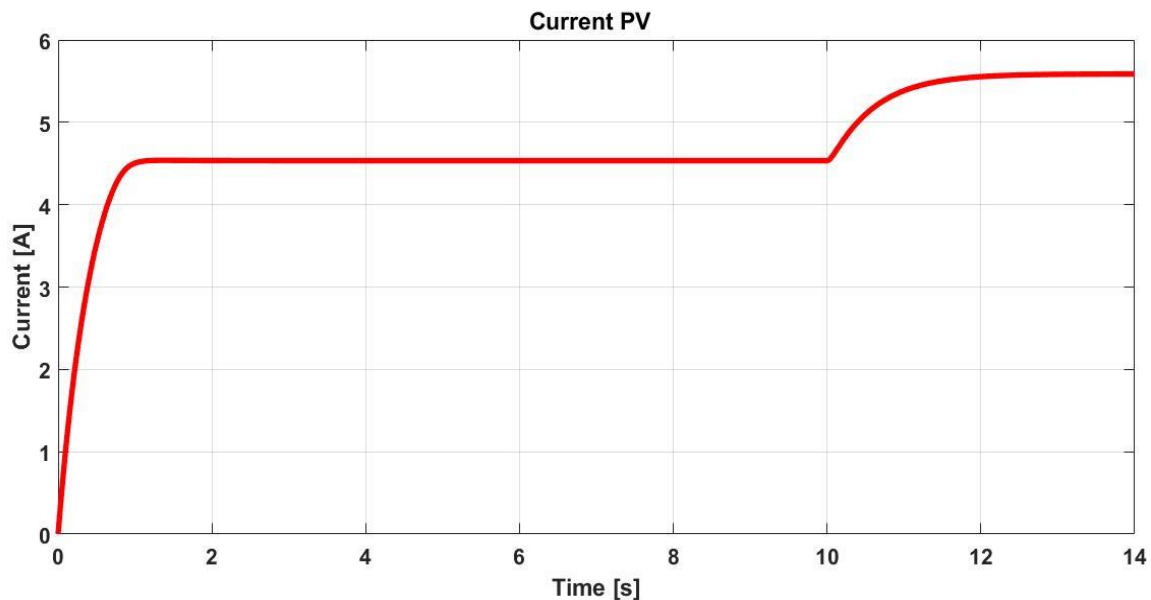


Figure 6-3: Photovoltaic current with breaker

In figure 6-3 can be seen the PV panel current graph where after lowering the load resistance at the time interval 10s the current is expecting to increase with decreasing the voltage level.

In the first 10 seconds when just 25 ohms resistance is connected as a load, the current is stable and is working around the maximum current of the module. After 10 second when the second resistance is connecting in parallel with the first resistance the voltage is decreasing as can be seen in the figure 6-2 and the current is increasing as we can see in figure 6-3.

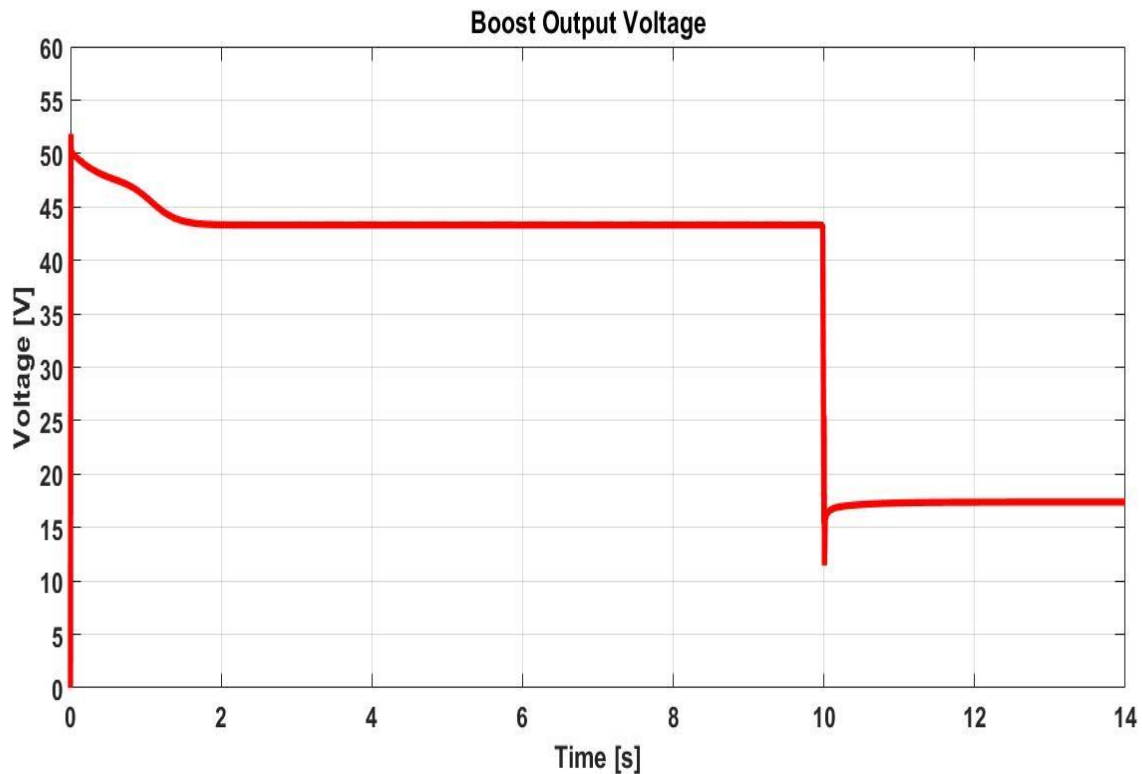


Figure 6 -4: Output Voltage of the Boost Converter

The desired output voltage of the system was chosen to be 44 Volts and in order to achieve this voltage level, a boost converter was used. The input voltage, output voltage, the load resistance value and the frequency has to be taken into account in the calculation process of the inductance and capacitance. After 10s when the breaker is opening and the second load resistance is connecting in parallel with the first load resistance, the boosted voltage has the same behavior as the PV voltage and a decrease can be observed. In order to produce the extra voltage from 18V to 44V the boost output current is expecting to drop.

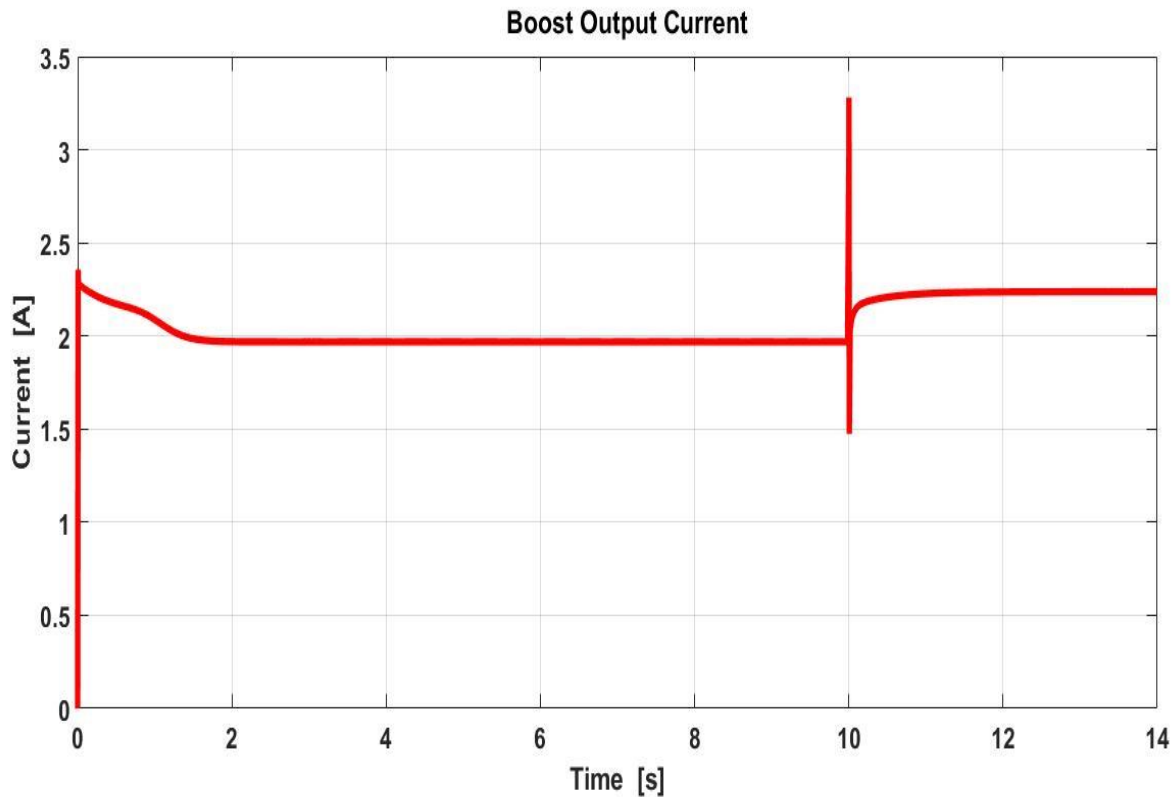


Figure 6-5: Output Current of the Boost Converter

The output current of the boost converter is dropping as expected in the first 10 second with around 2A and as we note in figure 6-5. After connecting the second resistance the current is slowly increasing and has the same behavior as the Photovoltaic current shown in figure 6-3.

The boosted voltage was achieved with the help of the MOSFET transistor which is receiving a PWM signal for opening and closing the gate of the transistor. As a consequence of the voltage rise the current is decreasing.

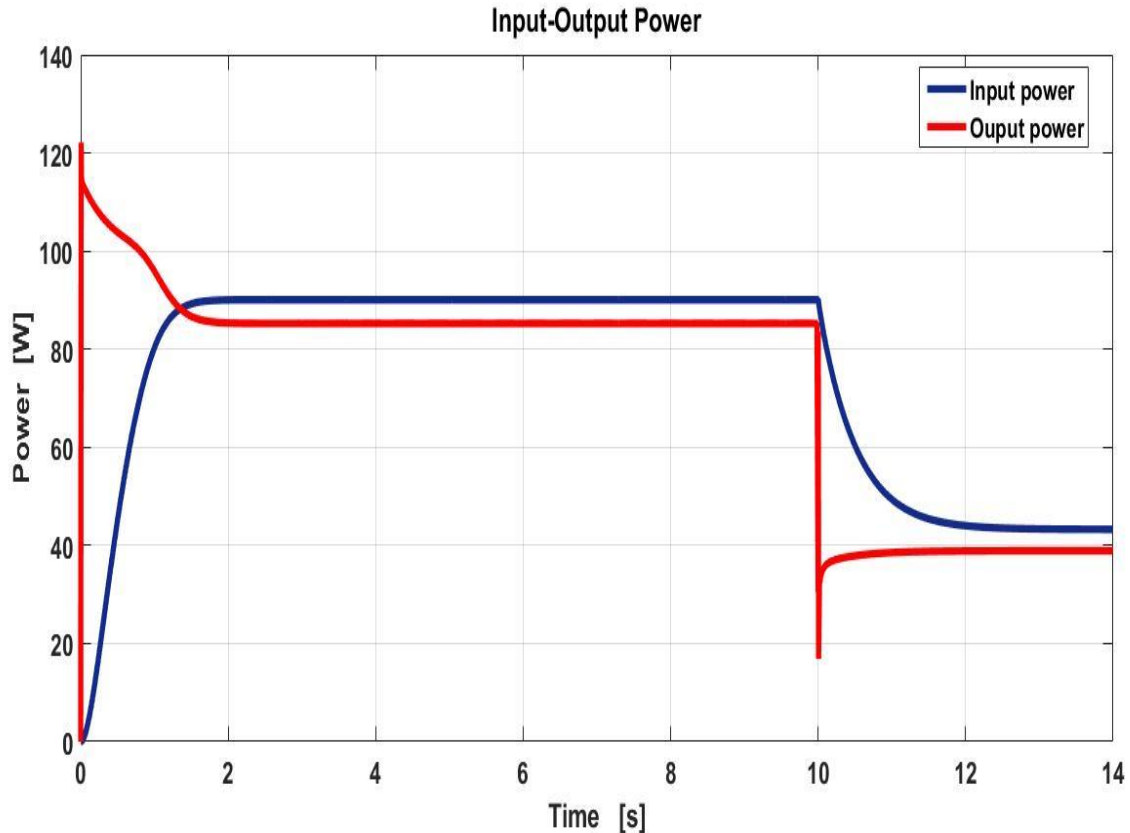


Figure 6-6: Input-Output Power under constant irradiance and temperature

The system was simulated under constant irradiance and constant temperature at standard test condition (STC) where the PV maximum power that can be extracted under this conditions is 90W. The photovoltaic module is connected to a maximum power point tracker which is using the Perturb and Observe algorithm in order to follow the maximum power point of the panel. As can be recognize in figure 6-6, the output power is following the input power with very low margins variations.

For the first 10 seconds the maximum power tracking is achieved and immediately after the breaker the power is dropping to approximately 40W because the load resistance is decreasing. More than half of the power is lost because of the load decrease and in this scenario the PV can't draw anymore the maximum available power. In a remote area where no connection to the grid is available the amount of power that is lost is influencing the overall efficiency of the PV system.

In order to overcome this problem, a battery need to be connected in parallel with the load because the MPPT charge controller is working most effective with battery connection.



The rest of the power which normally will be lost is now charged into the battery and during the night or during cloudy/rainy days the load can be supplied by the battery.

### 6.2 Constant Irradiance and constant Temperature with battery connected

The second model was simulated with constant irradiance and constant temperature as can be seen in the next picture. In this model a battery was connected on the output of the system in order to overcome the power losses problems presented in the first simulated model.

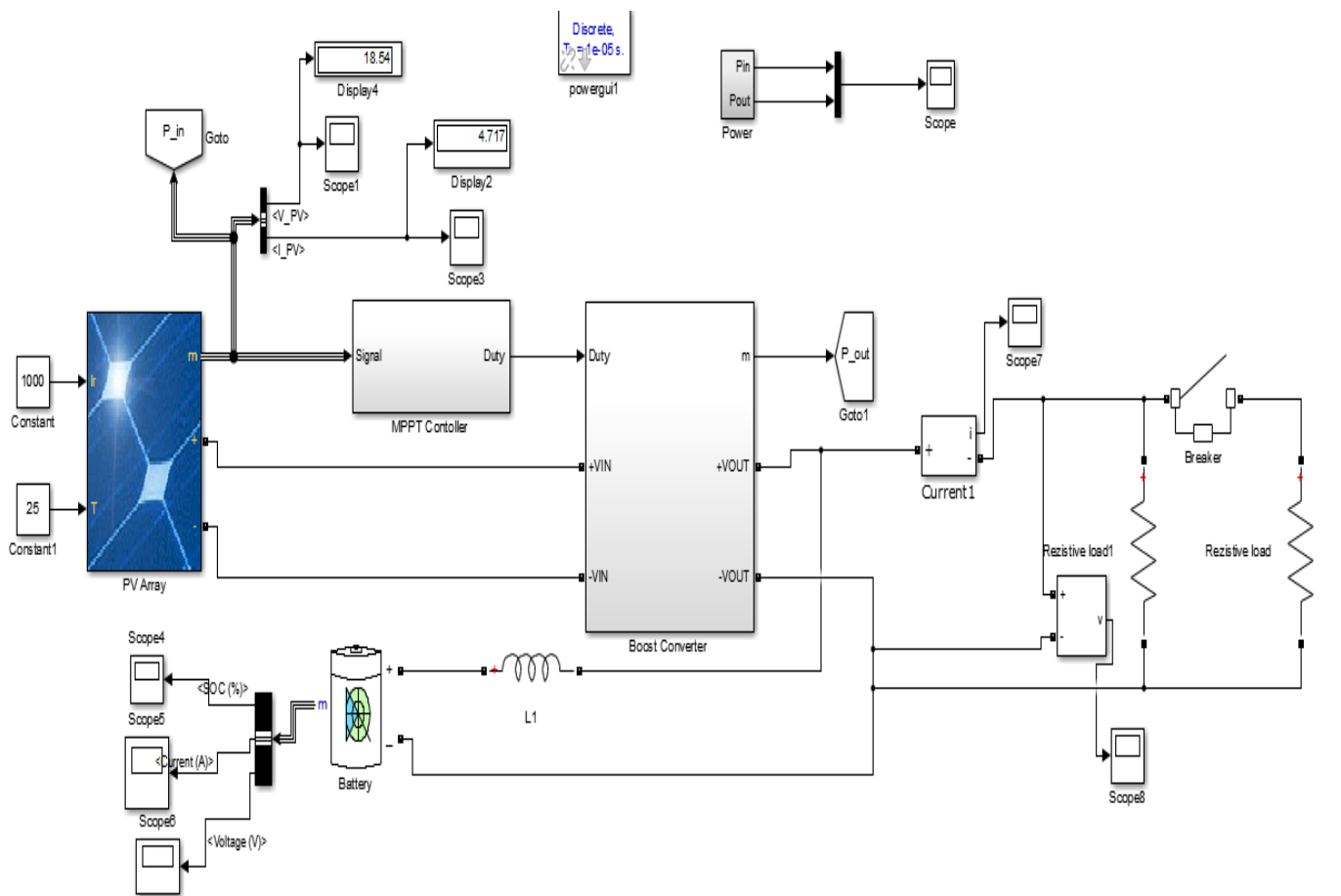


Figure 6-7: System schematic PV-MPPT -Boost converter –Battery with constant irradiance and constant temperature

In the above simulation the only difference from the simulation that can be found on Chapter 7.1 is that in this case a 44V (50Ah) battery is added to the model and was connected in parallel with the load resistance. After connecting the battery, the following graphs for voltage-current of the PV, boosted output current -voltage and power were plotted in order to observe the differences.

Firstly the PV voltage and current will be plotted and analyzed.

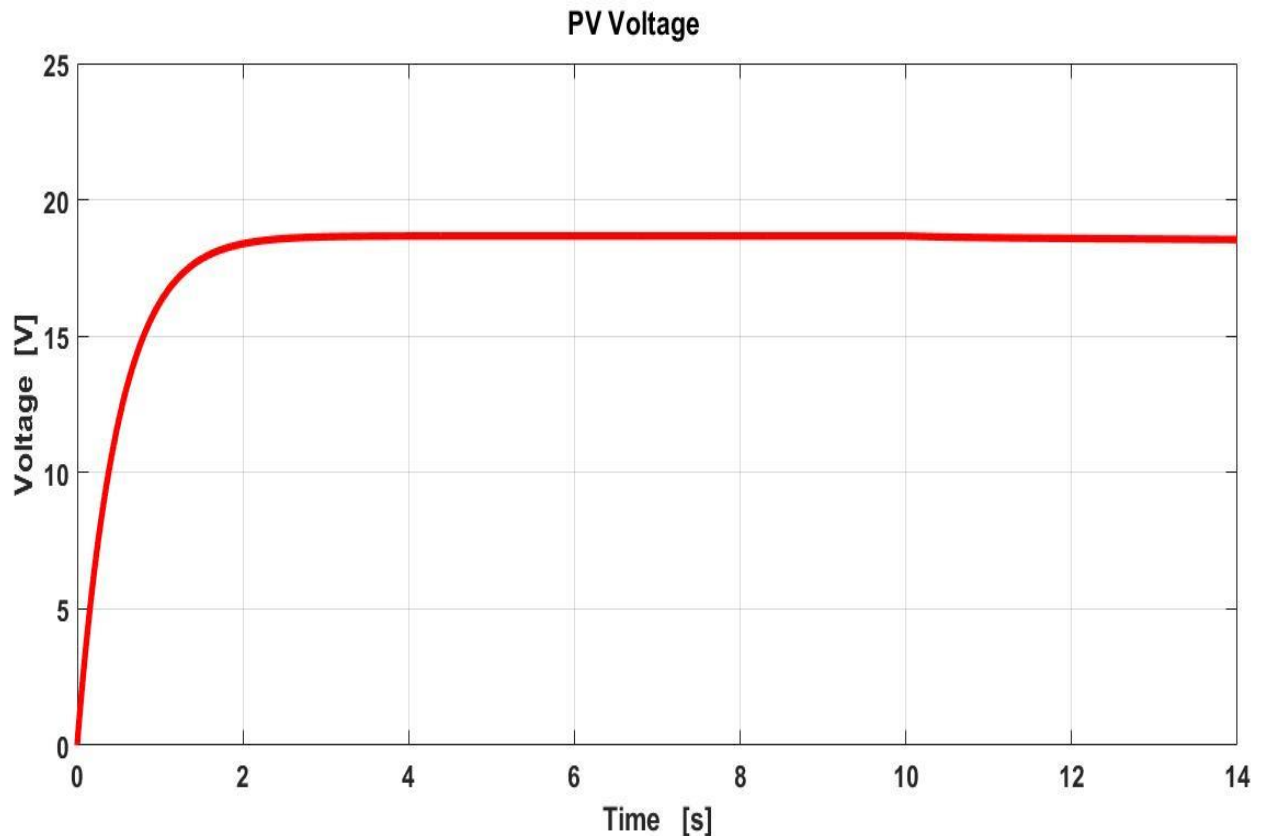


Figure 6 -8: Photovoltaic voltage with battery connection

In the above figure, the voltage of the PV module against time was plotted. It was used the same panel configuration - 90 W mono crystalline module as in the first simulation from Chapter 7.1 which was directly connected to a MPPT charge controller.

The same configuration of the boost converter was used, the only difference in the above Simulink model is the battery connection. The frequency chosen for this simulation was the same 20 kHz.

As can be notice in figure 6-8, the MPPT charge controller is forcing the module to operate at maximum voltage. Even after 10 second when the breaker is open and a change in the resistive load occurs the MPPT controller is working well and is maintaining the maximum voltage level.

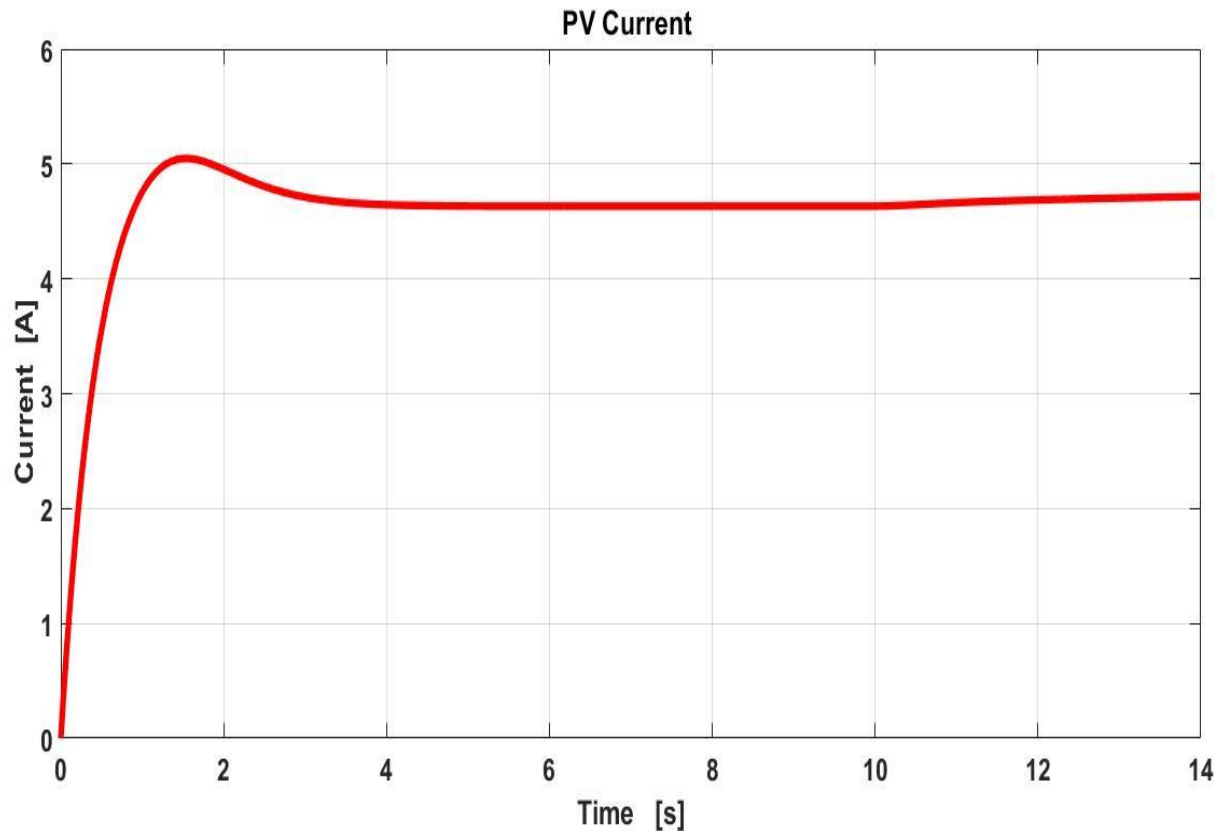


Figure 6-9: Photovoltaic Current with battery connection

The current of the photovoltaic module is also stable after two seconds and the operational current is achieved. Even after the breaker when a second resistive load is connected in parallel with the first resistive load, the current remains constant and no changes are occurring.

The MPPT charge controller together with the battery connected at the output of the system is maintaining the current at maximum operating point in order to extract the maximum available power. The aim of the MPPT is to work around maximum power to get maximum amperes into the battery.

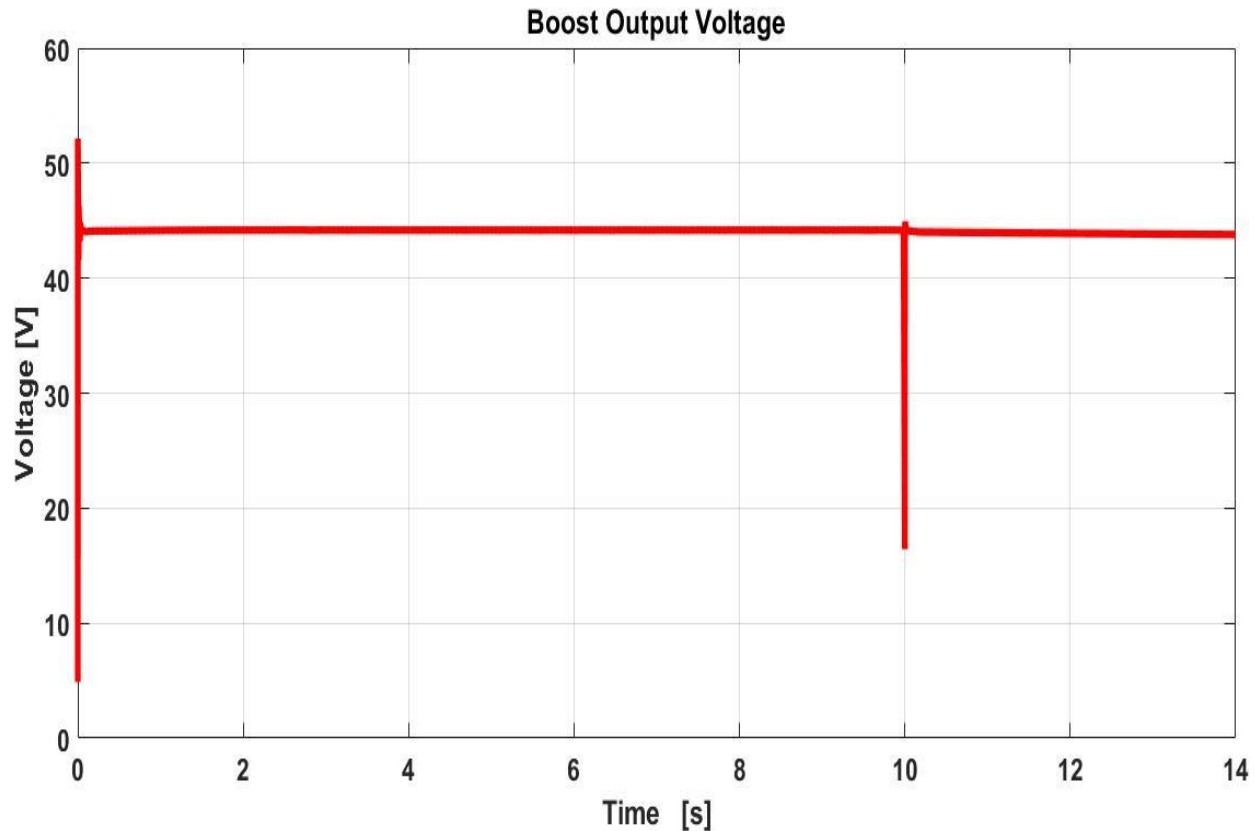


Figure 6-10: Output Voltage of the Boost Converter

The maximum output voltage of the PV is 18V at standard test conditions and with the help of the boost converter the voltage was stepped up to the desired voltage level of the system which was chosen in the design process. The input voltage, output desired voltage, the load resistance value and the frequency are very important parameters in the calculation process of inductance and capacitance.

After 10s when the breaker is opening and the second load resistance is connecting in parallel with the first load resistance, a big spike can be observed in the figure 6-10. The spike is indicate that a change in load occurs at that point, however the MPPT algorithm is keeping the boosted voltage constant. Because in this simulation a battery is coupled, no voltage drop occurs after the breaker and the same behavior is expected also for boost output current.

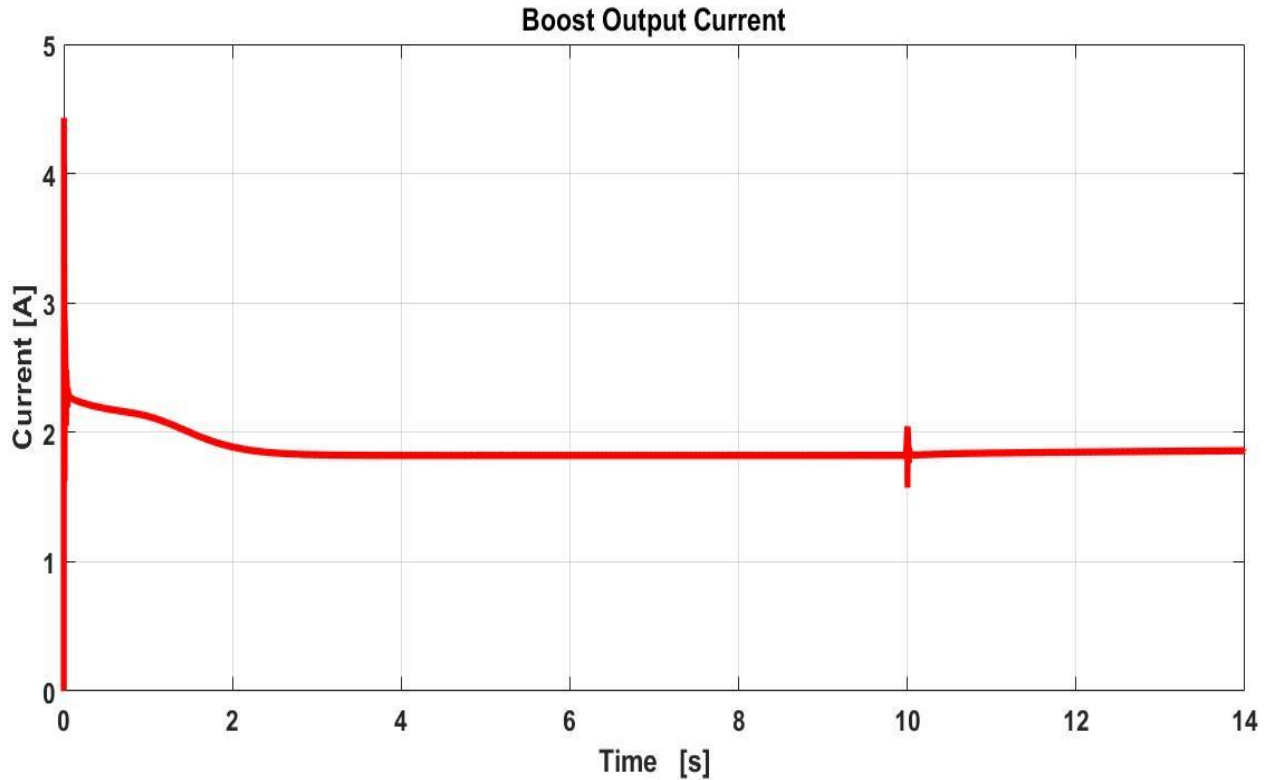


Figure 6-11: Output Current of the Boost Converter

The output current of the boost converter is dropping from around 5A to 2A, and the current drop is the effect of the voltage raise. After connecting the second resistance in parallel, the equivalent resistance of the parallel connection is lower than the load resistances but this drop in load resistance is not influencing anymore the current. Considering the connection of lead-acid battery at the output of boost converter the current continue to be constant after the breaker.

The boosted voltage was achieved with the help of the MOSFET transistor which by receiving a certain  $V_{gs}$  threshold voltage, the switch is opening or closing. As a consequence of the voltage rise the current has to decrease in order to keep the power at the maximum operating point.

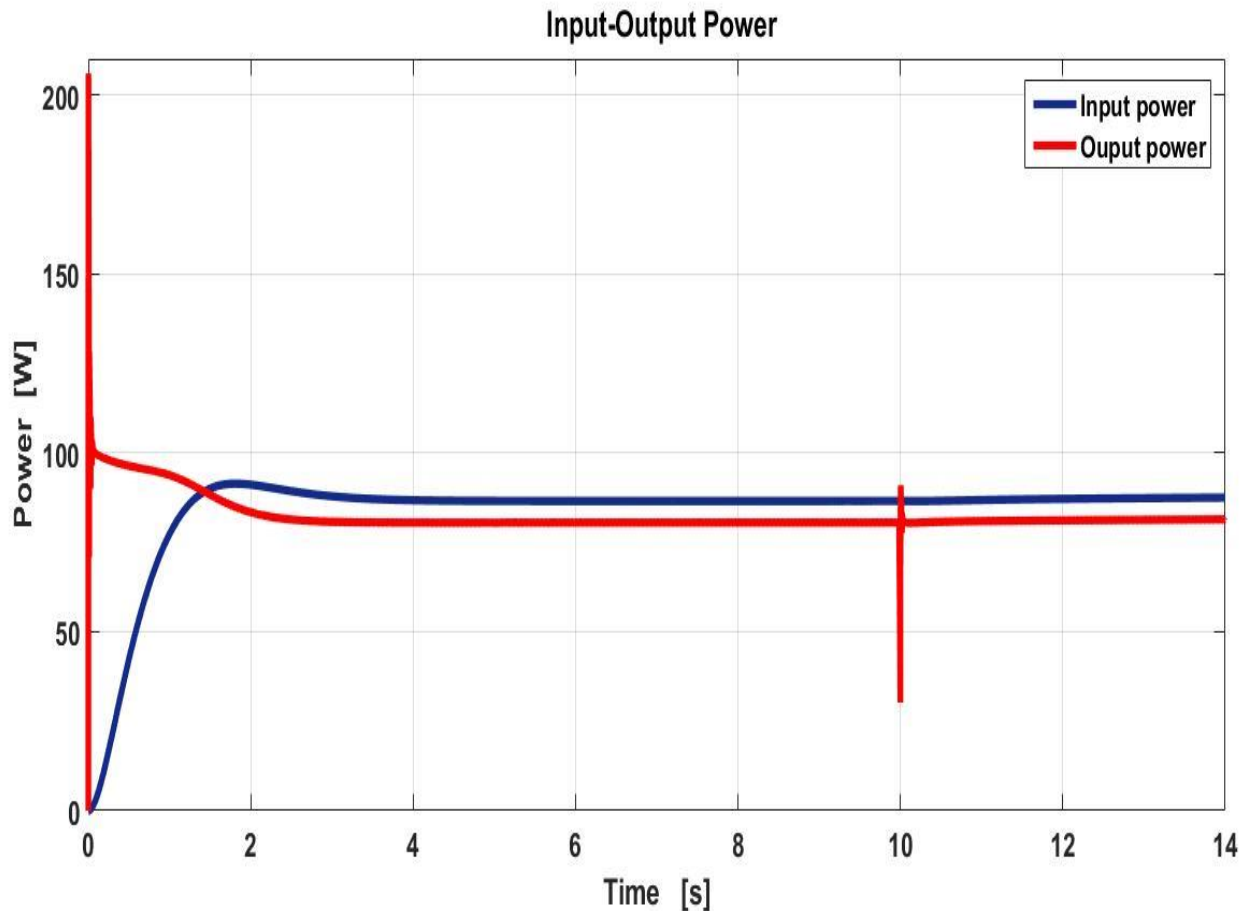


Figure 6-12: Input and Output Boosted Power

In this chapter the system was simulated under constant irradiance and constant temperature at standard test condition (STC) where the PV maximum power is 90W. The module is connected to a maximum power point tracker which is using the algorithm (P&O) in order to extract the maximum power out of the photovoltaic panel.

The input PV power and output boosted power are plotted in the above picture. The output power is following the input power with very low margins variations. For the first 10 seconds the maximum power tracking is achieved and immediately after the breaker a spike can be noticed in the output power, nevertheless the MPPT control algorithm is keeping the power constant without changes. In this case the extra power was fed into the battery and it can be used during the night or during cloudy days for the sake of providing enough power for continuously load operation.

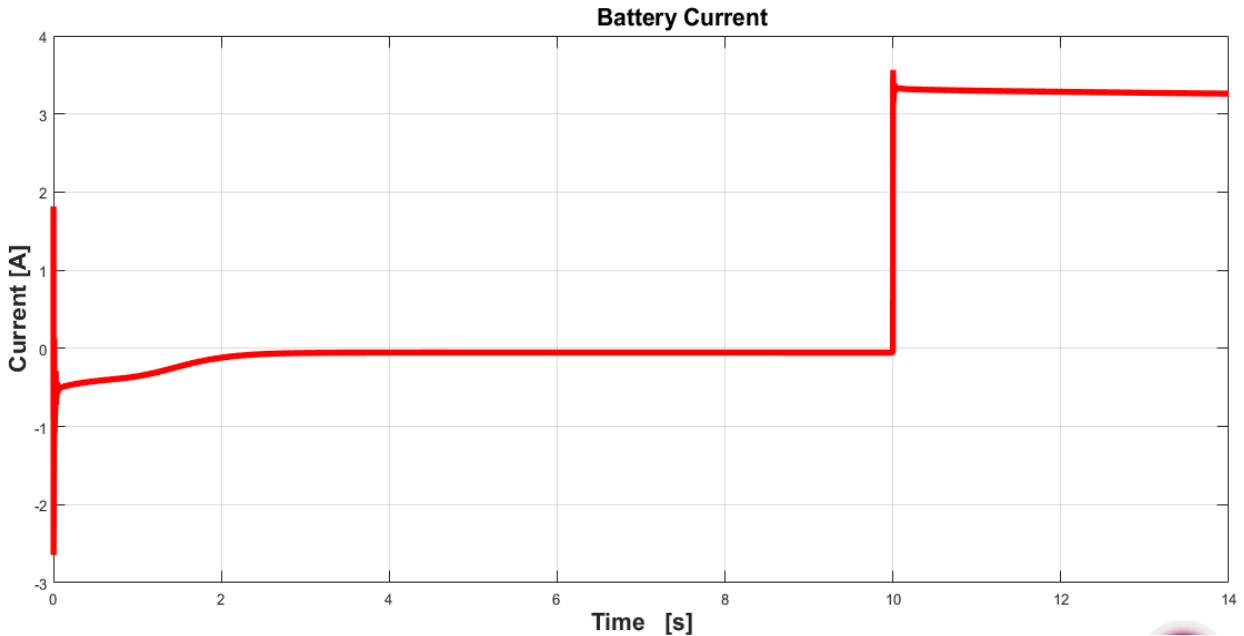


Figure 6 -13: Battery current

In figure 6-13 the battery current is plotted, where in the first 10s the current is zero because the load is absorbing the most of the available power. After the breaker when the resistance load is decreasing, the MPPT charge controller is maximizing the current that is feeding into the battery.

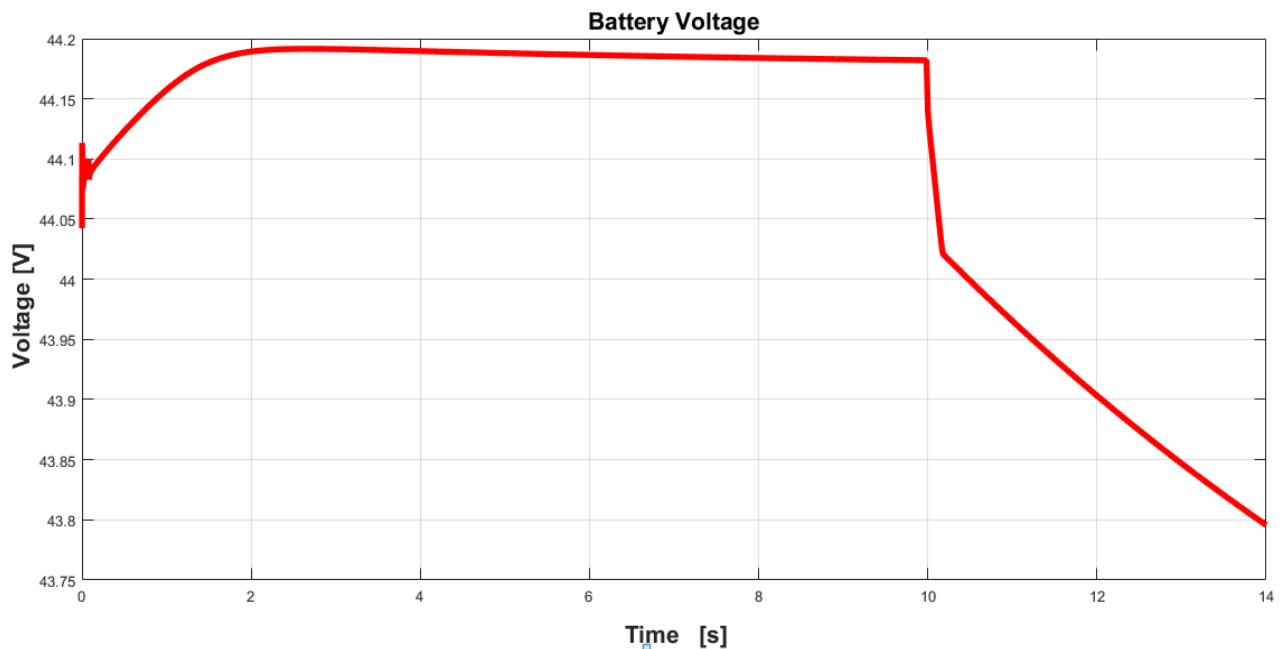


Figure 6 -14: Battery voltage

In figure 6-14, the voltage is plotted and a constant 44V is kept constant for the first 10s and immediately after the breaker, the voltage starts to decrease slowly.

### 6.3 Fluctuating Irradiance and fluctuating Temperature

After conducting the simulations from Chapter 7.1 and Chapter 7.2 both under Standard Test Conditions (STC), which means that the irradiance level is  $1000\text{W}/\text{m}^2$  and the module temperature is  $25^\circ\text{C}$ , in this Chapter a signal builder was made in order to simulate a “real environmental” scenario where the irradiance is fluctuating and also the module temperature is fluctuating. The signal builder was created in Simulink and can be seen in the figure below.

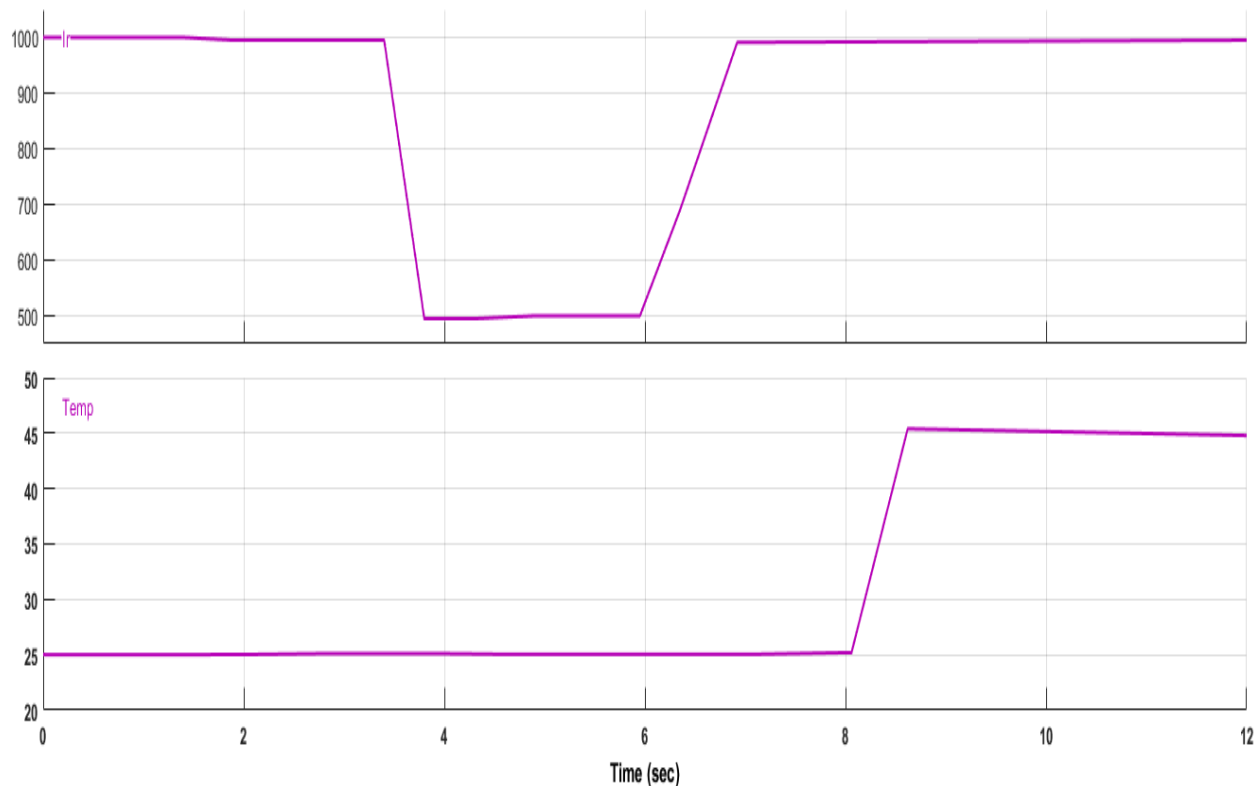


Figure 6 -15: Irradiance signal and Temperature signal

In the above picture the irradiance drops  $1000\text{W}/\text{m}^2$  to  $500\text{W}/\text{m}^2$  between the time interval 4-6seconds and after 6seconds the irradiance level is increasing back to  $1000\text{W}/\text{m}^2$  the standard test condition level. The module temperature is constant for the first 8seconds of the simulation and after 8s is increasing from  $25^\circ\text{C}$  the standard test conditions to  $45^\circ\text{C}$  degrees. The Simulink model contains also a breaker which will connects after 10s another 10ohms resistance to the system. The new resistance is connected in parallel with a 25ohms resistance.



The 44V (50Ah) battery used in the previous chapter is connected on the output of the converter in parallel with the load resistance.

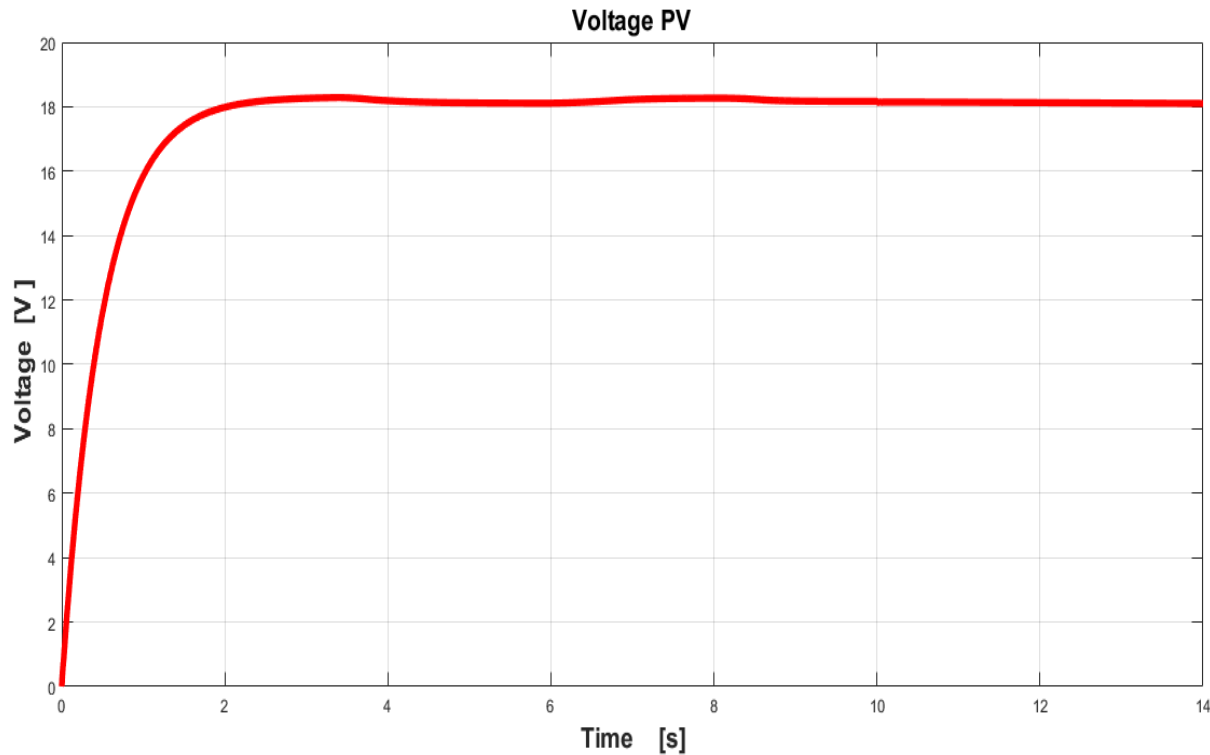


Figure: 6 -16: Photovoltaic voltage with irradiance variation and temperature variation

As already described in Chapter 5.1 the function of MPPT is to extract the maximum available power from PV module by forcing them to operate at the most efficient voltage ( $V_{mpp}$ ). The Perturb and Observe algorithm used for tracking the maximum power point checks the output of PV module, compares it to battery voltage then calculate the maximum power that the photovoltaic panel can harvest in order to charge the battery. The controller take this and convert it to the maximum voltage in order to fed maximum current into the battery.

The amount of voltage produced by the PV module is slightly affected by the irradiance changes, and small fluctuations can be observed in the above figure.

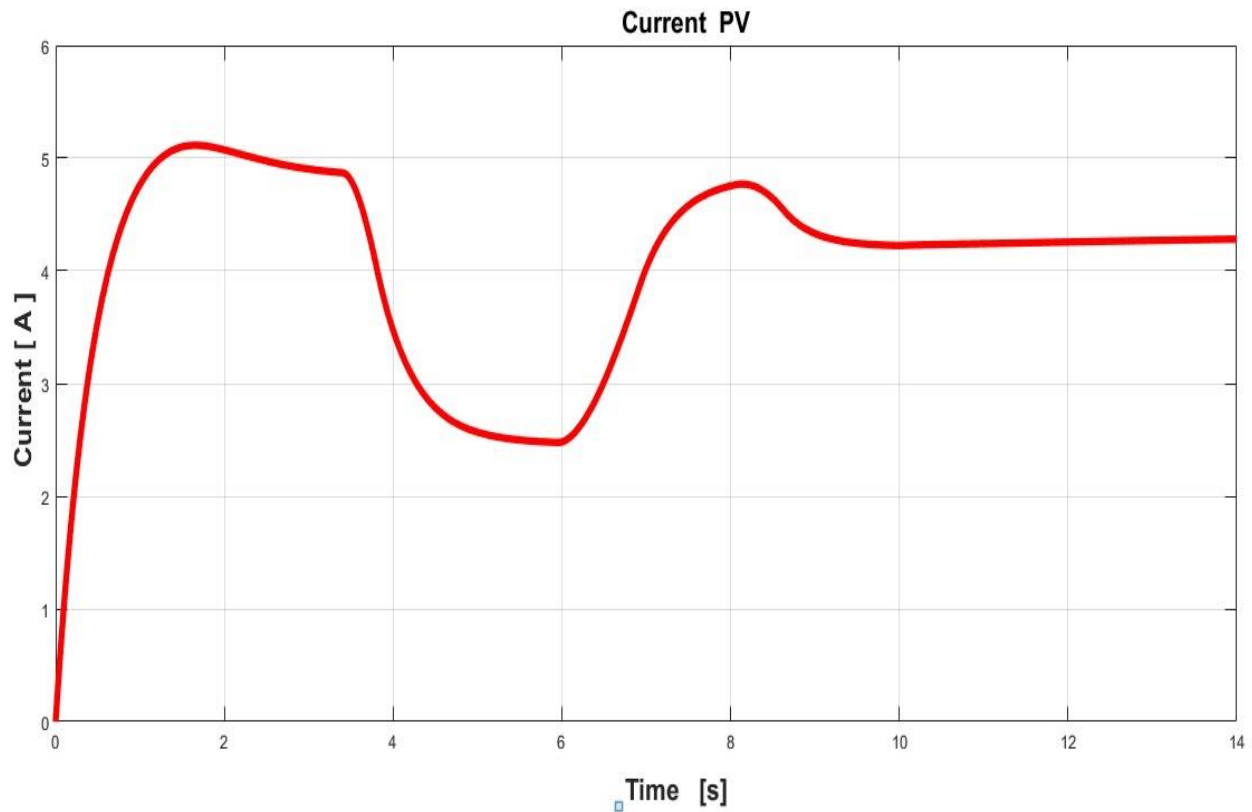


Figure 6 -17: Photovoltaic current with irradiance variation and temperature variation

The amount of current harvested by the photovoltaic module is directly influenced by the irradiance variations. Between the times interval 4-6 seconds the irradiance drops from  $1000\text{W}/\text{m}^2$  to  $500\text{W}/\text{m}^2$  and the PV current is also decreasing from 5A to 2.5A.

Within the increase in module temperature the power of module is expected to decrease and also the current is slightly dropping with temperature increase. After the 10s breaker the MPPT is keeping the current at a constant value and maximize the amount of current going into the battery.

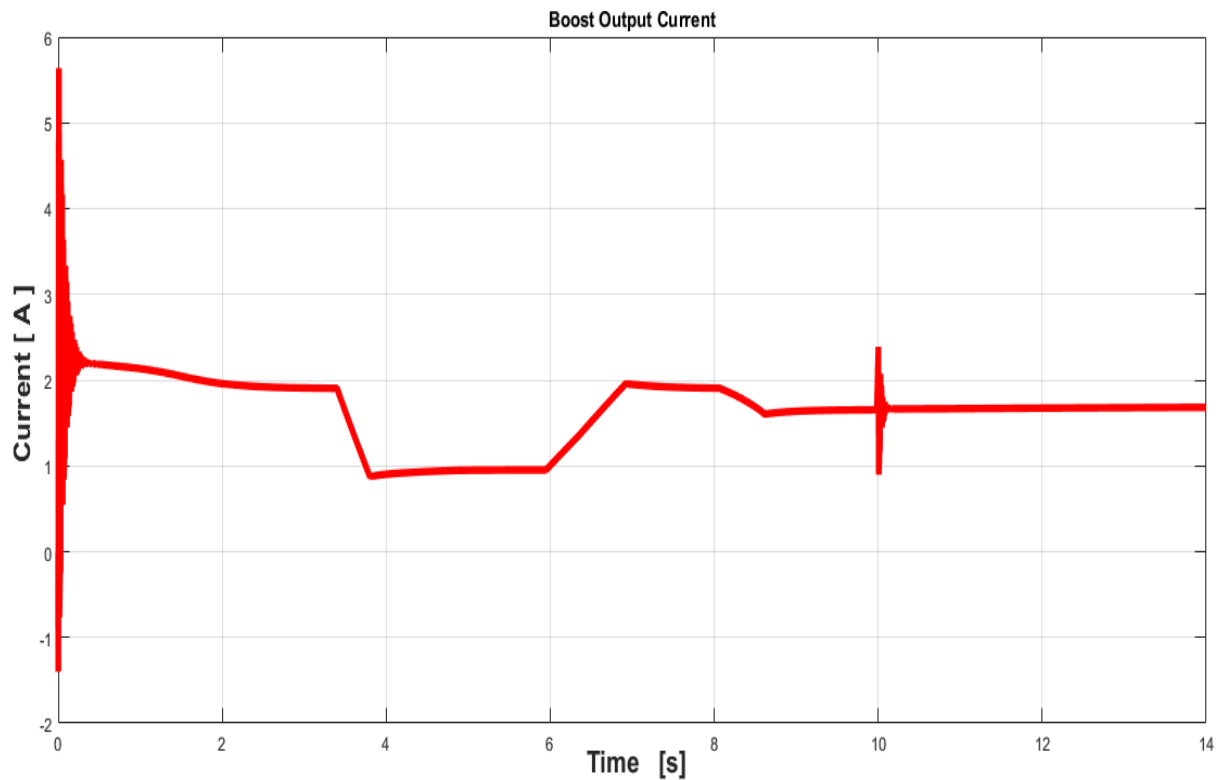


Figure 6 -18: Output current of the boost converter

The output current of the boost converter is dropping from around 5A the nominal current value to 2A, and the current decrease is the consequence of the voltage raise. The output current of the boost converter is following the irradiance curve and as the irradiance is dropping from  $1000\text{W}/\text{m}^2$  to  $500\text{W}/\text{m}^2$  the current has the same behavior. Shortly after the breaker the current is not anymore influenced by the load changes because of the lead-acid battery connected at the output of the boost converter which is now getting charged and is maintaining the output current constant.

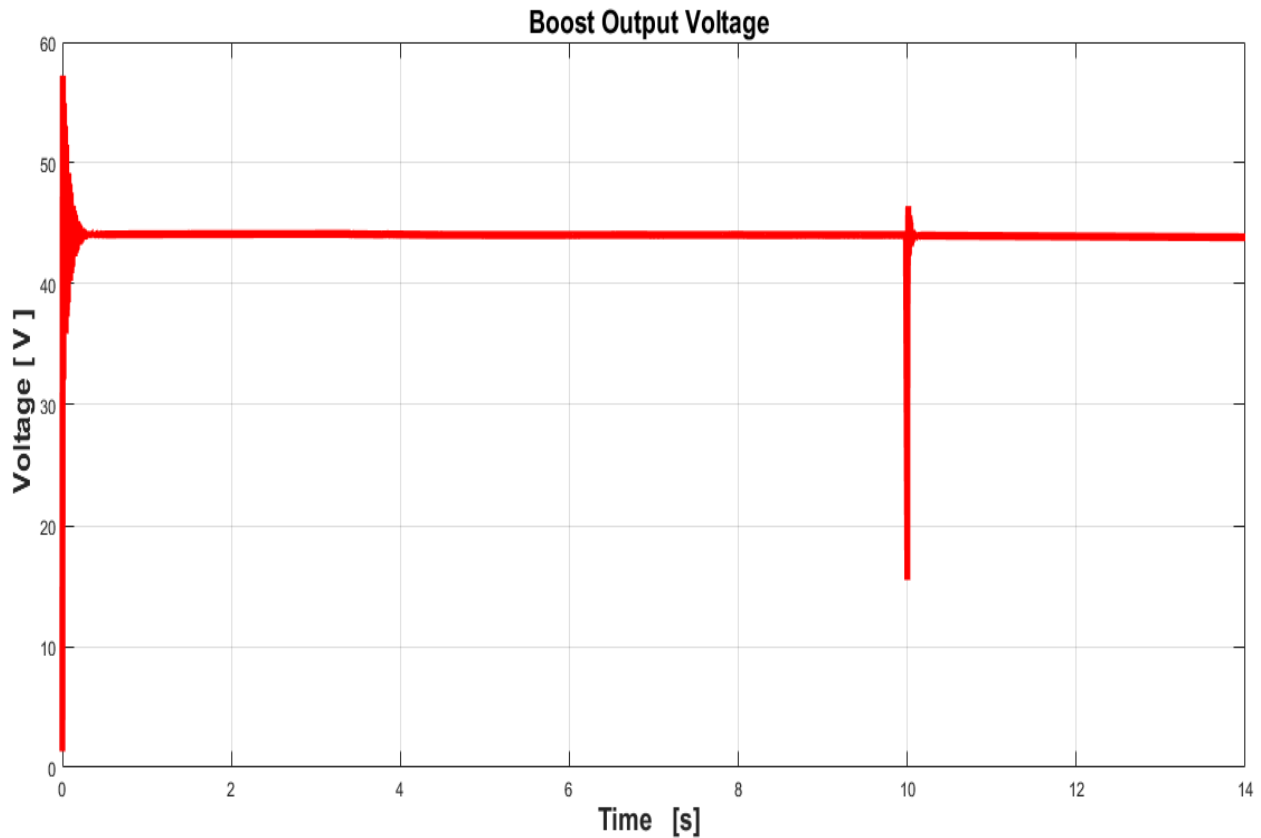


Figure 6 -19: Output Voltage of the Boost Converter

The boosted voltage was achieved with the help of the MOSFET transistor which is a voltage controlled component which by applying a voltage between the gate and the source the current is allowed to flow between the drain and the source. As a consequence of the voltage rise the current has to decrease in order to keep the power at the maximum operating point.

As can be seen in figure 6-19 the output voltage is not influencing by the irradiance changes or temperature changes and the aim of the controller to keep the output voltage at a constant desired value was achieved.

After 10s when the breaker is opening and the second load resistance is connecting in parallel with the first load resistance, a big spike can be observed in the figure 6-19. The spike is pointing out that a change in load occurs but the MPPT control algorithm is maintaining the boosted voltage constant. Because in this simulation a battery is connected, no voltage drop occurs after the breaker.

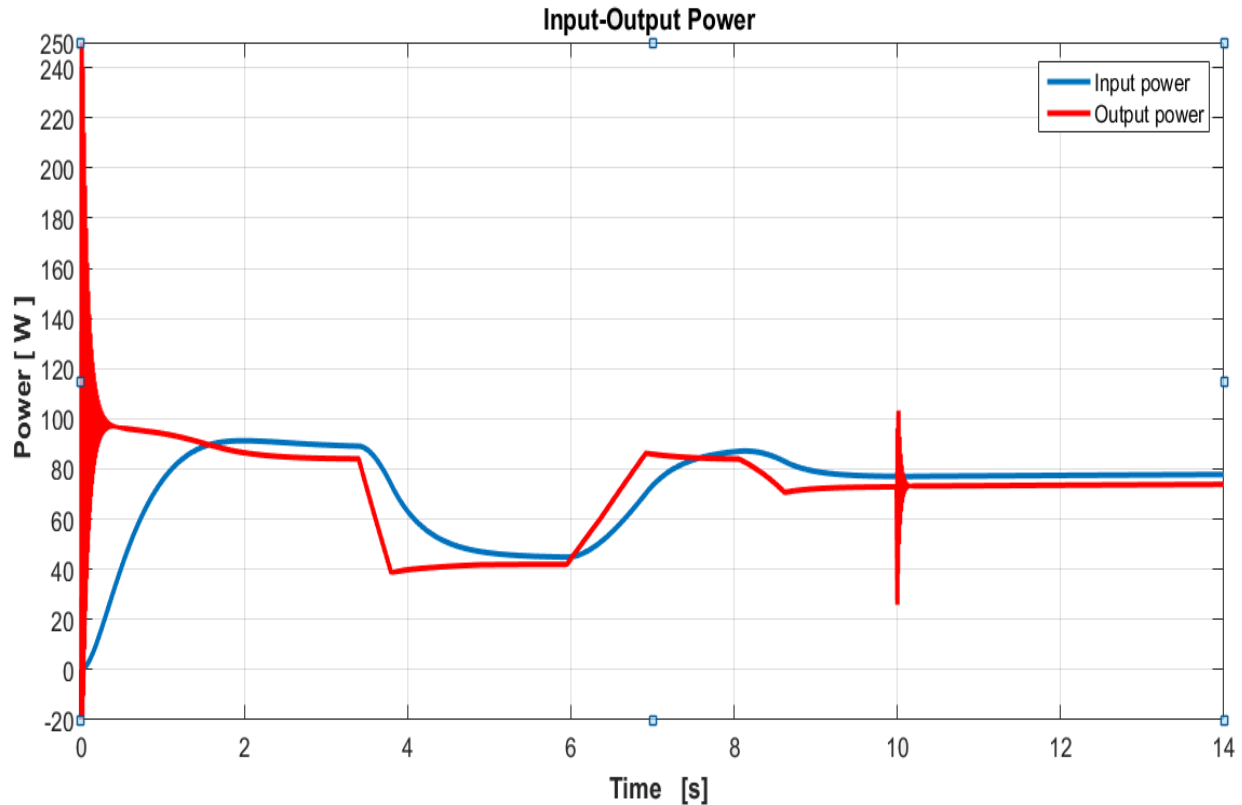


Figure 6-20: Input and Output Boosted Power

In this chapter the system was simulated under fluctuating irradiance and fluctuating temperature. MPPT solar charge controller is essential for any solar power systems and is used to extract maximum power from PV module. The input PV power and output boosted power are plotted in the above picture.

The input and output power of the first PV module can be observed in the above figure, where with blue is illustrated the input power and with red is representing the output power.

In the following time interval 4-6seconds the irradiance level is decreasing from  $1000 \text{ W/m}^2$  to  $500 \text{ W/m}^2$  and both powers are following the irradiance behavior.

The Perturb and Observe algorithm has a poor performance under rapidly irradiance changes and this behavior can be identify in the figure 6-20. For one second the MPPT algorithm is not working as expected but shortly after seven seconds the control algorithm is working again fine.

The poor performance of the P&O algorithm is mentioned in the most literature, but in the real environment the sudden changes in irradiance are not very common as the irradiance changes simulated in the model.

## 7. Experiments Chapter

### 7.1 Test Experiment

The tasks of this experiment are the boost converter performance. Before building the boost converter on a PCB, it was decided to scale down the prototype and to conduct a test experiment in order to observe the working principle of the boost converter.

In the design process of the boost converter, the values for the inductor and capacitor were calculated with the help of the equation Eq.4-20 and Eq.4-25. The boost converter was designed to step up the voltage from 6V to 30V. In this experiment I have used a pushbutton switch instead of a MOSFET transistor for opening and closing the switch.

**Table 4. Boost converter components**

Components	Characteristics
Inductor	23 $\mu$ H-1A
Capacitor	47 $\mu$ F -63V
Diode	Fast recovery rectifier diode
Switch	Push button switch
Led	5mm Led

In the above table can be found the components that were used in the experiment together with their electrical characteristics.

In the table 5 can be found the measurement instruments needed to conduct the test

**Table 5. Measurement instruments**

Experiment Setup	Type
Power Supply	EA-PS 2343-06B
Digital Multimeter	KEYSIGHT
Electronic Breadboard	test breadboard



Figure 7-1: Power Supply

The first step of the experiment was to set the power supply to 6V for the channel 1 and the current to 0.2A. After setting the voltage and current the power supply will be connected to the PCB test board and feed the components.

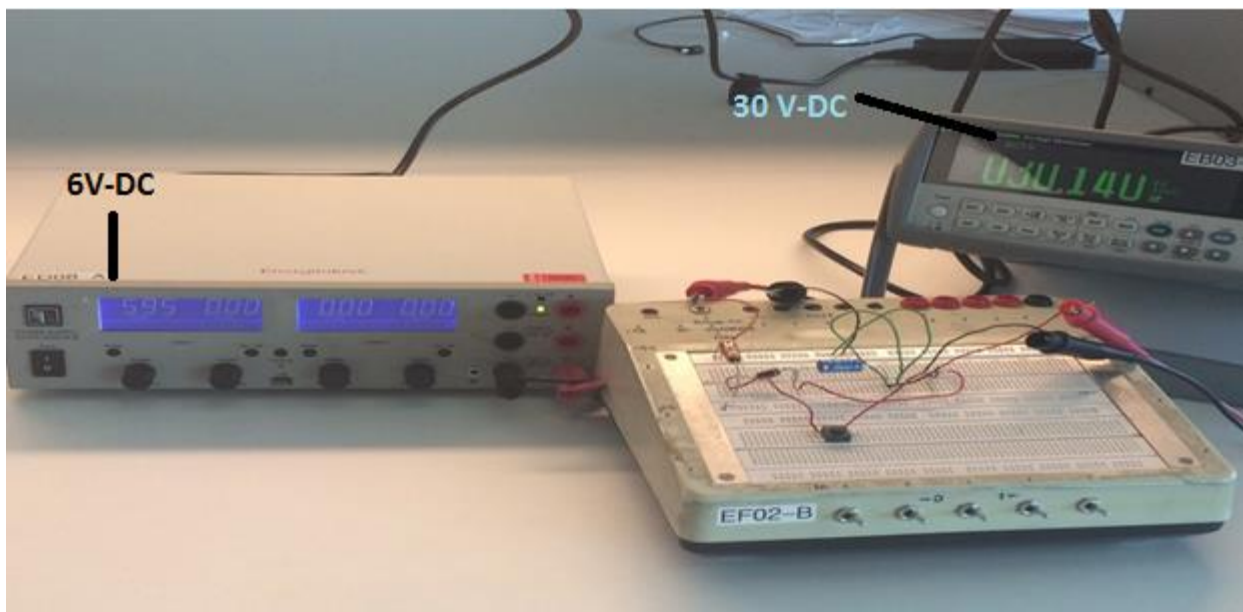


Figure 7-2. Experiment setup with the Power supply, Digital Multimeter, electronic breadboard

In the above figure the power supply is connected to the test board and on the output of the converter a digital multimeter is connected in order to measure the value of the boosted voltage. Because in this experiment wasn't used a MOSFET transistor with is controlled by a PWM signal, the voltage boost is done manually by pressing the push button with different frequencies. Pressing the button is equivalent with opening the gate of a transistor and by increasing the frequency the voltage will increase.

When the switch is open the energy which was stored in the inductor is getting transferred to the capacitor and the capacitor will start charging. When the digital multimeter was shown 30V, a 5 mm LED was connected to the capacitor output and was used as a load in order to discharge the capacitor.

After conducting several experiments in order to understand the boost converter performance, it was decided to start designing the boost converter taking into account the PV characteristics and the desired output boost voltage.

## 7.2 First Boost converter experiment

In this chapter, the design and construction of the boost converter used in the simulation will be described. The first step of the construction phase was to find the right electronic components. By taking into account the electrical characteristics of the module presented in Chapter 3.5, the desired output voltage of the boost converter and the load resistance was chosen.

In the table below the values for the minimum inductor and minimum capacitor where determined with the help of the equation Eq.4-20 and Eq.4-25. The converter is designed to boost the voltage from the 18V the  $V_{mpp}$  value of the PV to a constant 44V the desired output voltage value. The frequency chosen for the calculation of the component was 20 KHz.

The value for the duty cycle can be calculated from Eq.4.3. In the design process another important aspect to be taken into account is the output voltage ripples which in this case was chosen to be less than one percent.



**Table 6. Boost converter components**

Components	Characteristics
Inductor	70 $\mu$ H-11A
Capacitor	140 $\mu$ F -63V
Diode	Fast recovery rectifier diode 1N400
MOSFET	60V - 0.07 $\Omega$ - 16A
Resistive load	25 ohms

After choosing the right components and by following the boost converter schematic presented in Chapter 4. The first boost converter prototype was built.

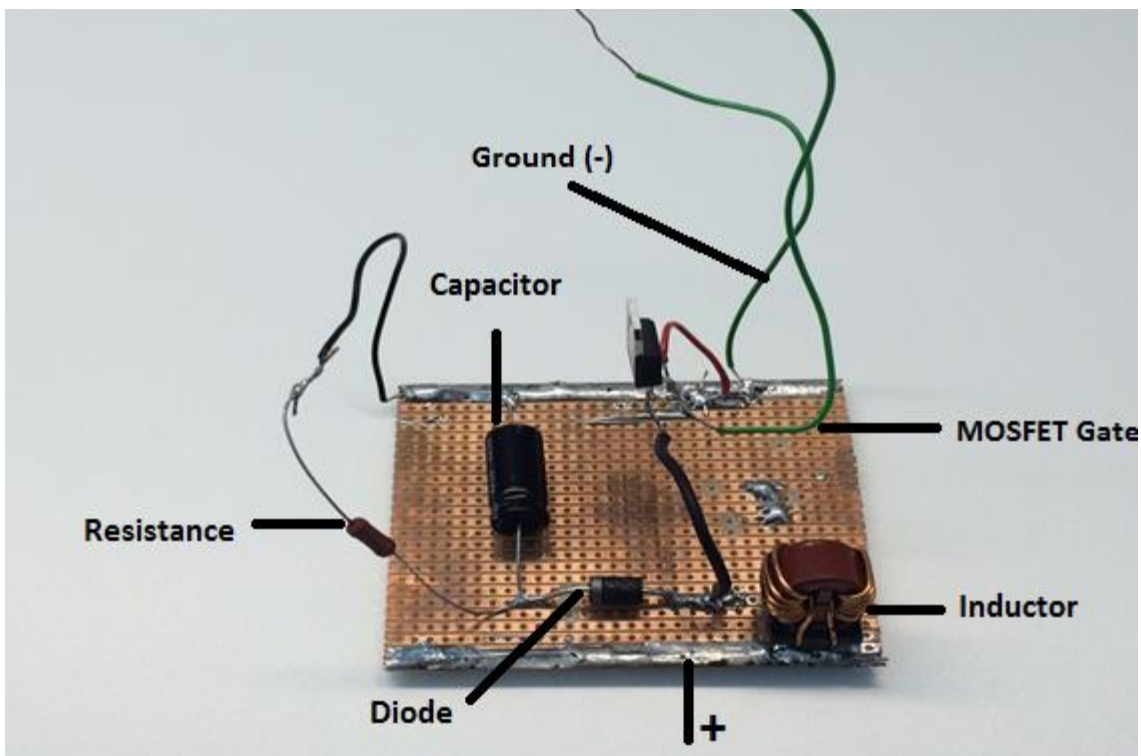


Figure 7-3: Boost converter first prototype

To provide a margin to ensure continuous current, the value for the inductor and capacitor presented in table 6 and used for building the boost converter are bigger than the value calculated in the Appendix [A .b’].

### 7.2.1 Experiment results

In order to test if the built converter is working, the following measurements instruments presented in the table below are used.

**Table 7. Measurement instruments**

Experiment Setup	Type
DC Power Supply	EA-PS 2343-06B
Digital Multimeter	KEYSIGHT
Digital Oscilloscope	Tektronix 200Mhz
Function Pulse Generator	TTI 50MHz

The DC power supply was used as the input for the converter. The amount of input voltage and input current which will supply the converter were selected with the help of the front bottoms available on the power supply. The voltage was firstly selected to 6V and the current to 0.4A. The function pulse generator was used to generate a PWM signals. The same 20 KHz frequency as the one used in the Simulink model was selected for the function pulse generator. The TTI function generator allows to use a square wave and allows you to vary the duty cycle between 20 and 80 percent. In figure7-4 the pulses can be seen on the oscilloscope screen together with the frequency and duty cycle.

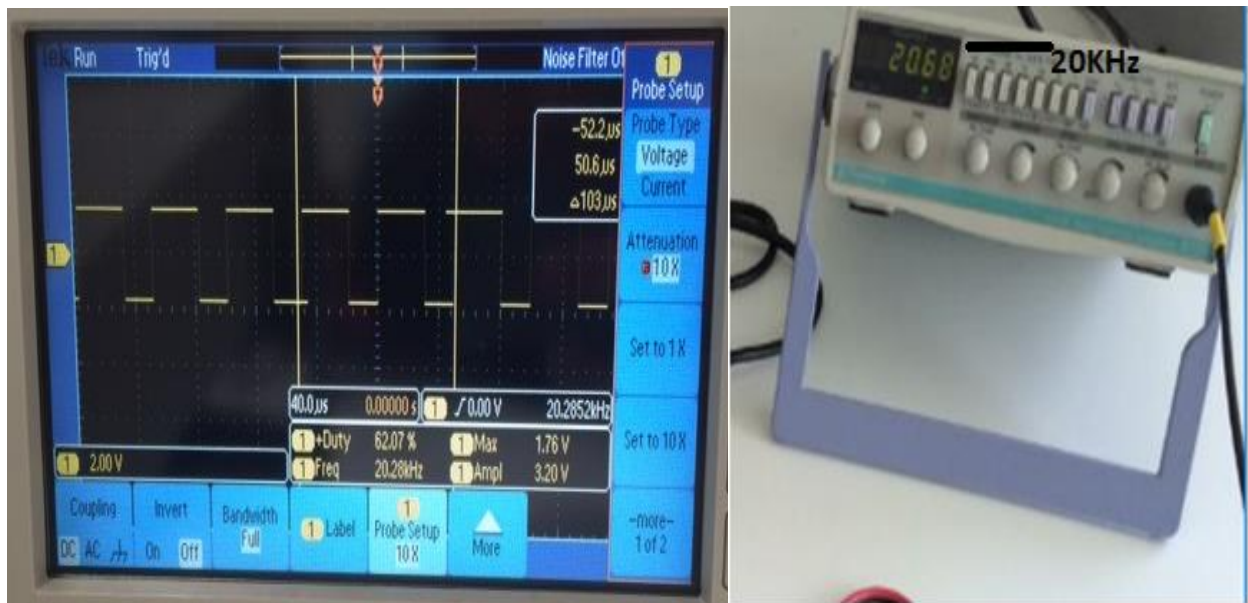


Figure 7-4: Digital Oscilloscope and Function pulse generator

The function pulse generator was connected to the gate of the MOSFET transistor in order to simulate the on/off operation of the transistor. The digital multimeter was connected on the output of the converter in order to measure the value of the output boosted voltage.

After few experiments the MOSFET the temperature of the transistor was increases and after few minutes it burned. The power dissipation in the transistor occurs during switching and is converting into heat. Each transistor have a limit on the current that they can safely handle and if the limit is exceeds because of the high voltages and currents that are present during the switching, the transistor can burn off. The first step in solving the current problem was to change the transistor and to try again the same experiment in order to observe again the behavior of the converter. The second step was to change the actual 25 ohms resistive load with a much higher resistance of 100 ohms.

Thereafter all the changes, another experiment was conducting but unfortunately the transistor experienced the same behavior as the previous one. After more research regarding the thermal management, according to Chapter 10.8 [14] it was obvious that the burning of the transistor were caused by exceeded his maximum thermal energy.

The solution for removing the thermal energy was to add a heat sink on top of the transistor.

### 7.3 Second boost converter experiment

In this chapter it will be described the second attempt of building a boost converter in order to solve the problems faced in the first experiment.

**Table.8 Components used for the second boost converter**

Components	Characteristics
Inductor	350 $\mu$ H-11A
Capacitor	160 $\mu$ F -63V
Diode	Fast recovery rectifier diode 1N400
MOSFET	60V - 0.07 $\Omega$ - 16A
Resistive load	100 ohms

A new boost converter was built with the above components characteristics but in this approach a heat sink was attached on top of the transistor in order to remove the thermal energy produced by switching losses. The heat sink lower the junction temperature for a certain power dissipation in a MOSFET transistor by decreasing the total thermal resistance of the junction to surroundings. [14]

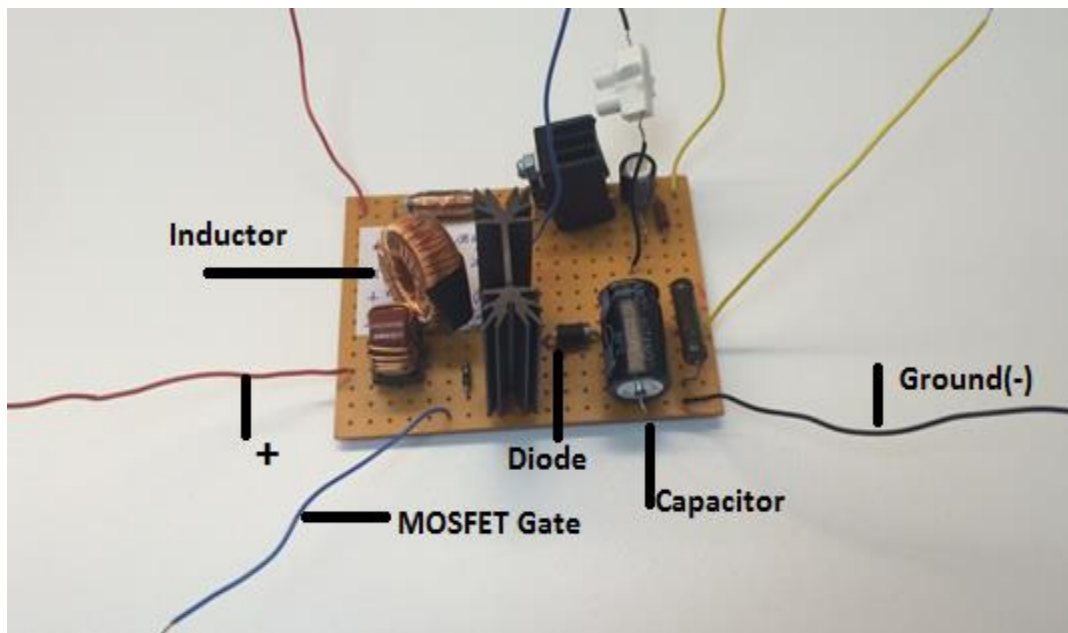


Figure 7-5: Boost converter second prototype

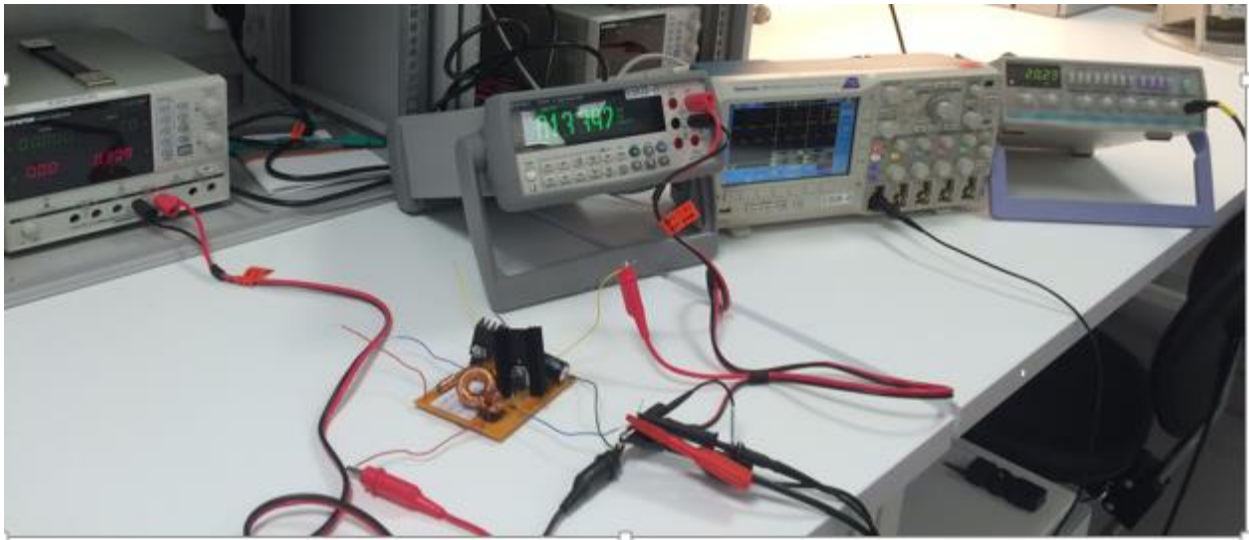


Figure 7-6 : Boost converter testing

For the testing part we used the same measurement instruments presented in table 7. The DC power supply was connected to the input of the converter, function pulse generator to the gate of the transistor and the digital multimeter to the output of the converter in order to measure the boosted output voltage.



Figure 7-7 : DC power supply- Digital Multimeter

Firstly, the input voltage was set to 11V and the input current to a small current value of 0.3A and with a frequency equals to 20KHz and a duty cycle of 60% the voltage was boosted to 30V.

The duty cycle describes the proportion of “ON” time of the transistor and by increasing the duty cycle the power is also increasing. The maximum duty cycle that can be simulated from the function pulse generator is around 80% but is not recommended to work with this high duty cycle because of possible damage of the components.

Unfortunately, after increasing the current and voltage to higher values, the MOSFET transistor burnt. The next aim after changing again the transistor was to couple the boost converter to the Simulink simulation and try to give a PWM signal to the gate of the MOSFET transistor with the help of an Arduino in order simulate the on/off operation of the transistor.

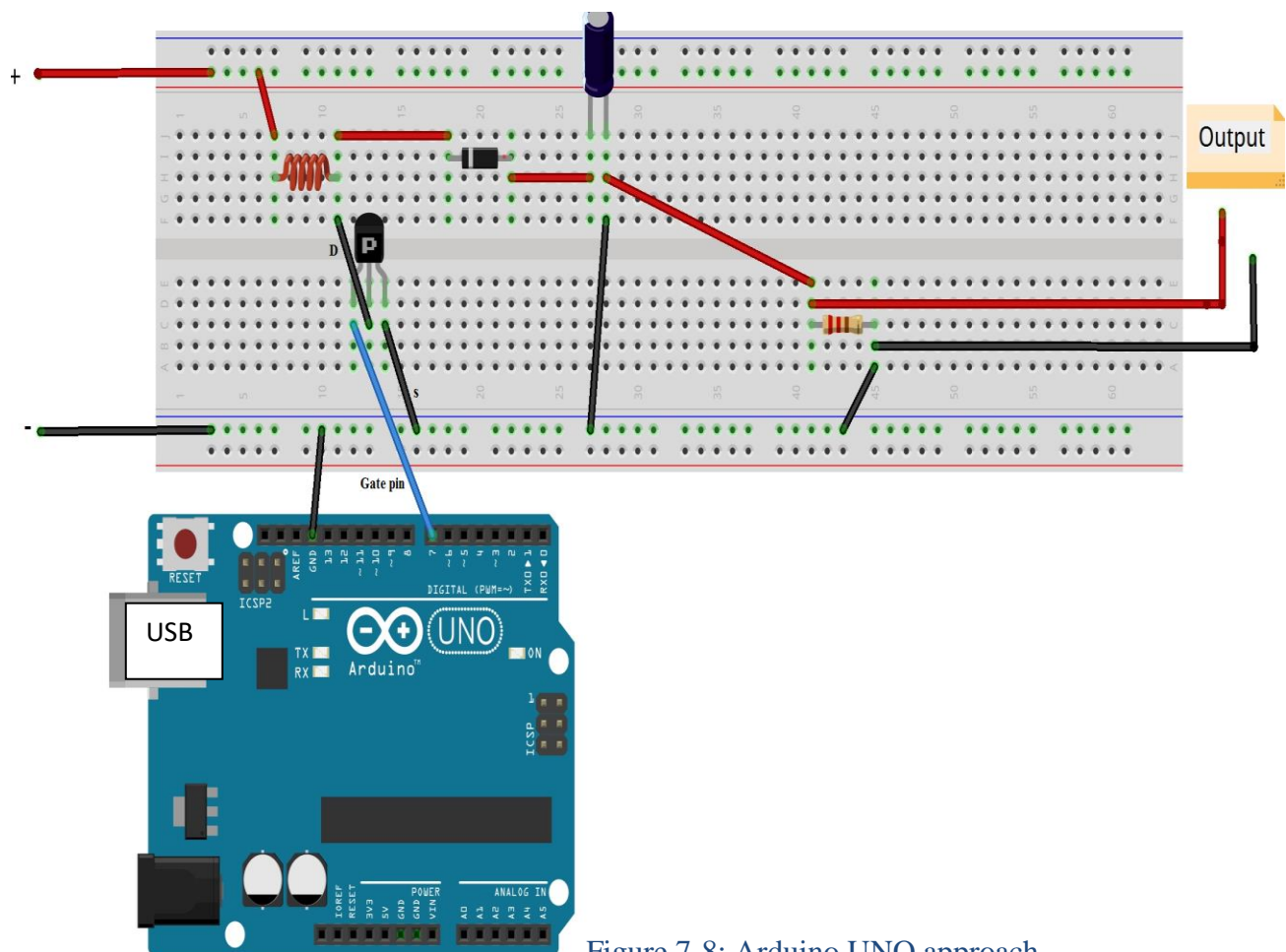


Figure 7-8: Arduino UNO approach

The Arduino UNO was chosen for trying to connect the Simulink model to the boost converter in order to control the gate of the transistor. This approach failed also after a lot of testing due to the fact that the Arduino has a limited output frequency of 400Hz and the frequency of the Simulation is 20Khz.

## 8. Conclusion

In this report the simulation of a stand-alone PV system was made. The maximum power point tracking charge controller algorithm was implemented and simulated in Simulink. The boost converter Simulink model was firstly build and validated through simulations. [Ch.4]

The next step was to couple the system and to analyze the behavior of the system under three different scenarios.

- Scenario 1 – Constant Irradiance and constant Temperature without a battery connection
- Scenario 2 – Constant Irradiance and constant Temperature with a battery connection
- Scenario 3 - Fluctuating Irradiance and fluctuating Temperature with a battery connection

The main purpose of the project was to implement a suitable control method in order to keep the output voltage stable and to extract the maximum available power from the panel.

For first simulated scenario [Ch.6-1] the maximum power point tracker method Perturb and Observe is working very well and the output voltage of the boost converter was reached the constant value chosen in the design process. The only loss of power was observed after the breaker when the load resistance was decreases.

The second scenario [Ch.6-2] is showing that MPPT charge controller is working most efficient together with a battery connected at the output of the system. MPPT controller monitors the output of PV module, compares it to battery voltage then is increasing or decreasing the duty cycle in order to arrive to the maximum power that PV panel can harvest to charge the battery and correlate it to the best voltage to obtain maximum current into battery.

For the third scenario where the irradiance and temperature are varying the controller is following the input power with very small margin variations and the efficiency is quite high for this scenario. The MPPT charge controller is most effective in cold weathers where the module temperature is low.

The practical implementation in order to validate the model couldn't be finish because of the different problems faced during the construction of the boost converter. One of the main problem that have to be solve is to find a suitable method for reducing the power dissipation that is taking place in the transistor during the on/off switching states.

## 8.1 Future research and improvements

The attention has to be paid mostly on the prototype construction of the boost converter, where the focused has to be on the MOSFET transistor which is the most important component in the circuit.

- More research in understanding the Transistor Snubber Circuit can be done.  
The Snubber circuits can possibly lower the power losses in the transistor during switching and protect the device from the switching stresses of high voltages and currents.
- The function pulse generator is not the most suitable method for applying a voltage between the gate and the source of the transistor and another procedure have to be found.

The Perturb and Observe algorithm is the most cost-efficient and easy to implement for any PV module without knowing any information about the panel but for abrupt irradiance changes is not the most efficient algorithm.

- Incremental Conductance algorithm is more suitable in the case of a very rapidly changes of the irradiance level. But the better efficiency of the algorithm is coming with a cost increasing.
- Normally, PV module works better at cold temperatures where the sun is most of time shining and the MPPT charged controller is used to extract maximum power available.
- In remote areas where no grid connection is available the system can be completely implemented.



## 9. Nomenclature

Symbol	Explanation	Unit
$\alpha_1$	The temperature coefficient of the current	[%/deg.C]
$A_{C1}$	Area of solar cell	[m <sup>2</sup> ]
°C	Celsius	[°]
D	Duty cycle	[%]
DC	Direct current	[-]
$D_{max}$	Maximum duty	[%]
DT	Length of time when the switch is closed	[s]
e	Electron charge	[C]
FF	Fill Factor	[%]
$f$	Switching frequency	[Hz]
G	Solar irradiation	[W/m <sup>2</sup> ]
G(t)	Incident solar irradiance	[W/m <sup>2</sup> ]
$G_{STC}$	Reference solar irradiation	[W/m <sup>2</sup> ]
$I_d$	Current flowing through the diode	[A]
$i_L$	Inductor current	[A]
$I_{L,max}$	Maximum inductor current	[A]
$I_{L,min}$	Minimum inductor current	[A]
$I_{mpp}$	Maximum power point current	[A]
I	Output Current of the Photovoltaic module	[A]
$I_d$	<i>Current</i> flowing through the diode	[A]
$I_{ph}$	Photo-induced current generated by the incident radiation	[A]
$I_{ph,STC}$	Photo-current at $G_{STC}$ and $T_{STC}$	[A]
$I_{sc}$	Short-Circuit Current	[A]
$I_{sh}$	Shunt current	[A]

$I_0$	Reverse saturation current of the diode	[A]
K	Boltzmann constant	[J/K]
L	Inductor	[H]
$L_{min}$	Minimum inductor current value	[H]
$P_{in}$	Input Power	[W]
$P_{mpp}$	Maximum power point	[W]
$P_{out}$	Output power of the boost converter	[W]
$P_0$	Output power of the boost converter	[W]
R	Load resistance	[ $\Omega$ ]
$r_c$	Equivalent series resistance	[ $\Omega$ ]
$R_L$	Load resistance	[ $\Omega$ ]
$R_{sh}$	Shunt resistance	[ $\Omega$ ]
$R_s$	Resistance series	[ $\Omega$ ]
$R_1$	Parasitic resistance of the inductor	[ $\Omega$ ]
$R_2$	Parasitic resistance of the transistor	[ $\Omega$ ]
T	Operating temperature of the PV cell	[ $^{\circ}$ C]
T	Switching period	[s]
$T_{STC}$	Reference cell temperature	[ $^{\circ}$ C]
U	Output voltage of the Photovoltaic module	[V]
$U_d$	Voltage though the diode	[V]
$U_s$	Voltage though series resistance	[V]
$V_s$	Input Source Voltage	[V]
$V_L$	Load Voltage	[V]
$V_{mpp}$	Maximum power point voltage	[V]
$V_{oc}$	Open circuit voltage	[V]

$V_o$	Output Voltage	[V]
$\Delta i_L$	Inductor current ripple	[%]
$v_L$	Voltage across the inductor	[V]
$\frac{\Delta V_o}{V_o}$	Output voltage ripple	[%]
$\Delta V_{0,ESR}$	Output voltage ripple due to capacitor equivalent series resistance	
$\eta$	Efficiency	[%]
$v_L$	Voltage across the inductor	[V]

## 9.1 Abbreviations

Symbol	Explanation
a	Diode ideal constant
AC	Alternate current
CCM	Continuous Conduction Mode
DC	Direct current
dI	Current derivative
dV	Voltage derivative
EG	Energy gap
I-V	Current-voltage
KWh	Kilowatt hour
MOSFET	Metal oxide semiconductor field effect transistor
MPPT	Maximum power point tracking
MW	Mega-watts
PV	Photovoltaic
P-V	Curve of an ideal photovoltaic

PWM	Pulse Width Modulation
STC	Standard test condition
P&O	Perturb and observe
SPE	Solar Power Europe
UN	United Nations
VU	Voltage unbalance
W	Watts
$\Delta t$	Time derivative

## 10. References

### Literature references

- [1] Fokko M. M. "Materials for Energy Conversion and Storage" Sustainable Energy Technology MSc Program within 3TU, ChemE , TU Delft University, October 2016
- [4] G.Dileep, S.N. Singh, "Maximum power point tracking of solar photovoltaic system using modified perturbation and observation method" Renewable and Sustainable Energy Reviews 50 pp.109-129, May 2015
- [6]R. I.Putri, S.Wibowo, M.Rifa, "Maximum power point tracking for photovoltaic using incremental conductance method" ,ICSEEA, pp.22-30, Energy Procedia 68, 2015
- [10]N.Femia, G.Petrone, G.Spgnuolo, M. Vitelli , "Power Electronics and Control Techniques for Maximum Energy Harvesting in Photovoltaic Systems" CRC Press December 2012
- [11] G.N.Tiwari, S.Dubey, "Fundamentals of Photovoltaic Modules and their Applications", RSC Energy Series No.2, pp.91-103, 2010
- [12] V.J. Fesharaki, M. Dehghani, J. J. Fesharaki, " The Effect of Temperature on Photovoltaic Cell Efficiency" International Conference on Emerging Trends in Energy Conservation – ETEC, November 2011
- [14] D.W Hart, "Power Electronics", pp 211-220, 2010
- [16] E.G.Eggum, "Application of Modular Multilevel Converter for Interfacing Grid-Connected Photovoltaic Conversion Plants", MSc. Thesis, NTNU, pp.31-36, June 2015
- [18] F.Olita, "Advance control and condition monitoring PV System", MSc. Thesis, Aalborg University, pp.6-10 June 2012
- [19] D.Apablaza, J.Munoz, "Interleaved Boost Converter for Multi-String Photovoltaic Topologies", IEEE PES Innovative Smart Grid Technologies Latin America, pp 479-484, 2015
- [21] D. Verma n, S.Nema, A.M.Shandilya, S.K.Dash, " Maximum power point tracking (MPPT) techniques: Recapitulation in solar photovoltaic systems", Renewable and Sustainable Energy Reviews 54, pp. 1018–1034, October 2015

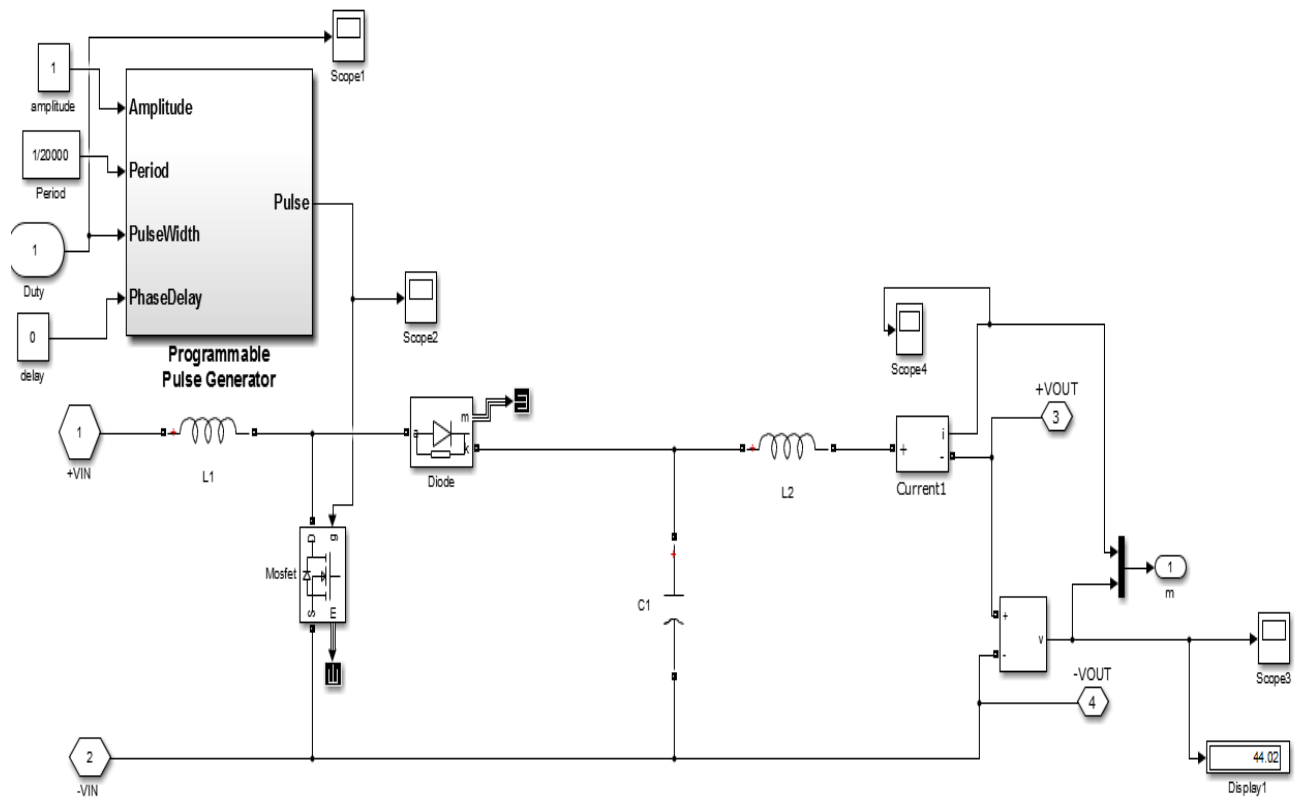
**Website references:**

- [2] <http://www.solarpowereurope.org/insights/global-market-outlook/> 22.02.2016  
O.Schafer, J.Watson Solar Power Europe, Principal authors and analysts: „Global Market Outlook for Photovoltaic 2015-2019
- [3] <http://www.cop21.gouv.fr/en/more-details-about-the-agreement/> 24.02.2016
- [5] [http://www.solarpowereurope.org/fileadmin/user\\_upload/documents/Solar\\_and\\_Mining/260116\\_Solar\\_storage\\_mining.pdf](http://www.solarpowereurope.org/fileadmin/user_upload/documents/Solar_and_Mining/260116_Solar_storage_mining.pdf)  
T.Hiling (THEnergy), J.Watson(SolarPowerEurope) ”Solar, storage and mining: New opportunities for solar power development”
- [7] <http://www.nrel.gov/ncpv/> 04.04.2016
- [8] <http://www.evwind.es/2015/06/12/photovoltaic-solar-energy-passes-1-global-threshold/52716> 15.03.2016
- [9] <http://denmark.dk/en/green-living/wind-energy/> 15.03.2016
- [13] <http://solarprofessional.com/articles/design-installation/field-applications-for-i-v-curve-tracers> 10.02.2016
- [15] <http://www.ti.com/lit/an/snva731/snva731.pdf> 17.04.2016
- [17] <http://se.mathworks.com/discovery/mppt-algorithm.html> 20.04.2016
- [20] <http://suncatchertci.com/products/solar-photovoltaics/> [cover page] 08.06.2016
- [22] <http://se.mathworks.com/videos/implement-maximum-power-point-tracking-algorithms-using-matlab-and-simulink-108209.html>

## Appendices:

### A. Boost Converter

#### a. Subsystem of the Converter



## b. Matlab .m file for calculating inductor and capacitance value

```
%calculating duty cycle
%Input values

Vs = 18;           % [V] Input Source Voltage (PV)
Vout = 44;        % [V] Output desired Voltage
R1 = 25;          % [ohms] Resistance load before the breaker
R2 = 15;          % [ohms] Resistive load after the breaker
f = 20000;        % [HZ] frequency
delta_V = 0.01;  % [%] Output voltage ripple less than 1%
```

```
D = 1-(Vs/Vout)
```

```
L = [D*(1-D)^2*R1]/(2*f)
```

```
C = D/(R1*delta_V*f)
```

**b' .**

```
D =
```

```
0.5909
```

```
L =
```

```
6.1807e-05
```

```
C =
```

```
1.1818e-04
```

## c. Perturb and Observe .m file

```
function D = PerturbandObserve_cod(V_PV, I_PV, T)
```

```
% define internal values as persistent variables
persistent Pn Po difP d dd n;
```

```
%initialize the internal values
```

```
if isempty(V_PV)
```

```
    V_PV=20;
```

```
end
```

```
if isempty(I_PV)
```



```

    I_PV=0;
end
if isempty(Pn)
    Pn=0;
end
if isempty(Po)
    Po=0;
end
if isempty(difP)
    difP=0;
end
if isempty(d)
    d=1;
end
if isempty(dd)
    dd=0;
end
if isempty(n)
    n=1;
end

if (T>n*0.02)
    n=n+1;
    % calculated measured array power
    Pn=V_PV*I_PV;
    difP=Pn-Po;
    Po=Pn;
    if (dd==0) % to avoid dP/dd=inf
        if difP>1
            dd=0.01;
            d=d+dd;
        elseif (difP<-1)
            dd=-0.01;
            d=d+dd;
        else
            dd=0;
        end
    else
        if ((difP>-1)&&(difP<1)) % leave little margin
            dd=0;
            d=d+dd;
        elseif ((difP/dd)>0) % increase the duty cycle-positive slope
            dd=0.01;
            d=d+dd;
        else % decrease the duty cycle-negative slope
            dd=-0.01;
            d=d+dd;
        end
    end
end

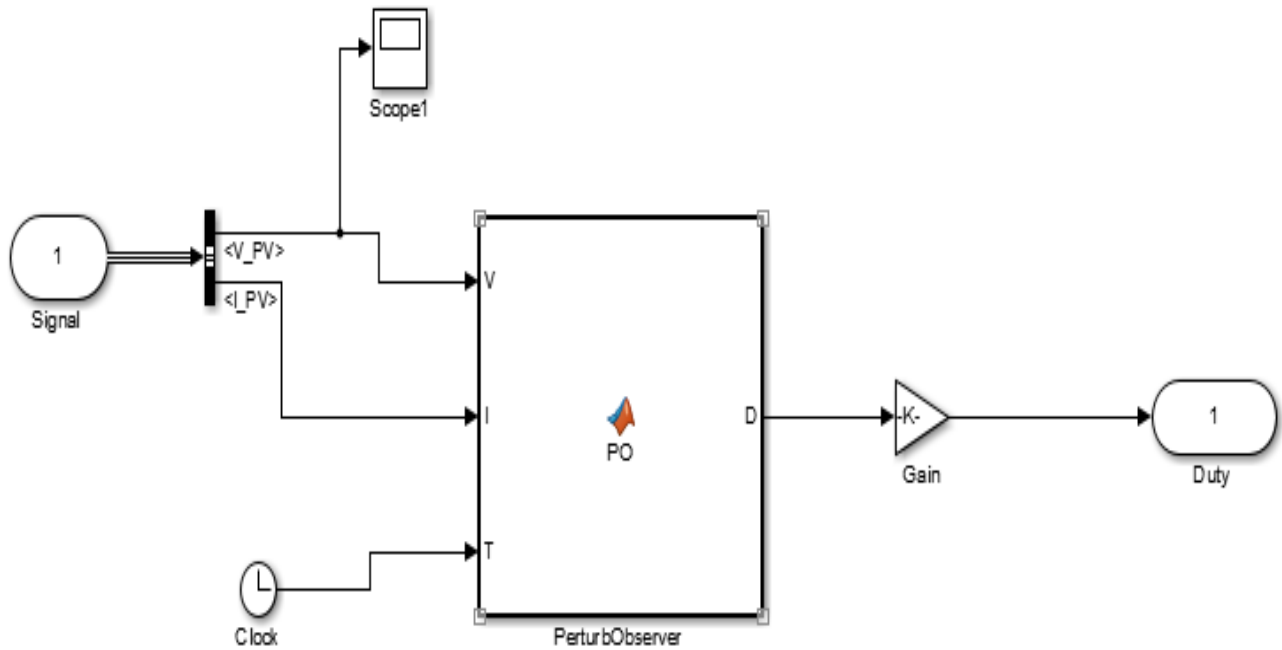
D=d/(d+1); % calculate duty

end

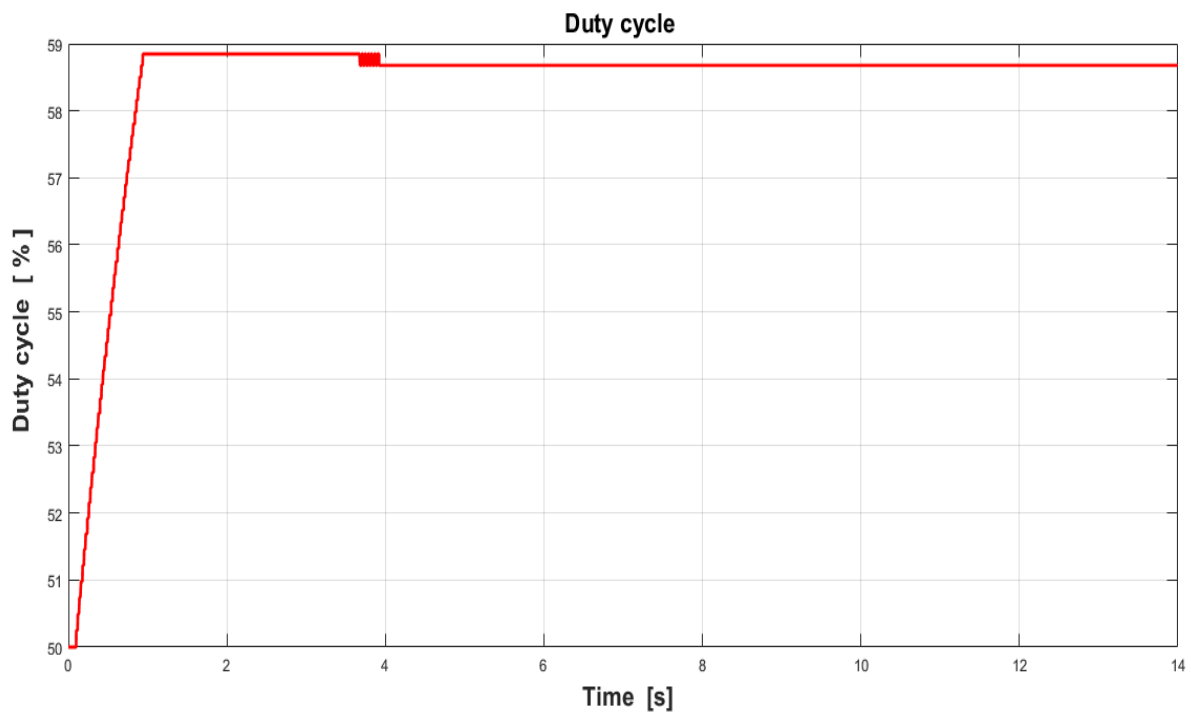
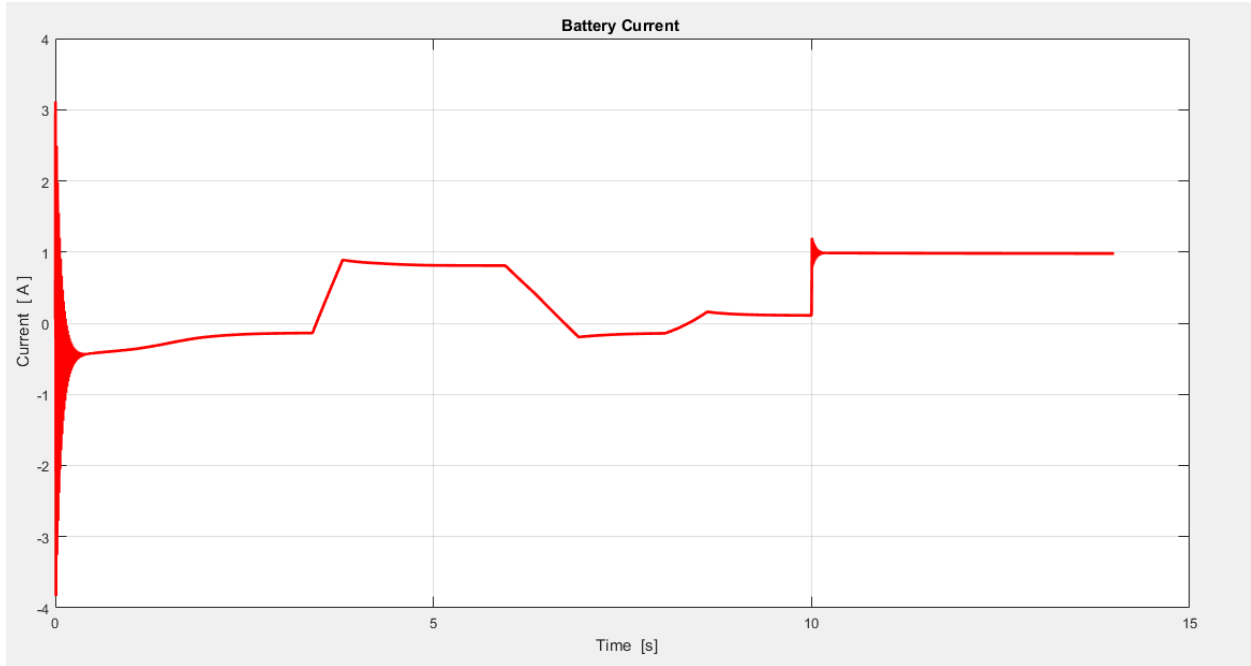
```

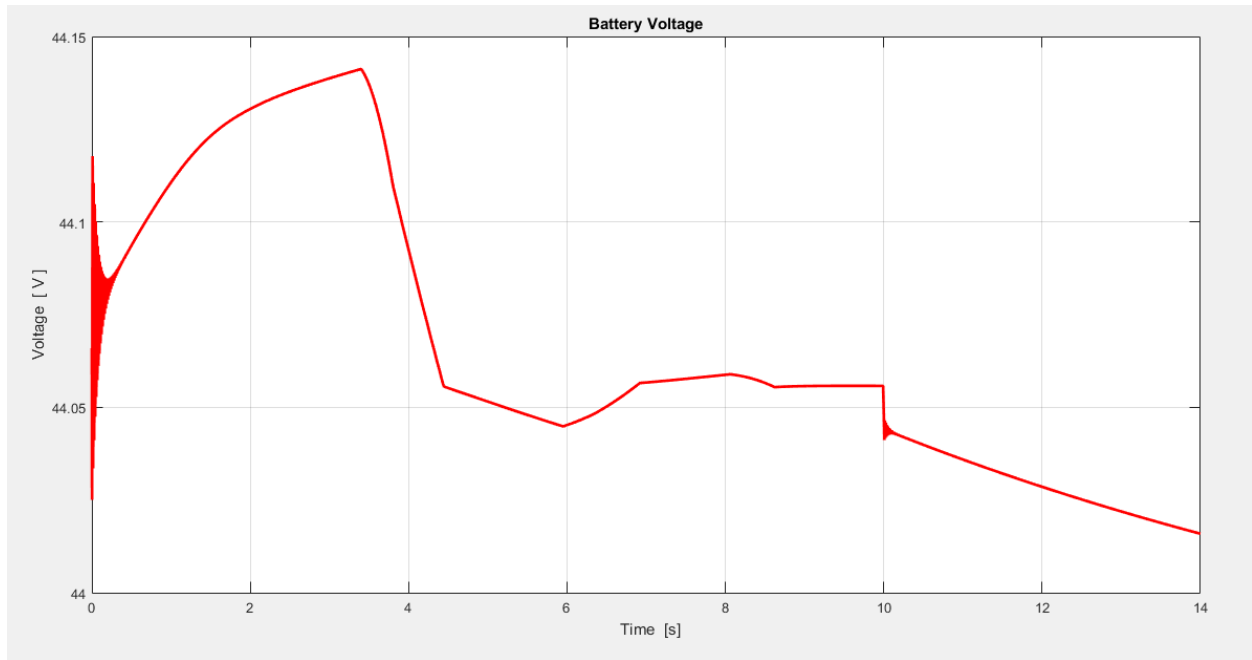
[22]

## Perturb and Observe subsystem.




## B. Battery graphs Chapter 6.3





## C. Photovoltaic Panel Array

### a. Block Parameters defined by the user in Simulink

 Block Parameters: PV Array ✕

PV array (mask) (link)

Implements a PV array built of strings of PV modules connected in parallel. Each string consists of modules connected in series. Allows modeling of a variety of preset PV modules available from NREL System Advisor Model (Jan. 2014) as well as user-defined PV module.

Input 1 = Sun irradiance, in W/m2, and input 2 = Cell temperature, in deg.C.

---

Parameters Advanced

Array data

Parallel strings

Series-connected modules per string

Display I-V and P-V characteristics of ...

array @ 1000 W/m2 & specified temperatures ▾

T\_cell (deg. C) [ 45 25 ]

Plot

---

Module data

Module: User-defined ▾

Plot I-V and P-V characteristics when a module is selected

Maximum Power (W)	Cells per module (Ncell)
<input style="width: 100%;" type="text" value="90.464"/>	<input style="width: 100%;" type="text" value="40"/>
Open circuit voltage Voc (V)	Short-circuit current Isc (A)
<input style="width: 100%;" type="text" value="21.5"/>	<input style="width: 100%;" type="text" value="5.81"/>
Voltage at maximum power point Vmp (V)	Current at maximum power point Imp (A)
<input style="width: 100%;" type="text" value="17.6"/>	<input style="width: 100%;" type="text" value="5.14"/>

Model parameters

Light-generated current IL (A)

Diode saturation current I0 (A)

Diode ideality factor

Shunt resistance Rsh (ohms)

### b. Diode current equation in detail

The diode I-V characteristics for a single module are defined by the equations

$$I_d = I_0 \left[ \exp \left( \frac{V_d}{V_T} \right) - 1 \right]$$

$$V_T = \frac{kT}{q} \times nI \times N_{cell}$$

where:

$I_d$	= diode current (A)
$V_d$	= diode voltage (V)
$I_0$	= diode saturation current (A)
$nI$	= diode ideality factor, a number close to 1.0
$k$	= Boltzman constant = 1.3806e-23 J.K-1
$q$	= electron charge = 1.6022e-19 C
$T$	= cell temperature (K)
$N_{cell}$	= number of cells connected in series in a module

## D. Datasheets for Inductor, Diode, Capacitor, MOSFET Transistor

### a. Fast recovery rectifier diode datasheet



**PFR850 → 856**

#### FAST RECOVERY RECTIFIER DIODE

PRELIMINARY DATA SHEET

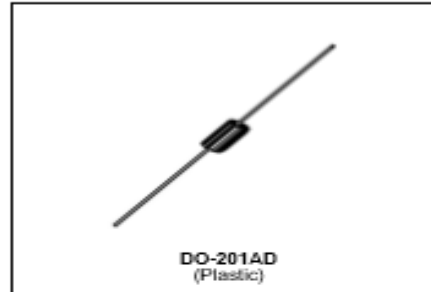
- LOW FORWARD VOLTAGE DROP
- HIGH SURGE CURRENT CAPABILITY

#### APPLICATIONS

- AC-DC POWER SUPPLIES AND CONVERTERS
- FREE WHEELING DIODES, etc.

#### DESCRIPTION

Their high efficiency and high reliability combined with small size and low cost make these fast recovery rectifier diode very attractive components for many demanding applications.



#### ABSOLUTE RATINGS (limiting values)

Symbol	Parameter		Value	Unit
$I_{FRM}$	Repetive peak forward current	$t_D < 20\mu s$	100	A
$I_F(AV)$	Average forward current*	$T_a = 90^\circ C$ $\delta = 0.5$	3	A
$I_{FSM}$	Surge non repetitive forward current	$t_D = 10ms$ Sinusoidal	100	A
$P_{tot}$	Power dissipation *	$T_a = 90^\circ C$	3.5	W
$T_{stg}$ $T_J$	Storage and junction temperature range		-40 to +175 -40 to +175	$^\circ C$
$T_L$	Maximum lead temperature for soldering during 10s at 4mm from case		230	$^\circ C$

Symbol	Parameter	PFR					Unit
		850	851	852	854	856	
$V_{RRM}$	Repetitive peak reverse voltage	50	100	200	400	600	V
$V_{RESM}$	Non repetitive peak reverse voltage	75	150	250	450	650	V

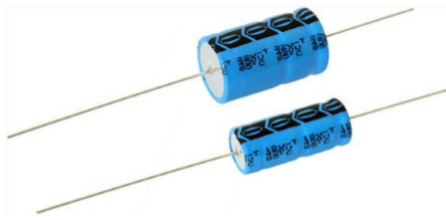
## b. Aluminum Capacitor Axial Standard datasheet


[www.vishay.com](http://www.vishay.com)

030/031 AS

Vishay BCcomponents

### Aluminum Capacitors Axial Standard



041/043 ASH

#### FEATURES

- Polarized aluminum electrolytic capacitors, non-solid electrolyte
- Axial leads, cylindrical aluminum case, insulated with a blue sleeve
- Taped version available for automatic insertion
- Charge and discharge proof
- Useful life: 3000 h at 85 °C
- Standard dimensions
- Material categorization: For definitions of compliance please see [www.vishay.com/doc?99912](http://www.vishay.com/doc?99912)

RoHS  
COMPLIANT

#### ADDITIONAL ELECTRICAL DATA

PARAMETER	CONDITIONS	VALUE
<b>Voltage</b>		
Surge voltage		$U_s \leq 1.15 \times U_R$
Reverse voltage		$U_{rev} \leq 1 \text{ V}$
<b>Current</b>		
Leakage current	After 1 min at $U_R$ : Case $\varnothing D \times L = 4.5 \text{ mm} \times 10 \text{ mm}$ Case $\varnothing D \times L = 6 \text{ mm} \times 10 \text{ mm}$ to $10 \text{ mm} \times 25 \text{ mm}$ $U_R = 100 \text{ V}$	$I_{L1} \leq 0.05 C_R \times U_R$ or $5 \mu\text{A}$ , whichever is greater $I_{L1}$ for $CV \leq 1000$ : $\leq 0.01 C_R \times U_R$ or $1 \mu\text{A}$ , whichever is greater $I_{L1}$ for $CV > 1000$ : $\leq 0.006 C_R \times U_R + 4 \mu\text{A}$ $I_{L1} = 0.02 C_R \times U_R + 4 \mu\text{A}$
	After 5 min: $U_R = 6.3 \text{ V}$ to $63 \text{ V}$ $U_R = 100 \text{ V}$	$I_{L5} \leq 0.002 C_R \times U_R + 5 \mu\text{A}$ $I_{L5} \leq 0.006 C_R \times U_R + 4 \mu\text{A}$
<b>Inductance</b>		
Equivalent series inductance (ESL)	Case $\varnothing D \times L$ mm:	
	4.5 x 10	typ. 10 nH
	6 x 10	typ. 22 nH
	8 x 11	typ. 85 nH
	6.5 x 18	typ. 25 nH

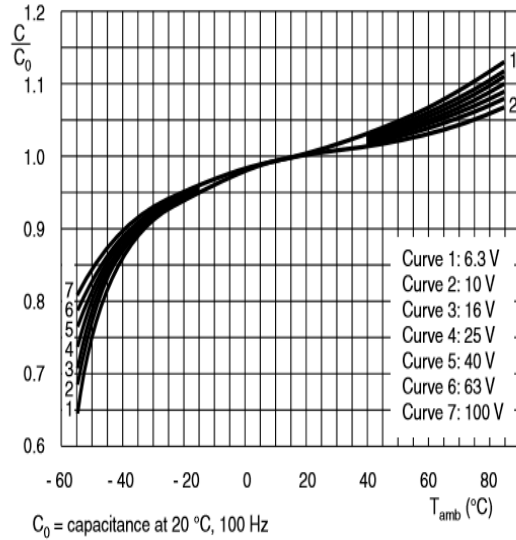
**CAPACITANCE (C)**

Fig. 4 - Typical multiplier of capacitance as a function of ambient temperature

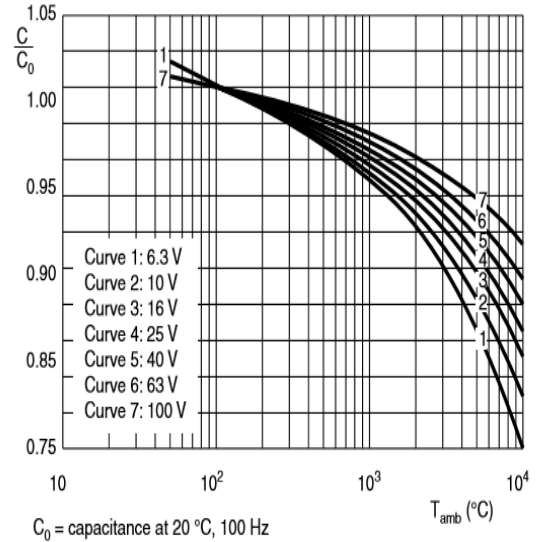


Fig. 5 - Typical multiplier of capacitance as a function of frequency

<b>QUICK REFERENCE DATA</b>	
<b>DESCRIPTION</b>	<b>VALUE</b>
Nominal case sizes ( $\varnothing$ D x L in mm)	4.5 x 10 to 10 x 25
Rated capacitance range, $C_R$	1 $\mu$ F to 1000 $\mu$ F
Tolerance on $C_R$	- 10 % to + 50 %
Rated voltage, $U_R$	6.3 V to 100 V
Category temperature range	- 40 °C to + 85 °C
Endurance test at 85 °C	2000 h
Useful life at 85 °C	3000 h
Useful life at 40 °C, 1.4 x $I_R$ applied	80 000 h
Shelf life at 0 V, 85 °C	500 h
Based on sectional specification	IEC 60384-4/EN130300
Climatic category IEC 60068	40/085/56



Table 4

MULTIPLIER OF RIPPLE CURRENT ( $I_R$ ) AS A FUNCTION OF FREQUENCY			
FREQUENCY (Hz)	$I_R$ MULTIPLIER		
	$U_R = 6.3 \text{ V TO } 10 \text{ V}$	$U_R = 16 \text{ V TO } 25 \text{ V}$	$U_R = 40 \text{ V TO } 100 \text{ V}$
50	0.95	0.90	0.85
100	1.00	1.00	1.00
300	1.07	1.12	1.20
1000	1.12	1.20	1.30
3000	1.15	1.25	1.35
$\geq 10\,000$	1.20	1.30	1.40

## 2. First experiment prototype-Capacitor datasheet



### ECA SERIES

- Standard Miniature Axial Type Aluminum Electrolytic Capacitors.
- Life 2000 hours at 85°C
- Small size allows wider choice of capacitance and voltage for automatic insertion.

#### Characteristics

<b>Voltage Range</b>	10 to 100 VDC				160 to 450 VDC				
<b>Capacitance Range</b>	0.47 to 10000uF				0.47 to 220uF				
<b>Temperature Range</b>	-40 to +85°C				-25 to +85°C				
<b>Capacitance Tolerance</b>	+20% -20% (at 20°C, 120Hz)								
<b>Leakage Current</b>	I $\leq$ 0.01CV or 3uA, whichever is greater 3 minutes after Rated Voltage applied				I $\leq$ 0.03CV or 3uA, whichever is greater 3 minutes after Rated Voltage applied				
<b>Dissipation Factor (tan <math>\delta</math>)</b>	Rated Voltage (V)	10	16	25	35	50	63	100	
	Dissipation Factor	0.20	0.17	0.15	0.12	0.10	0.10	0.08	
<b>Stability at Low Temperature</b>	For capacitance > 1000uF, add 0.02 for every 1000uF, (at 20°C, 120Hz)								
	Impedance ration at 120Hz								
	Rated Voltage (V)	10	16	25	35	50	63	100	
	Z-25°C/Z 20°C	3	2	2	2	2	2	2	
Z-40°C/Z 20°C	6	4	4	3	3	3	3		
<b>Load Life</b>	After the rated voltage has been applied for 2000 hours at 85°C	Rated Voltage (V)	160	200	250	350	400	450	
		Z-25°C/Z 20°C	2	2	3	5	15	15	
<b>Shelf Life</b>	After storage for 500 hours at 85°C, with no voltage applied and being stabilized at +20°C, Capacitor shall meet the limit specified in load life.	Capacitance change		Within $\pm$ 20% of initial value					
		D.F. tan $\delta$		150% or less of initial specified value					
		Leakage current		Less than initial specified value					

### Case Size of Standard Products & Maximum Ripple Current ( mA rms 85°C 120Hz)

Cap. uF	6.3V		10V		16V		25V		35V		50V		63V						
	Size	R.C.	Size	R.C.	Size	R.C.	Size	R.C.	Size	R.C.	Size	R.C.	Size	R.C.					
0.47												→	6.3x12.5	11					
1			ALL BLANK VOLTAGE ON SLEEVE MARKING IS SAME VOLTAGE "→" POINT TO										→	6.3x12.5	17				
2.2																	→	6.3x12.5	28
3.3																	→	6.3x12.5	35
4.7																	→	6.3x12.5	45
10																→	6.3x12.5	65	6.3x12.5
22										→	6.3x12.5	100	6.3x12.5	115					
33								→	6.3x12.5	105	8x16	125	8x16	140					
47						→	6.3x12.5	130	6.3x12.5	140	8x16	150	8x16	190					
100				→	6.3x12.5	185	8x16	190	8x16	230	8x16	250	10x21	300					
220				→	8x16	320	8x16	320	10x17	370	10x21	440	13x21	490					
330		→	8x16	330	8x16	360	10x17	420	10x21	470	13x21	520	13x26	680					
470		→	8x16	400	8x16	470	10x17	520	13x21	580	13x21	740	16x28	880					
1000		→	10x17	630	10x21	710	13x21	830	13x26	1100	16x33	1350	16x37	1550					
2200		→	13x21	970	13x26	1150	16x28	1300	16x33	1550	18x37	1700	18x37	2200					
3300		→	13x26	1250	16x28	1400	16x33	1650	18x37	1950	22x42	2200	22x42	2360					
4700		→	16x28	1500	16x33	1700	18x37	2050	22x37	2400	22x42	2500	25x42	2950					
6800		→	16x33	1850	18x37	2150	22x42	2550	25x42	2600									
10000		→	18x37	2350	22x42	2700	22x42	2800	25x42	2800									

### c. MOSFET transistor



## STP16NF06L STP16NF06LFP

N-CHANNEL 60V - 0.07  $\Omega$  - 16A TO-220/TO-220FP  
STripFET™ II POWER MOSFET

TYPE	V <sub>DSS</sub>	R <sub>DS(on)</sub>	I <sub>D</sub>
STP16NF06L	60 V	<0.09 $\Omega$	16 A
STP60NF06LFP	60 V	<0.09 $\Omega$	11 A

- TYPICAL R<sub>DS(on)</sub> = 0.07  $\Omega$
- EXCEPTIONAL dv/dt CAPABILITY
- LOW GATE CHARGE AT 100 °C
- LOW THRESHOLD DRIVE

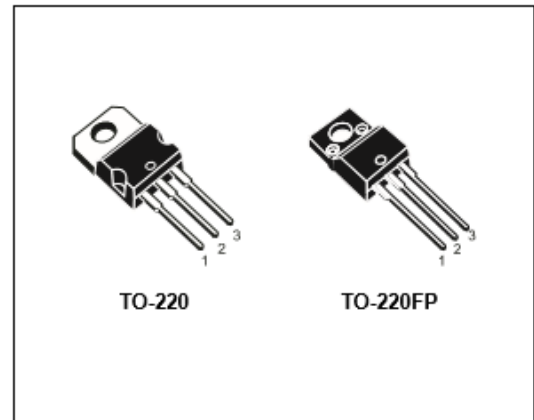
#### DESCRIPTION

This Power MOSFET is the latest development of STMicroelectronics unique "Single Feature Size™" strip-based process. The resulting transistor shows extremely high packing density for low on-resistance, rugged avalanche characteristics and less critical alignment steps therefore a remarkable manufacturing reproducibility.

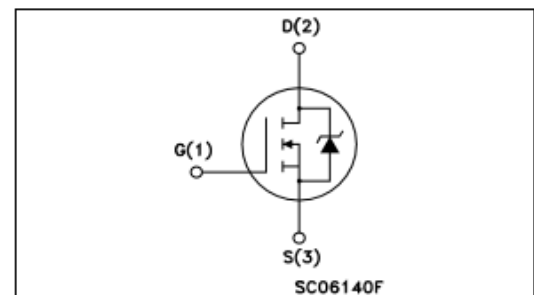
#### APPLICATIONS

- MOTOR CONTROL, AUDIO AMPLIFIERS
- HIGH CURRENT, HIGH SPEED SWITCHING
- SOLENOID AND RELAY DRIVERS
- DC-DC & DC-AC CONVERTERS
- AUTOMOTIVE ENVIRONMENT

#### ABSOLUTE MAXIMUM RATINGS



#### INTERNAL SCHEMATIC DIAGRAM



## ABSOLUTE MAXIMUM RATINGS

Symbol	Parameter	Value		Unit
		STP16NF06L	STP16NF06LFP	
$V_{DS}$	Drain-source Voltage ( $V_{GS} = 0$ )	60		V
$V_{DGR}$	Drain-gate Voltage ( $R_{GS} = 20 \text{ k}\Omega$ )	60		V
$V_{GS}$	Gate- source Voltage	$\pm 16$		V
$I_D$	Drain Current (continuous) at $T_C = 25^\circ\text{C}$	16	11(*)	A
$I_D$	Drain Current (continuous) at $T_C = 100^\circ\text{C}$	11	7.5(*)	A
$I_{DM}(\bullet)$	Drain Current (pulsed)	64	44(*)	A
$P_{tot}$	Total Dissipation at $T_C = 25^\circ\text{C}$	45	25	W
	Derating Factor	0.3	0.17	W/ $^\circ\text{C}$
$dv/dt$ (1)	Peak Diode Recovery voltage slope	23		V/ns
$E_{AS}$ (2)	Single Pulse Avalanche Energy	127		mJ
$V_{ISO}$	Insulation Withstand Voltage (DC)	-----	2500	V
$T_{stg}$	Storage Temperature	-55 to 175		$^\circ\text{C}$
$T_j$	Operating Junction Temperature			

(\*) Pulse width limited by safe operating area.

(\*) Current Limited by package's thermal resistance

(1)  $I_{SD} \leq 16\text{A}$ ,  $di/dt \leq 210\text{A}/\mu\text{s}$ ,  $V_{DD} \leq V_{(BR)DSS}$ ,  $T_j \leq T_{jMAX}$ .(2) Starting  $T_j = 25^\circ\text{C}$ ,  $I_D = 8\text{A}$ ,  $V_{DD} = 30\text{V}$ 

August 2002

1/9

## ELECTRICAL CHARACTERISTICS (continued)

## SWITCHING ON

Symbol	Parameter	Test Conditions	Min.	Typ.	Max.	Unit
$t_{d(on)}$ $t_r$	Turn-on Delay Time Rise Time	$V_{DD} = 30\text{V}$ $I_D = 8\text{A}$ $R_G = 4.7\ \Omega$ $V_{GS} = 4.5\text{V}$ (Resistive Load, Figure 3)		10 37		ns ns
$Q_g$ $Q_{gs}$ $Q_{gd}$	Total Gate Charge Gate-Source Charge Gate-Drain Charge	$V_{DD} = 48\text{V}$ $I_D = 16\text{A}$ $V_{GS} = 5\text{V}$		7.3 2.1 3.1	10	nC nC nC

## SWITCHING OFF

Symbol	Parameter	Test Conditions	Min.	Typ.	Max.	Unit
$t_{d(off)}$ $t_f$	Turn-off Delay Time Fall Time	$V_{DD} = 30\text{V}$ $I_D = 8\text{A}$ $R_G = 4.7\ \Omega$ $V_{GS} = 4.5\text{V}$ (Resistive Load, Figure 3)		20 12.5		ns ns

## SOURCE DRAIN DIODE

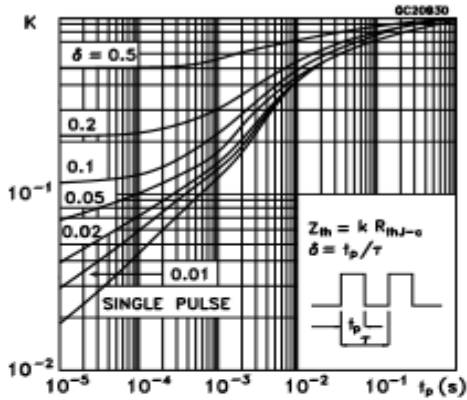
Symbol	Parameter	Test Conditions	Min.	Typ.	Max.	Unit
$I_{SD}$ $I_{SDM}(\bullet)$	Source-drain Current Source-drain Current (pulsed)				16 64	A A
$V_{SD}(\bullet)$	Forward On Voltage	$I_{SD} = 16\text{A}$ $V_{GS} = 0$			1.3	V
$t_{rr}$ $Q_{rr}$ $I_{RRM}$	Reverse Recovery Time Reverse Recovery Charge Reverse Recovery Current	$I_{SD} = 16\text{A}$ $di/dt = 100\text{A}/\mu\text{s}$ $V_{DD} = 16\text{V}$ $T_j = 150^\circ\text{C}$ (see test circuit, Figure 5)		50 67.5 2.7		ns nC A

(\*) Pulsed: Pulse duration = 300  $\mu\text{s}$ , duty cycle 1.5 %.

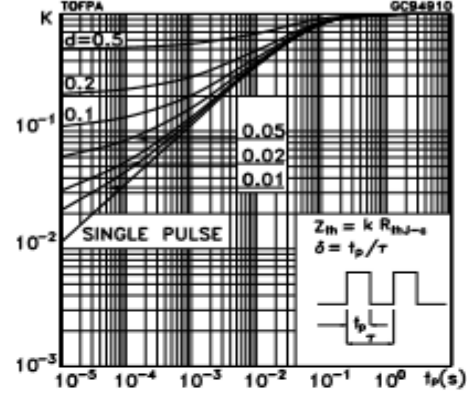
(\*) Pulse width limited by safe operating area.

STP16NF06L/FP

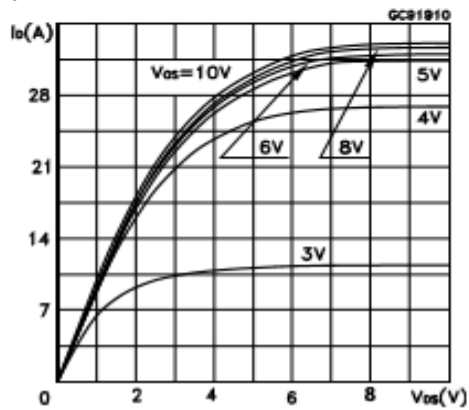
Thermal Impedance



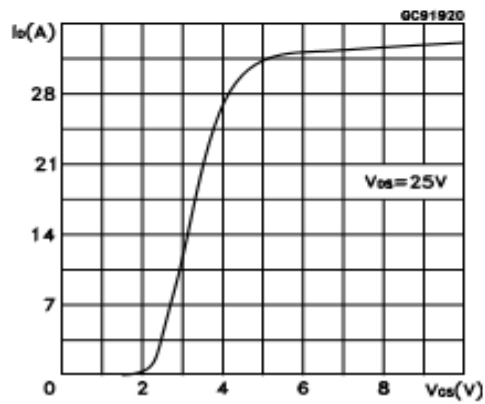
Thermal Impedance for TO-220FP



Output Characteristics

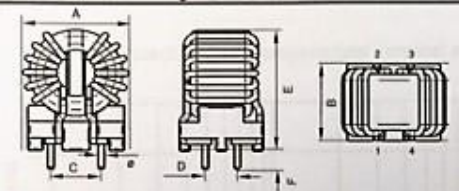


Transfer Characteristics



d. Inductor

**A Mechanische Abmessungen / dimensions:**




		S	
A	18,5 max	mm	
B	14,5 max	mm	
C	7,7 ± 0,5	mm	
D	5,0 ± 0,5	mm	
E	22,0 max.	mm	
F	3,5 ± 0,5	mm	
ø	1,0 typ.	mm	

**B Elektrische Eigenschaften / electrical properties:**

Eigenschaften / properties	Testbedingungen / test conditions	Wert / value	Einheit / unit	tol.	
Leerlauf-Induktivität / inductance	100 kHz / 0,1 mA / 20 °C	$L_0$	350	µH	±30%
DC-Widerstand / DC-resistance	@ 20 °C	$R_{DC}$	5,5	mΩ	±10%
Nennstrom / rated current	@ 70 °C	$I_N$	8,50	A	max.
Nennspannung / rated voltage	50 Hz	$U_N$	250	V	max.

**C Schaltbild / schematic:**



**D Prüfgeräte / test equipment:**

WAYNE KERR WK3260B/WK3265 für/for Lr und/and Rec  
 HP 34401 A für/for I/N

**E Testbedingungen / test conditions:**

Luftfeuchtigkeit / humidity: 33%  
 Umgebungstemperatur / temperature: +20 °C  
 Prüfspannung / testing voltage: 1500 V, 50 Hz  
 5mA, 2 sec

**F Werkstoffe & Zulassungen / material & approvals:**

Socket / base: UL94V-0  
 Draht / wire: Class F  
 Kleber / glue: UL94V-2  
 Abstandhalter / spacer: UL94V-0

**G Eigenschaften / general specifications:**

Klimabeständigkeit/ climatic class: 40/125/21  
 Betriebstemp. / operating temperature: -40 °C - + 125 °C  
 Übertemperatur / temperature rise: < 55 K  
 It is recommended that the temperature of the part does not exceed 125 °C under worst case operating conditions.

Freigabe erteilt / general release:

Kunde / customer	Unterschrift / signature	Wüth Elektronik	IKa	Version 1	19-01-20
			Name	Änderung / modification	Datum / date

The electronic component has been designed and developed for usage in general electronic equipment. Before incorporating this component into any equipment where higher safety and reliability is especially required or if there is the possibility of direct damage or injury to human body, for example in the range of aerospace, aviation, nuclear control, submarine, transportation control, train control, ship control, transportation signal, disaster prevention, medical, public information network etc. Würth Elektronik eides GmbH shall be informed before the design-in stage. In addition, sufficient reliability evaluation checks for safety must be performed on every electronic component which is used in electrical circuits that require high safety and reliability functions or performance.

**Würth Elektronik eides GmbH & Co. KG**

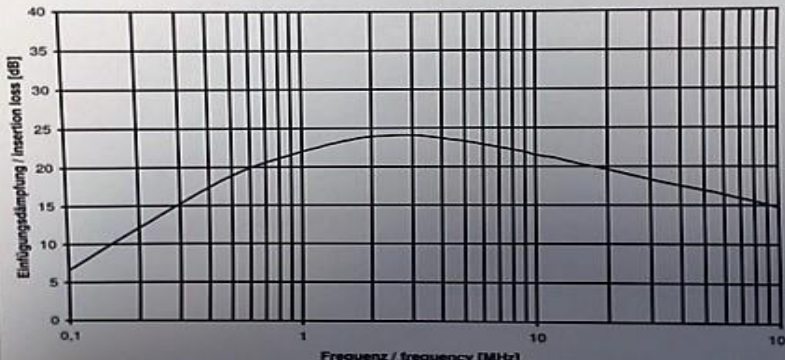
**Spezifikation für Freigabe / specification for release**

Kunde / customer :  
 Artikelnummer / part number : 7448229004  
 Bezeichnung : STROMKOMP. DROSSEL WE-CMB HC  
 description : COMMON MODE CHOKE WE-CMB HC

**compliant RoHS** **WE** **WÜRTH ELEKTRONIK**  
 DATUM / DATE : 2009-01-20

**H Einfügedämpfung / insertion loss:**

**typischer Dämpfungsverlauf / typical attenuation curve**



common mode

